



Nagasaki University



**Graduate School of Biomedical
Sciences**

**Development and validation of new analytical methods for
clinically important aldehydes**

By

Mahmoud Hamed Mahmoud Hamed Elmaghrabey

**A Dissertation Submitted to the
Graduate School of Biomedical Sciences
Nagasaki University**

In Partial Fulfillment of the Requirements

For the Degree of

DOCTOR OF PHILOSOPHY

(Pharmaceutical Sciences, Analytical Chemistry)

Japan

2016

Dedication

To the Soul of My Father

To My Mother

To My Beloved Wife

List of publications

- 1- Mahmoud H. El-Maghrabey, Naoya Kishikawa, Kaname Ohyama, Naotaka Kuroda, *Analytical method for lipoperoxidation relevant reactive aldehydes in human sera by high-performance liquid chromatography-fluorescence detection*, *Analytical Biochemistry* 464 (2014) 36–42. DOI: 10.1016/j.ab.2014.07.002.
- 2- Mahmoud H. El-Maghrabey, Naoya Kishikawa, Kaname Ohyama, Takahiro Imazato, Yukitaka Ueki, Naotaka Kuroda, *Determination of human serum semicarbazide-sensitive amine oxidase activity via flow injection analysis with fluorescence detection after online derivatization of the enzymatically produced benzaldehyde with 1,2-diaminoanthraquinone*, *Analytica Chimica Acta* 881 (2015) 139–147. DOI: 10.1016/j.aca.2015.04.006.
- 3- Mahmoud El-Maghrabey, Naoya Kishikawa, Naotaka Kuroda, *9,10-Phenanthrenequinone as a Mass-Tagging Reagent for Ultra-Sensitive Liquid Chromatography Tandem Mass Spectrometry Assay of Aliphatic Aldehydes in Human Serum*, *Journal of Chromatography A*, 1462 (2016) 80–89. DOI: 10.1016/j.chroma.2016.07.082.

Table of contents

Subject	Page
List of publications.....	i
Table of contents.....	ii
List of abbreviations.....	viii
List of tables.....	xi
List of figures.....	xiv
Preface.....	xxii

Chapter I: General introduction

Introduction.....	1
1-1. Endogenous sources and harmful effects of aldehydes	2
1-1-1. Lipid peroxidation	2
1-1-2. Carbohydrate or ascorbate autoxidation	5
1-1-3. Carbohydrate metabolism	6
1-1-4. Amine oxidases-catalyzed metabolic activation	6
1-1-5. Cytochrome P ₄₅₀ -catalyzed metabolic activation	9
1-1-6. Myeloperoxidase-catalyzed metabolic activation	9
1-2. Challenges in analytical determination of aldehydes	10
1-3. Aim of the thesis	12

Chapter II: Analytical method for lipoperoxidation relevant reactive aldehydes in human sera by high-performance liquid chromatography-fluorescence detection

2-1. Introduction	13
2-2. Experimental	16
2-2-1. Materials and reagents	16
2-2-2. Instrumentations and chromatographic conditions	17
2-2-3. Clinical samples	18
2-2-4. Assay procedure for aliphatic aldehydes in human serum	19
2-2-5. Validation procedure	19
2-2-6. Statistical analysis	20
2-3. Results and discussion	20
2-3-1. Fluorescence characteristics of the products	20
2-3-2. Optimization of chromatographic conditions	21
2-3-3. Optimization of derivatization conditions	23
2-3-4. Validation of the proposed method	26
2-3-5. Application to the analysis of serum samples from healthy and diseased human subjects	28
2-3-6. Comparison of the analytical performance of the proposed method and published literature	32
2-4. Conclusions	33

Chapter III: 9,10-Phenanthrenequinone as a mass-tagging reagent for ultra-sensitive liquid chromatography tandem mass spectrometry assay of aliphatic aldehydes in human serum

3-1. Introduction	35
3-2. Experimental	38
3-2-1. Chemicals and reagents	38
3-2-2. Instrumentation and LC-ESI-MS/MS conditions	39
3-2-3. Clinical samples	41
3-2-4. Derivatization procedure	41
3-2-5. Serum samples treatment	41
3-2-6. Validation procedure	41
3-3. Results and discussion	43
3-3-1. Preliminary screening for candidate derivatizing agents	43
3-3-2. The MS/MS fragmentation pattern of PQ-aldehydes derivatives	52
3-3-3. PQ selectivity for aldehydes.....	54
3-3-4. Optimization of derivatization conditions	56
3-3-5. Optimization of HPLC separation and MS/MS monitoring	58
3-3-6. Validation study	60
3-3-7. Application of the proposed LC/ESI-MS/MS method to determination of the target aldehydes in human serum	63
3-3-8. Comparison of the developed method and reported methods for aldehydes determination in biological fluids	66
3-4. Conclusions	68

Chapter IV: Development of an isotope-coded derivatization LC-MS/MS assay for reactive aldehydes in human serum using ¹⁴N/¹⁵N ammonium acetate and 9,10-phenanthrenequinone

4-1. Introduction	69
4-2. Experimental	73
4-2-1. Materials and reagents	73
4-2-2. Instrumentation and LC/ESI-MS/MS conditions	73
4-2-3. Clinical samples	74
4-2-4. Derivatization procedure for elucidation of product ion spectra	75
4-2-5. Assessment of ICD technique for relative quantification	75
4-2-6. Serum samples treatment and ICD protocol	75
4-2-7. Validation procedure	76
4-2-8. Statistical analysis	77
4-3. Results and discussion	78
4-3-1. The MS/MS fragmentation of PQ-aldehydes derivatives.....	78
4-3-2. Optimization of derivatization conditions	81
4-3-3. Optimization of vHPLC separation and MS/MS monitoring ...	83
4-3-4. Results of the assessment study of ICD technique for relative quantification	84
4-3-5. Validation of the method	87
4-3-6. Selection and optimization of the extraction procedure and recovery study.....	88
4-3-7. Application of the proposed ICD LC/ESI-MS/MS method to determination of the target aldehydes in human serum	93
4-3-8. Comparison of the proposed and reported methods for simultaneous determination of HNE and HHE	97
4-3-9. Comparison of the proposed and reported ICD LC-MS/MS methods for of aldehydes	99
4-4. Conclusions	100

Chapter V: Determination of human serum semicarbazide-sensitive amine oxidase activity via flow injection analysis with fluorescence detection after online derivatization of the enzymatically produced benzaldehyde with 1,2-diaminoanthraquinone

5-1. Introduction	101
5-2. Experimental	103
5-2-1. Materials and reagents	103
5-2-2. Instrumentation and FIA conditions	104
5-2-3. Confirmation of the identity of benzaldehyde-DAAQ derivative.	105
5-2-4. Fluorescence measurement of benzaldehyde after reaction with DAAQ	105
5-2-5. Clinical samples	106
5-2-6. Sample preparation procedure for SSAO enzyme activity	106
5-2-7. Method validation	106
5-2-8. Statistical analysis	108
5-3. Results and discussion	108
5-3-1. Fluorescence spectra and identification of benzaldehyde-DAAQ derivative	108
5-3-2. Optimization of derivatization conditions	110
5-3-3. Optimization of FIA conditions	112
5-3-4. Pretreatment of serum samples for determination of SSAO activity and Michaelis-Menten constant (K_m)	115
5-3-5. Validation study	117
5-3-6. Interference investigation	120
5-3-7. Application of the proposed method to determination of the SSAO activity in healthy and diabetic sera	123
5-3-8. Comparison of performance of the proposed method with that of reported literature for SSAO activity determination	124
5-4. Conclusions	126

General conclusions 127
References..... 131
Acknowledgment..... 143

List of abbreviations

Abbreviation	Meaning
ACR	Acrolein
AGEs	Advanced glycation end products
4-APC	4-(2-(Trimethylammonio)ethoxy)benzenaminium halide
BODIPY-aminozide	1,3,5,7-Tetramethyl-8-aminozide-difluoroboradiaza-s-indacene
CHD	1,3-Cyclohexanedione
CID	Collision induced dissociation
CL	Chemiluminescence
DAAQ	1,2-Diaminoanthraquinone
DAO	Tissue diamine oxidase
DBD-H	4-(<i>N,N</i> -Dimethylaminosulphony)-7-hydrazino-2,1,3 benzoxadiazole
DMAB	4-Dimethylaminobenzil
DMSO	Dimethyl sulfoxide
DNPH	2,4-Dinitrophenylhydrazine
DNSH	Dansylhydrazine
EI-MS	electron impact-mass spectrometry
FDA	Food and Drug Administration
FIA	Flow injection analysis
FL	Fluorescence
GC-MS	Gas chromatography-mass spectrometry
GO	Glyoxal
h	Hour
HHE	4-Hydroxy-2-hexenal
HLB	Hydrophilic-lipophilic balance

Abbreviation	Meaning
HNE	4-Hydroxy-2-nonenal
ICD	Isotope-coded derivatization
IS	Internal standard
K'	The apparent K_m
K_m	Michaelis-Menten constant
LC	Liquid chromatography
LC/ESI-MS/MS	Liquid chromatography electrospray ionization tandem mass spectrometry
LDL	Low density lipoproteins
LLE	Liquid-liquid extraction
LOD	Limit of detection
LOQ	Limit of quantification
LPRRAs	Liperoxidation relevant reactive aldehydes
MAO	Monoamine oxidase
MDA	Malondialdehyde
MNBDH	<i>N</i> -methyl-4-hydrazino-7-nitrobenzo-furazan
MPIA	4-(1-methyl-1 <i>H</i> -phenanthro[9,10- <i>d</i>]imidazol-2-yl) phenlamine
MPO	Myeloperoxidase
MRM	Multiple reaction monitoring
MS	Mass spectrometry
PAD	1,10-Phenanthroline-5,6-dione
PAO	Polyamine oxidase
PBS	Phosphate buffer saline
PFBHA	<i>O</i> -2,3,4,5,6-(Penta-fluorobenzyl)hydroxylamine
PPT	Protein precipitation

Abbreviation	Meaning
PQ	9,10-Phenanthrenequinone
PUFAs	Polyunsaturated fatty acids
PTFE	Polytetrafluoroethylene
<i>r</i>	Correlation coefficient
ROS	Reactive oxygen species
% RSD	%Relative standard deviation
RT-PCR	Reverse transcription polymerase chain reaction
S	Seconds
SD	Standard deviation
SE	Standard error
SPE	Solid phase extraction
SSAO	Semicarbazide-sensitive amine oxidase
S/N	Signal-to-noise ratio
TCPH	2,4,6-Trichlorophenylhydrazine
t_R	Retention time
UV	Ultraviolet
V'	The apparent V_{max}
V_{max}	The maximum reaction velocity

List of Tables

	Title	Page
Table 2.1	Calibration ranges, regression equations, correlation coefficients and detection limits for the target aldehydes in spiked serum.....	27
Table 2.2	Accuracy and precision of the proposed method for the determination of the target aldehydes in spiked serum.....	28
Table 2.3	Statistical analysis of the results for determination of the target aldehydes in healthy, diabetic and rheumatic patients' sera.....	30
Table 3.1	Optimum MS/MS conditions for the analysis of PQ derivatives of the studied aliphatic aldehydes.....	40
Table 3.2	The optimum MS/MS conditions for the studied α,β -diketo reagents.....	44
Table 3.3	Collective regression data, LOD, LOQ, accuracy and precision at LOQ for the studied aldehydes in serum	61
Table 3.4	Accuracy and precision of the proposed method for the determination of the studied aliphatic aldehydes in spiked serum samples.....	62
Table 3.5	Results of recovery study of the target of aliphatic aldehydes from spiked serum samples after salting-out LLE.....	63

	Title	Page
Table 3.6	Levels of the target aliphatic aldehydes in healthy human serum.....	65
Table 3.7	Comparison of the proposed and reported methods for determination of aldehydes in biological fluids	67
Table 4.1	Optimum MS/MS conditions for the analysis of PQ derivatives of the studied aldehydes	74
Table 4.2	LOD, LOQ, calibration ranges, regression equations and correlation coefficient for the target aldehydes in spiked serum..	87
Table 4.3	Accuracy and precision of the proposed method for the determination of the target aldehydes in spiked serum	88
Table 4.4	Statistical analysis of the results for determination of the target aldehydes in healthy, diabetic, rheumatic, and cardiac disorders patients' sera.....	95
Table 4.5	Comparison of the developed and reported methods for simultaneous determination of HHE and HNE	98
Table 5.1	Accuracy and precision of the proposed method for the determination of benzaldehyde in the spiked enzymatic reaction mixtures	119
Table 5.2	Results of recovery study of benzaldehyde from spiked enzymatic reaction mixtures.....	119

	Title	Page
Table 5.3	Effects of some aldehydes normally exist in human serum on the determination of benzaldehyde (100 nmol/mL)	121
Table 5.4	Statistical analysis of the results for determination of the SSAO activity in healthy and diabetics human subjects' sera.....	123
Table 5.5	Critical comparison of the performance of the proposed and reported methods for determination of SSAO activity.....	124
Table 5.6	Statistical comparison of the proposed FIA method and a reference method for the determination of SSAO activity in human sera.....	125

List of Figures

	Title	Page
Fig. 1.1	Scheme for lipid peroxidation process showing structures of the proposed intermediates and the produced aldehydes.....	3
Fig. 1.2	Formation of 4-hydroxyphenylacetaldehyde and indoleacetaldehyde by MAO and formation of formaldehyde and methylglyoxal by serum SSAO.....	7
Fig. 1.3	Formation of aldehydes <i>via</i> MPO-catalyzed metabolic activation.....	10
Fig. 2.1	Structures of the studied LPRRAs, where (A) GO, (B) ACR, (C) MDA and (D) HNE.....	13
Fig. 2.2	Scheme for the fluorogenic derivatization reaction of the target aldehydes with 2,2'-fural and ammonium acetate.....	15
Fig. 2.3	Schematic diagram of the HPLC-FL system P ₁ : pump 1, P ₂ : pump 2, I: injector, ODS column: Cosmosil 5C ₁₈ -MS II column (250 mm × 4.6 mm, 5μm particle size), FLD: fluorescence detector, R: read out, buffer: citrate phosphate buffer (pH 5.0; 5.0 mM)	18
Fig. 2.4	Fluorescence spectra of MDA-2,2'-fural derivative and reagent blank. (A), (B): excitation and emission spectra of MDA-2,2'-fural derivative, respectively, (A'), (B)': excitation and emission spectra of reagent blank, respectively.	21

	Title	Page
Fig. 2.5	Representative chromatograms of (A) reagent blank, (B) standard mixture of the studied aldehydes (5 nmol/mL each), where: 1=GO, 2=ACR, 3=MDA, 4=HNE, * acrolein dimer.....	23
Fig. 2.6	Effect of 2,2'-fural concentration on the relative peak area of the studied aldehydes derivatives (5.0 nmol/mL)	24
Fig. 2.7	Effect of ammonium acetate concentration on the relative peak area of the studied aldehydes derivatives (5.0 nmol/mL)	25
Fig. 2.8	Effect of reaction temperature on the relative peak area of the studied aldehydes derivatives (5.0 nmol/mL)	25
Fig. 2.9	Effect of reaction time on the relative peak area of the studied aldehydes derivatives (5.0 nmol/mL)	26
Fig. 2.10	Chromatograms of (A) healthy human serum, (B) human serum spiked with a standard mixture of the studied aldehydes (5.0 nmol/mL each), (C) diabetic patient serum, and (D) rheumatoid arthritis patient serum; where peaks 1-4: as in Fig. 2.5.....	29
Fig. 3.1	Reaction pathway of the mass tagging of the target aliphatic aldehydes with PQ and ammonium acetate.....	38

	Title	Page
Fig. 3.2	Schematic diagram of the LC/ESI-MS/MS system P: pump, AI: auto injector, ODS column: Cosmosil 3C ₁₈ -AR II column (100 mm × 4.6 mm, 3μm particle size), MS/MS: triple quadrupole tandem mass spectrometry detector, R: read out.....	40
Fig. 3.3	Structures of the initially screened α,β -diketo reagents for the derivatization of the target aldehydes.....	43
Fig. 3.4	Product ion spectra of heptanal derivatives of PQ using (A) ESI ⁺ mode and (B) ESI ⁻ mode.....	45
Fig. 3.5	Product ion spectra of heptanal derivatives of <i>p</i> -anisil using (A) ESI ⁺ mode and (B) ESI ⁻ mode.....	46
Fig. 3.6	Product ion spectra of heptanal derivatives of benzil using (A) ESI ⁺ mode and (B) ESI ⁻ mode.....	47
Fig. 3.7	Product ion spectra of heptanal derivatives of DMAB using (A) ESI ⁺ mode and (B) ESI ⁻ mode.....	48
Fig. 3.8	Product ion spectra of heptanal derivatives of 2,2'-furil using (A) ESI ⁺ mode and (B) ESI ⁻ mode.....	49
Fig. 3.9	Product ion spectra of heptanal derivatives of PAD using (A) ESI ⁺ mode and (B) ESI ⁻ mode.....	50
Fig. 3.10	Product ion spectrum of heptanal derivative of 2,2'-pyridil using ESI ⁺ mode.....	51

	Title	Page
Fig. 3.11	Relative peak areas of heptanal derivatives of the studied reagents using ESI ⁺ and ESI ⁻ modes.....	52
Fig. 3.12	The MS/MS fragmentation pattern of the formed product from the reaction of target aldehydes and PQ.....	53
Fig. 3.13	Total ion spectra of (A) propanal derivative resulted from the reaction of propanal with PQ and ammonium acetate in presence of acetic acid and (B) reaction mixture of acetone with PQ and ammonium acetate in presence of acetic acid using ESI ⁺	55
Fig. 3.14	Effect of PQ concentration on the relative peak area of the studied aldehydes derivatives (50.0 nM)	56
Fig. 3.15	Effect of ammonium acetate concentration on the relative peak area of the studied aldehydes derivatives (50.0 nM)	57
Fig. 3.16	Effect of reaction temperature on the relative peak area of the studied aldehydes derivatives (50.0 nM)	57
Fig. 3.17	Effect of reaction time on the relative peak area of the studied aldehydes derivatives (50.0 nM)	58
Fig. 3.18	Product ion spectrum of PQ-IS derivative.....	59
Fig. 3.19	Recovery of the studied aldehydes from serum after protein PPT with methanol (10 or 20 folds dilution of serum), sub-zero temperature LLE, and salting-out LLE.....	64

	Title	Page
Fig. 3.20	Representative chromatograms of the target aliphatic aldehydes and IS in serum after derivatization with PQ where (A) propanal, (B) butanal, (C) pentanal, (D) hexanal, (E) heptanal, (F) octanal, (G) nonanal, (H) decanal and (I) IS (100 nM)	65
Fig. 4.1	Structures of HNE and HHE.....	69
Fig. 4.2	Reaction pathway of the target aldehydes with PQ and ¹⁴ N/ ¹⁵ N ammonium acetate.....	72
Fig. 4.3	Scheme of the quantification procedure based on ICD.....	76
Fig. 4.4	Product ion spectra of (A) HHE-PQ- ¹⁴ N and (B) HHE-PQ- ¹⁵ N derivatives.....	79
Fig. 4.5	Product ion spectra of (A) HNE-PQ- ¹⁴ N and (B) HNE-PQ- ¹⁵ N derivatives.....	80
Fig. 4.6	Effect of PQ concentration on the relative peak area of the studied aldehydes derivatives (100.0 nM)	81
Fig. 4.7	Effect of ammonium acetate concentration on the relative peak area of the studied aldehydes derivatives (100.0 nM)	82
Fig. 4.8	Effect of reaction temperature on the relative peak area of the studied aldehydes derivatives (100.0 nM)	82

	Title	Page
Fig. 4.9	Effect of reaction time on the relative peak area of the studied aldehydes derivatives (100.0 nM)	83
Fig. 4.10	Chromatogram of ¹⁴ N and ¹⁵ N labeled aldehydes for (A) HHE and (B) HNE; mass spectrum of the ion pair of ¹⁴ N and ¹⁵ N labeled aldehydes for (C) HHE and (D) HNE.....	85
Fig. 4.11	MS intensity ratios of ¹⁴ N and ¹⁵ N labeled HHE (A) and HNE (B) with the amount of 1:2, 1:1, and 2:1; and ion pairs of ¹⁴ N and ¹⁵ N labeled HHE (C) and HNE (D) in 1:10, 1:5, 1:2, 1:1, 2:1, 5:1 and 10:1 mixed solutions showed a good linear regression.....	86
Fig. 4.12	Recovery of the studied aldehydes from serum after PPT with methanol (MeOH) or acetonitrile (ACN), salting out LLE, subzero-temperature LLE, LLE with chloroform/MeOH mixture and SPE with HLB cartridge.....	89
Fig. 4.13	Effect of (A) salt type and (B) salt amount used during salting out LLE on the %recoveries of the target analytes.....	90
Fig. 4.14	Effect of the solvent used for salting-out LLE on the %recoveries of target analytes.....	91

	Title	Page
Fig. 4.15	Chromatograms of (A) healthy human serum, (B) diabetic patient serum, (C) rheumatoid arthritis patient serum, and (D) cardiac disorder patient serum; where peaks 1=HHE-PQ- ¹⁴ N, 2=HHE-PQ- ¹⁵ N, 3=HNE-PQ- ¹⁴ N, and 4=HNE-PQ- ¹⁵ N.....	94
Fig. 5.1	Suggested mechanism for benzaldehyde reaction with DAAQ..	103
Fig. 5.2	Schematic diagram of the used FIA system.....	105
Fig. 5.3	Fluorescence spectra of benzaldehyde-DAAQ (10.0 μM benzaldehyde and 8.0 mM DAAQ) derivative and reagent blank (8 mM DAAQ alone). (A), (B): excitation and emission spectra of benzaldehyde-DAAQ derivative, respectively, (A'), (B'): excitation and emission spectra of reagent blank, respectively.....	109
Fig. 5.4	Effect of DAAQ concentration on the fluorescence intensity of the reaction product with benzaldehyde (100 nmol/mL).....	110
Fig. 5.5	Effect of (A) type of catalyst and (B) acetic acid concentration (%) on the fluorescence intensity of DAAQ-benzaldehyde derivative.....	111
Fig. 5.6	Effect of the reaction temperature (°C) on the fluorescence intensity of DAAQ-benzaldehyde derivative.....	112

	Title	Page
Fig. 5.7	Effect of total flow rate of the carrier and fluorogenic reagent streams on the fluorescence intensity of DAAQ-benzaldehyde derivative.....	113
Fig. 5.8	Effect of reaction coil volume and flow rate on the fluorescence intensity of DAAQ-benzaldehyde derivative.....	114
Fig. 5.9	FIA signals for the determination of benzaldehyde spiked to the enzymatic reaction mixture. Concentrations of benzaldehyde are: (a) 0 nmol/mL (blank), (b) 0.2 nmol/mL, (c) 5 nmol/mL, (d) 20 nmol/mL, (e) 50 nmol/mL, (f) 80 nmol/mL, (g) 100 nmol/mL and (h) 150 nmol/mL.....	115
Fig. 5.10	Nonlinear fitting of Michaelis–Menten plot of SSAO activity versus benzylamine concentration in the enzymatic reaction mixture using GraphPad Prism trial version 6.05.....	116

Preface

This thesis is submitted for the partial fulfillment of the doctor degree of philosophy in pharmaceutical sciences. The research described here has been conducted under the Japanese Government (MEXT) Scholarship Program for the year 2012 and supervised by Professor Naotaka Kuroda in the Department of Analytical Chemistry for Pharmaceutics, Course of Pharmaceutical Sciences, Graduate School of Biomedical Sciences, Nagasaki University, Japan, in the period from October 2013 to September 2016.

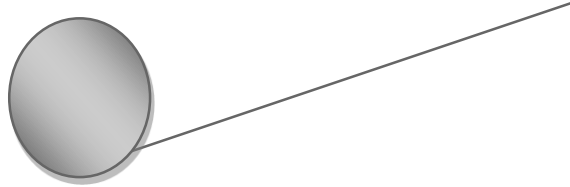
This thesis is based on research in the field of pharmaceutical analytical chemistry. The thesis is aimed at the development of new analytical methods for the determination of clinically important aldehydes and the activity of an aldehyde-producing enzyme in serum of healthy and diseased human subjects. The thesis comprises five chapters in 144 pages containing 21 Tables, 58 Figures and 162 references.

Japan, 2016

Mahmoud Hamed El-Maghrabey

Chapter I

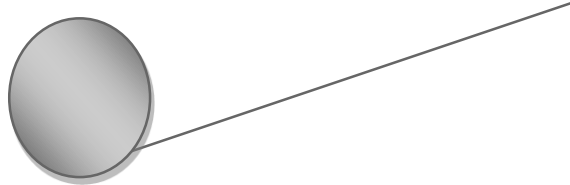
General introduction



Introduction

Aldehydes comprise a group of reactive compounds that are widespread naturally. They can be formed endogenously by lipid peroxidation, carbohydrate or ascorbate autoxidation, amineoxidases, cytochrome P_{450s}, or myeloperoxidase (MPO)-catalyzed metabolic activation. As well, aldehydes are very common components in many foods, usually in small amounts but sometimes they exist in large amounts. The most commonly distributed aldehydes in foods include acetaldehyde which is a natural component in many fruits and vegetables, cinnamaldehyde which is highly contained in cinnamon and peas, and benzaldehyde which exists in almonds and cherries. Also, anise and vanilla extracts contain anisaldehyde and salicylaldehyde, respectively. Aldehydes are also widely used as additives/preservatives in the cosmetics, detergents (*e.g.* benzaldehyde, cinnamaldehyde, anisaldehyde, vanillin, and C₇-C₁₃ aliphatic aldehydes) and food industries (*e.g.* benzaldehyde, 4-hydroxybenzaldehyde, salicylaldehyde, cinnamaldehyde, vanillin and furfural) ^{1,2}.

Aldehydes have also been identified in various matrices such as water, beverages and atmosphere. Also, some therapeutic drugs are aldehydes (*e.g.* josamycin, tylosin, spiramycin and streptomycin) or even produce reactive aldehyde metabolites which cause toxic side effects ¹. Two anticancer agents, cyclophosphamide and ifosfamide, are metabolized by cytochrome P_{450s} producing acrolein (ACR) and crotonaldehyde which resulted in hemorrhagic cystitis and neurotoxicity ³. Sudoxicam, a non-steroidal anti-inflammatory drug, is metabolized to glyoxal (GO), and it was withdrawn due to hepatotoxicity ¹. Also, the antiepileptic drug felbamate causes hepatotoxicity and aplastic anemia due to its major metabolite atropaldehyde ⁴. Misonidazole, anticancer drug, is



reduced by cytochrome P₄₅₀ reductase to DNA-adduct-forming GO⁵. In addition, the anti HIV drug abacavir gives a reactive aldehyde intermediate which is capable to covalently bind proteins⁶.

Aldehydes are relatively reactive organic compounds containing a polarized carbon-oxygen double bond. They have significant dipole moments due to the higher electronegativity of oxygen atom compared to carbon atom. The carbon atom constitutes an electrophilic site that reacts easily with nucleophiles. When α and β -carbons have a double bond “ α,β -unsaturated aldehyde e.g. ACR and crotonaldehyde”, the molecule becomes more reactive. Due to the conjugation with the carbonyl group, the β -carbon is positively polarized; hence it becomes a site for nucleophilic attack. This partial positive charge is affected by the presence of substituent. 4-Hydroxy group substituent (as in case of 4-hydroxy-2-nonenal (HNE) and 4-hydroxy-2-hexenal (HHE)) has an electron withdrawing effect imparting higher electrophilicity to the β -carbon^{2,7}.

In view of the fact that the main objective of this thesis is focused on the analysis of reactive aldehydes produced endogenously in human plasma, a brief discussion about the main sources of endogenous aldehydes and their influences on human body will be given in the following section.

1-1. Endogenous sources and harmful effects of aldehydes

1-1-1. Lipid peroxidation

Oxidants, including reactive oxygen species (ROS), are always produced in cells through normal metabolic processes. Oxidative stress occurs when the level of oxidants within the cell exceeds the levels of antioxidants⁸. The increased levels of intracellular oxidants lead to peroxidation of membrane-derived lipids. Such process forms many

products *via* a sequence of oxidation and cleavage reactions producing various types of peroxides (Fig. 1.1) ⁹⁻¹¹. The most significant products are aldehydes originated from ω -6 polyunsaturated fatty acids (PUFAs) (*e.g.* linoleic acid), including alkanals (*e.g.* pentanal and hexanal), 2-alkenals (*e.g.* ACR, crotonaldehyde, and trans-2-nonenal), dialdehydes (*e.g.* GO and malondialdehyde (MDA)), 4-hydroxy-2-alkenals (*e.g.* HNE), and 2,4-alkadienals (*e.g.* heptadienal and nonadienal) ^{9,10,12,13}.

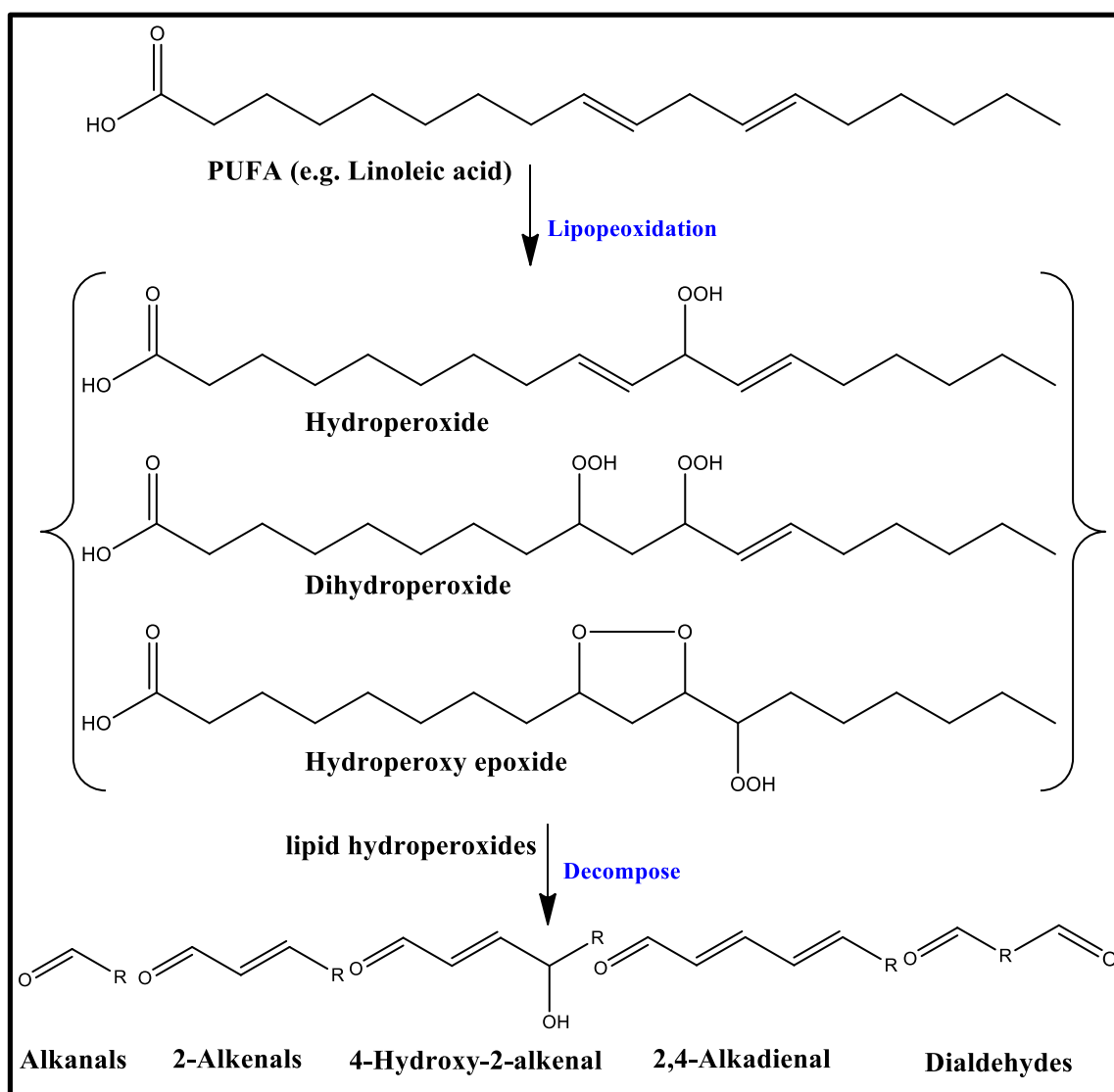


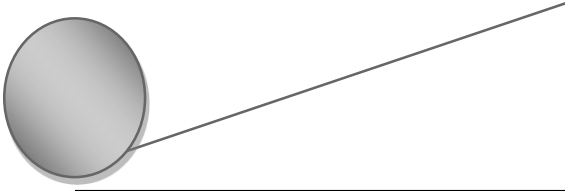
Fig. 1.1: Scheme for lipid peroxidation process showing structures of the proposed intermediates and the produced aldehydes

MDA is the most abundant aldehyde produced; constituting about 70% of the total aldehydes resulted from lipid peroxidation ¹⁰. Meanwhile, hexanal and HNE comprises 15 and 5% of total aldehydes, respectively ¹⁴. ACR was recently recognized as a product of lipid peroxidation process, but it has been long identified as an environmental contaminant ¹³.

The harmful effects of aldehydes includes disturbance of proteins and enzymes functions, formation of DNA adducts and further damage of lipids. High levels of aldehydes produced by lipid peroxidation are associated with many diseases; hence, they have been widely used as biomarkers of diseases progression. High levels of ACR has been detected in brains of patients with Alzheimer's disease ¹⁵, a study of Calingasan et al. ¹⁶ recommended the use of the levels of ACR-modified proteins as biomarkers of this disease. Additionally, high levels of HNE ¹⁷ and crotonaldehyde-protein adducts ¹⁸ have also been detected in brains of patients with Alzheimer's disease.

HNE is very reactive with proteins having the ability of Michael addition and Schiff base formation. Elevated levels of HNE-protein adducts have been detected in plasma of rat model of hypertension ¹⁹. In addition, the role of HNE in atherosclerosis has been confirmed by its high levels detected in fibrotic plaques and low density lipoproteins (LDL) ²⁰. Elevation of HNE level has also been detected in serum of diabetic patients ²¹.

MDA can react through Schiff base formation with free amino groups of proteins, DNA and lipids ²². Elevated levels of MDA and its adducts are associated with many diseases such as hepatitis ²³, cancer ²⁴, neurodegenerative diseases ²⁵ and diabetes mellitus ²⁶.

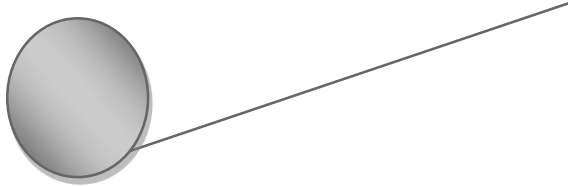


A significant increase in the levels of HNE and ACR has been detected in plasma of rheumatoid arthritis patients (2-folds increase relative to healthy control group), while HHE, MDA, 4-oxo-2-nonenal and crotonaldehyde showed about 66, 42, 41 and 18% increase, respectively²⁷. The role of HNE and MDA in the pathogenesis of cardiovascular diseases such as atherosclerosis has also been established *via* immunohistochemical analyses of atherosclerotic lesions from human aorta using antibodies against aldehydes adducts *e.g.* HNE-histidine, MDA-lysine. Strong positive results were detected in cells and primarily macrophages²⁸.

Dicarbonyls “oxoaldehydes”, such as GO, are of a significant concern due to their ability to covalently cross-link proteins due to formation of Amadori intermediate products and advanced glycation end-products (AGEs). Protein cross-linking has been found to be associated with pathophysiologies of aging and the long-term complications of diabetes and atherosclerosis¹. The plasma levels of GO and its advanced lipid peroxidation end-products are increased by more than three to four folds in diabetic and renal failure patients relative to healthy subjects²⁹.

1-1-2. Carbohydrate or ascorbate autoxidation

GO, unlike methylglyoxal, is a main degradation product of lipid peroxidation. It is also a main DNA oxidative degradation product resulted from the oxidation of deoxyribose C₄/C₅' carbons by ROS leading to breaking of DNA strand. Consequently, GO could form adducts with DNA guanine. GO is the only dicarbonyl produced in glucose autoxidation by cleavage of C₂-C₃ bond of glucosone or other intermediates¹. Dicarbonyls produced during fructosyl-lysine autoxidation were GO > 3-deoxyglucosone > methylglyoxal³⁰. Ascorbate autoxidation has also a role in age-induced



cataractogenesis, which is associated with glycation of proteins by oxidized catabolites of ascorbate in the lens ³¹.

GO is also produced through transition metal-catalyzed autoxidation of the enediol tautomer of glycolaldehyde ³². Another dicarbonyl, hydroxypyruvaldehyde, is formed by the autoxidation of glyceraldehyde or dihydroxyacetone ³³. These dicarbonyls are the most reactive carbonyls. At low concentration levels (micromolar concentrations) they could form cross-link and glycate proteins and inactivate enzymes. On the other hand, glucose needs high concentration (about 20 mM) and very long autoxidation times to produce protein carbonylation and enzyme inactivation ³⁴.

1-1-3. Carbohydrate metabolism

Methylglyoxal, contrast to GO, is produced enzymatically from triose phosphate intermediates, *i.e.* glyceraldehyde 3-phosphate and dihydroxyacetone phosphate, formed in the glycolic metabolism of glucose or from threonine and ketone bodies metabolism. It has also been evidenced that triose phosphate formation by the pentose phosphate pathway contributes to the production of methylglyoxal from xylitol, ribose, and deoxyribose, which are more efficient than glucose. The rate of methylglyoxal endogenous production has been anticipated to be about 120 $\mu\text{mol/day}$ ³⁵.

1-1-4. Amine oxidases-catalyzed metabolic activation

Monoamine oxidase (MAO) and polyamine oxidase (PAO) are FAD-dependent oxidases. MAO exists in the outer membrane of mitochondria and it is inhibited by pargyline, clorgyline, quinacrine, or deprenyl, while PAO exists in the cytosol and peroxisomes and it is inhibited by quinacrine. MAO presents in two forms, MAO-A (*e.g.* serotonin substrate) and MAO-B (*e.g.* phenethylamine and dopamine substrates). MAO

acts by catalyzing the deamination of amines, such as tyramine and tryptamine forming hydrogen peroxide, ammonia and the corresponding aldehydes (Fig. 1.2). Both of ammonia and phenylacetaldehyde are detoxified by mitochondria. As well, MAO-catalyzed metabolism of the neurotransmitter gamma-aminobutyric acid produces succinic semialdehyde¹.

PAO acts on diamine or polyamine substrates (*e.g.* spermine, acetylspermine and diacetylspermine) producing hydrogen peroxide but without ammonia. Oxidation of spermine by PAO forms spermidine and 3-aminopropanal. 3-Aminopropanal is a strong lysomotropic neurotoxin, additionally it spontaneously forms ACR. Both of 3-aminopropanal and ACR are the most cytotoxic products in brain injury³⁶.

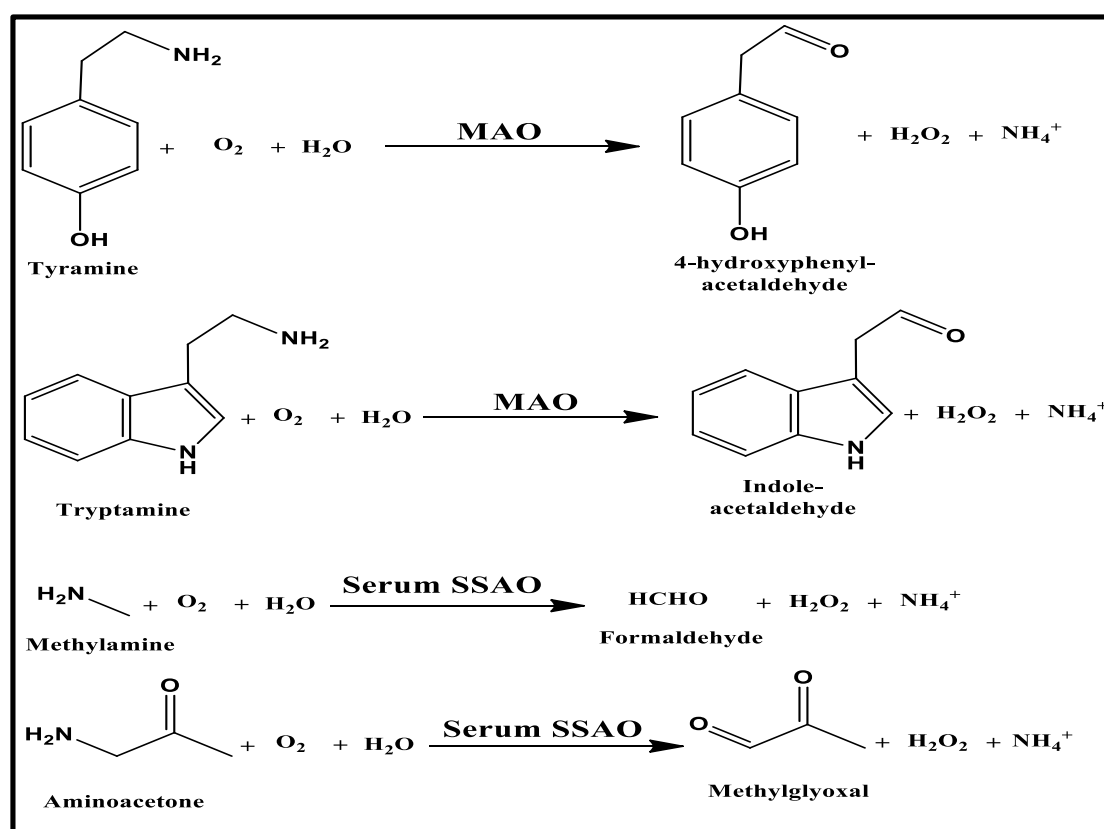
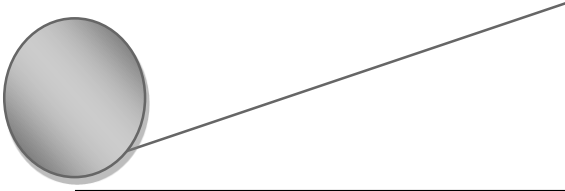


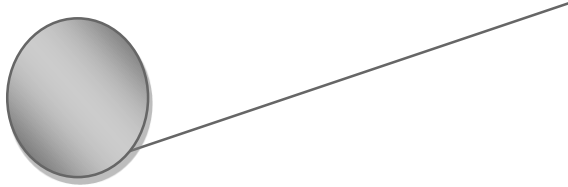
Fig. 1.2: Formation of 4-hydroxyphenylacetaldehyde and indoleacetaldehyde by MAO and formation of formaldehyde and methylglyoxal by serum SSAO



The copper-dependent amine oxidases (semicarbazide-sensitive amine oxidase, SSAO) including serum amine oxidase (serum SSAO) and tissue diamine oxidase (tissue DAO) are inhibited by copper chelating agents like semicarbazide and aminoguanidine. DAO is generally located in kidney and intestinal mucosa, but it is also stimulated by putrescine or injury in the heart, liver and brain. Serum SSAO presents in the vascular system as soluble or membrane forms, for example in the kidney cells, cardiovascular smooth muscles and cartilage. Serum SSAO and DAO act by detoxification of xenobiotic amines, but they generate toxic aldehydes, hydrogen peroxide and ammonia, which contribute to the vascular damage and advanced protein aggregation found in vascular disorders, such as diabetic complications, atherosclerosis, Alzheimer's disease and aging¹.

DAO uses the diamines putrescine, cadaverine and spermine, and generates aminoaldehydes. ACR is produced from spermidine while 3-aminopropanal/MDA is produced from 1,3-propanediamine. On the other hand, MAO catalyzes the oxidative deamination of spermine, spermidine, or the industrial chemical allylamine in the plasma producing the highly toxic ACR³⁷. As well, formaldehyde is also produced by the action of serum SSAO on methylamine (Fig. 1.2) which is a metabolite of epinephrine, sarcosine and creatinine, and a gut bacterial product. Also, serum SSAO uses aminoacetone, a decarboxylation product produced by the metabolism of threonine, to produce methylglyoxal (Fig. 1.2)¹.

The ACR produced by serum SSAO in the coronary artery was thought to be linked to the coronary artery contraction causing myocardial necrosis that is induced by allylamine³⁸. Increased levels of serum SSAO and methylglyoxal were also detected in uncontrolled cases of diabetes. It has also been suggested that increased levels of



methylglyoxal and formaldehyde produced by serum SSAO from aminoacetone and methylamine, respectively, resulted in cross-linking of proteins of vascular endothelial cells and cell injury associated with diabetic atherosclerosis ³⁹. High levels of serum SSAO is also increased in patients with congestive heart failure. Amine oxidase inhibitors generally stop the cytotoxicity of polyamine oxidation products. Currently, aminoguanidine is the only DAO and serum SSAO inhibitor used in the clinic ¹.

1-1-5. Cytochrome P₄₅₀-catalyzed metabolic activation

Cytochrome P₄₅₀ catalyzes the oxidation of alcohols such as glycerol, ethylene glycol, 1,2-propane diols, or polyhydroxylated alcohols containing vicinal diols forming aldehydes with one less carbon atom than the initial alcohol substrates ^{40,41}. CYP2E1 catalyzes the endogenous formation of methylglyoxal from ketone bodies. Acetone is hydroxylated to hydroxyacetone (acetol) which is in turn hydroxylated to methylglyoxal ⁴².

1-1-6. Myeloperoxidase-catalyzed metabolic activation

Plasma contains MPO and hydrogen peroxide (generated from activated neutrophils at locations of inflammation), in addition to chloride (0.1 M) and α -amino acids (4–5 mM). The oxidation of protein arginine, lysine or proline catalyzed by MPO/hydrogen peroxide by radical mechanism produces semialdehydes. Where, the oxidation of alanine, valine, and serine resulted in the formation of formaldehyde ⁴³. The intermediate chloramines during the MPO/hydrogen peroxide/Cl⁻ or HOCl-catalyzed oxidation of threonine give ACR and 2-hydroxypropanal as main products. Meanwhile, glycolaldehyde was produced as a main product from serine *via* intermediate chloramines (Fig. 1.3) ⁴⁴.

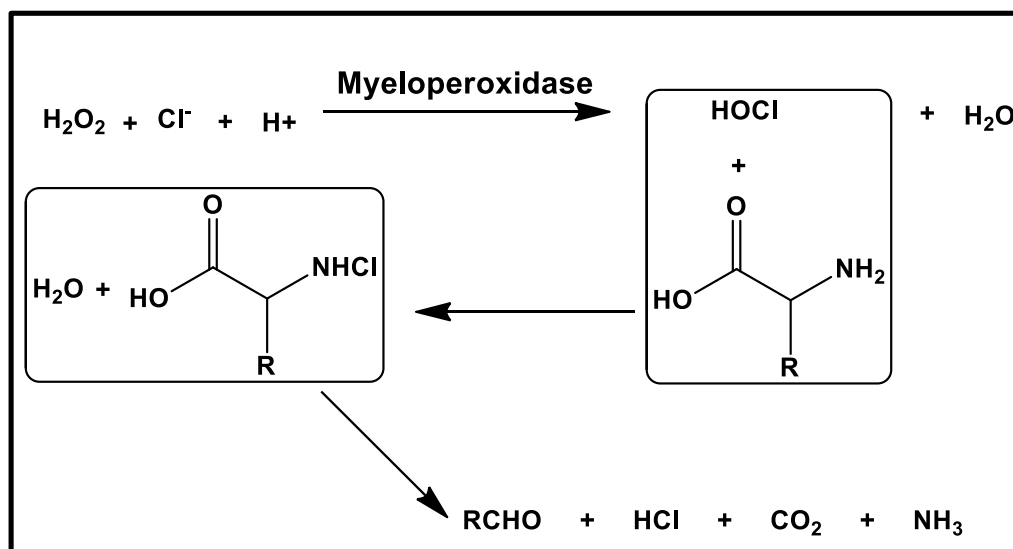
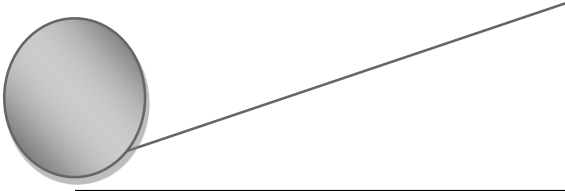


Fig. 1.3: Formation of aldehydes *via* MPO-catalyzed metabolic activation

The formation of these aldehydes in the blood vessels probably resulted in the propagation of diabetic vascular disease. The aldehydes yield is expected to be greater than that was found due their autoxidation by peroxidases. This is important from toxicology point of view, because the electronically excited carbonyl intermediates and hydroperoxy-aldehyde intermediates produced by peroxidases from some aldehydes are reactive DNA oxidants ⁴⁵.

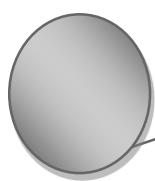
1-2. Challenges in analytical determination of aldehydes

Quantification of aldehydes in biological fluids at trace and ultra-trace levels is one of the most difficult experimental procedures representing a challenge to analytical chemists for many reasons. First, aldehydes are small molecules and most of them are very hydrophilic in nature. So, their retention at common liquid chromatography (LC) columns is difficult. Second, the aliphatic aldehydes exhibit very weak ultraviolet (UV) absorbance making their detection at UV detector very difficult. Although, α,β -unsaturated aldehydes have the advantage of presence of a chromophoric group and



subsequent possibility of UV detection at 220 nm, a limitation for application of this technique to *in vivo* determination of these aldehydes is still existing due to the lack of sensitivity and precision. Thirdly, the high polarity of aldehydes represents a main problem for detection by mass spectrometry (MS) due to their poor ionization and fragmentation properties⁴⁶. A fourth problem associated with the analytical determination of aldehydes is their high reactivity enabling them to form adducts with endogenous biomolecules such as DNA and proteins. Hence, it is very difficult to recover them from biological matrices owing to high water solubility¹¹. Fifth, the poor stability of aldehydes is of a great concern. When extracted from urine, aldehydes suffer from degradation to aliphatic carboxylic acids⁴⁷. In addition, the volatile nature of aldehydes represents a sixth limitation for their analytical determination¹¹.

In all these analytical challenges, the concept of derivatization can play a very important role. Derivatization decreases the polarity of aldehydes and improves their retention and chromatographic behavior on LC columns. Also, it enables the detection of aldehydes at UV, fluorescence (FL) and chemiluminescence (CL) detectors. As well, derivatization improves the MS detectability of aldehydes by enhancing their ionization efficiency and fragmentation properties. Additional advantages gained by derivatization are increasing the stability of aldehydes, improvement of their separation from matrix components and improvement of their chromatographic separation⁴⁷. The choice of the derivatizing agent, the analytical method and the extraction procedure play a very important role for selective and sensitive determination of aldehydes



1-3. Aim of the thesis

Due to the clinical importance of *in vivo* measuring of aldehydes, imparted from their significance as key parameters for monitoring lipid peroxidation, AGEs and activity of amine oxidases, in this study our main goal is to develop highly sensitive, selective and reliable analytical methods for trace analysis of some clinically important aldehydes in human serum. We also aimed at using these methods to monitor the differences between the levels of these aldehydes in the serum of healthy and diseased human subjects. The planned analytical strategy to achieve these goals is to apply the condensation reaction of aldehydes with α,β -diketo compounds in presence of ammonium acetate forming imidazole derivatives which could be detected by FL or MS detection. These methods will help to provide information about the relationship between the levels of these aldehydes and the onset of different diseases. Also, we aim at developing an analytical method capable of monitoring serum SSAO activity *via* measuring the aldehyde formed after introduction of exogenous amine substrate to a biological matrix containing the enzyme. Thus we can determine the alteration in the activity of the enzyme at different clinical conditions. For this purpose, we intend to use the acid-catalyzed condensation reaction of α,β -diamino compound with aldehyde forming highly fluorescent imidazole derivative.

Chapter II

Analytical method for lipoperoxidation relevant reactive aldehydes in human sera by high-performance liquid chromatography-fluorescence detection

Mahmoud H. El-Maghrabey, Naoya Kishikawa, Kaname

Ohyama, Naotaka Kuroda, Analytical Biochemistry 464

(2014) 36–42. DOI: 10.1016/j.ab.2014.07.002.

2-1. Introduction

Among the carbonyl compounds produced as a result of lipid peroxidation, alkanals are the least reactive. Alkenals containing unsaturated bond, such as ACR, are usually an order of magnitude more reactive than the alkanals. 4-Hydroxy-2-alkenals, such as HNE, are extremely reactive due to increased reactivity of the α,β -unsaturated bond by the close proximity of the electron withdrawing hydroxyl at C₄ and the C₁-carbonyl group. The di-aldehydes, such as GO and MDA, are also very reactive since the two aldehydic moieties can form Schiff bases with amino acids⁸. In consequence, these four lipoperoxidation relevant reactive aldehydes (LPRRAs); GO, ACR, MDA and HNE (Fig. 2.1) are considered the most reactive and harmful, and could be used as good biomarkers of oxidative damage and disease progression²⁸. So there is a strong need for a method that could simultaneously determine these LPRRAs to investigate their patterns in healthy and diseased conditions.

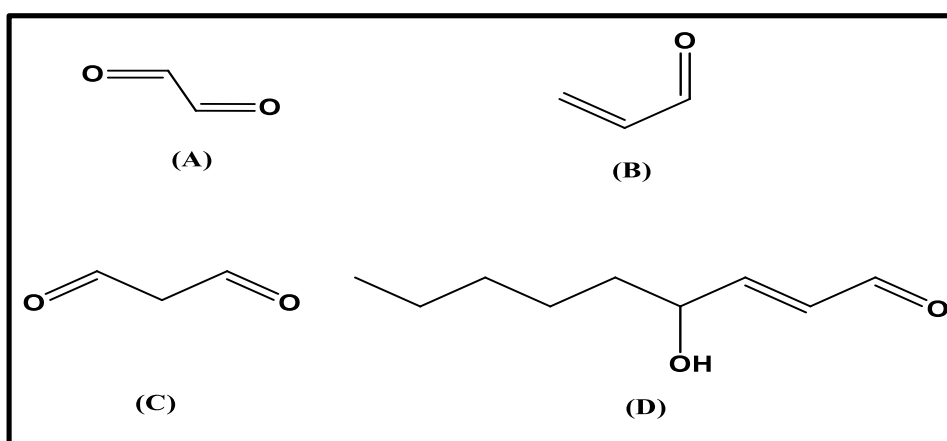
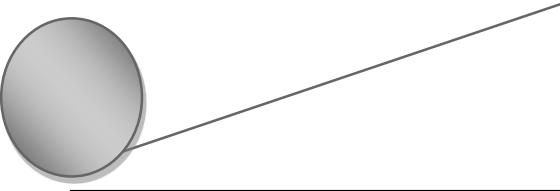


Fig. 2.1: Structures of the studied LPRRAs, where (A) GO, (B) ACR, (C) MDA and (D) HNE



Levels of these LPRRAs have been determined in different matrices either individually or in combination with each other or with other carbonyl compounds as has been reviewed by Shibamoto ¹¹. Some methods were recently published for determination of GO such as gas chromatography-MS (GC-MS) ⁴⁸, GC-flame ionization detection ⁴⁹ and High performance liquid chromatography (HPLC)-FL following derivatization with 5,6-diamino-2,4-hydroxypyrimidine sulfate ⁵⁰ or 4-methoxy-*o*-phenylenediamine ⁵¹. ACR has also been determined by HPLC-FL after derivatization with luminarin ⁵², 3-aminophenol ⁵³, or 1,2-diamino-4,5-dimethoxybenzene ⁵⁴, and by HPLC-peroxyoxalate CL after fluorescence labeling with 4-(*N,N*-dimethylaminosulfonyl)-7-hydrazino-2,1,3-benzoxadiazole (DBD-H) ⁵⁵. MDA has been determined by LC and GC methods ⁵⁶, HPLC-CL using potassium permanganate/formaldehyde system ⁵⁷, capillary electrophoresis-FL after derivatization with thiobarbituric acid ⁵⁸ and surface-enhanced Raman spectroscopy after derivatization with thiobarbituric acid ⁵⁹. As for HNE, HPLC-UV detection based on derivatization with 2,4-dinitrophenylhydrazine (DNPH) ⁶⁰, HPLC-FL after derivatization with DBD-H ⁶¹ and GC-electron capture detection ⁶² have been reported for its determination.

Only one GC method with nitrogen phosphorous detection was developed for the simultaneous determination of ACR, MDA and HNE in lipids following derivatization with *N*-methylhydrazine ⁶³. A LC-MS method was reported for the simultaneous determination of several classes of aldehydes including ACR, MDA and HNE in exhaled breath condensate after derivatization with DNPH ⁶⁴. These methods involved the use of expensive instrumentation that are not available in many laboratories and were only applied to either lipids ⁶³ or exhaled breath condensate ⁶⁴. This initiates the present study

to develop and validate a new analytical method for the simultaneous determination of LPRRAs in human serum and estimation of their pattern in diseased conditions.

1,2-Di(2-furyl)-1,2-ethanedione (2,2'-furyl) is an α,β -diketo compound that has been used in our laboratory as a new fluorogenic derivatization reagent for determination of a number of saturated aliphatic aldehydes in human serum⁶⁵. 2,2'-Furyl reacts with aldehydes in the presence of ammonium acetate forming highly fluorescent imidazole derivatives (Fig.2.2). The selectivity, sensitivity, and superiority of 2,2'-furyl over other reported aldehydes-derivatizing reagents⁶⁵ encouraged us to use it for pre-column derivatization of the four LPRRAs (GO, ACR, MDA and HNE) prior to HPLC-FL. We aim at applying the proposed method for the determination and comparison of the patterns of these LPRRAs in sera of healthy human subjects, diabetes mellitus and rheumatoid arthritis patients.

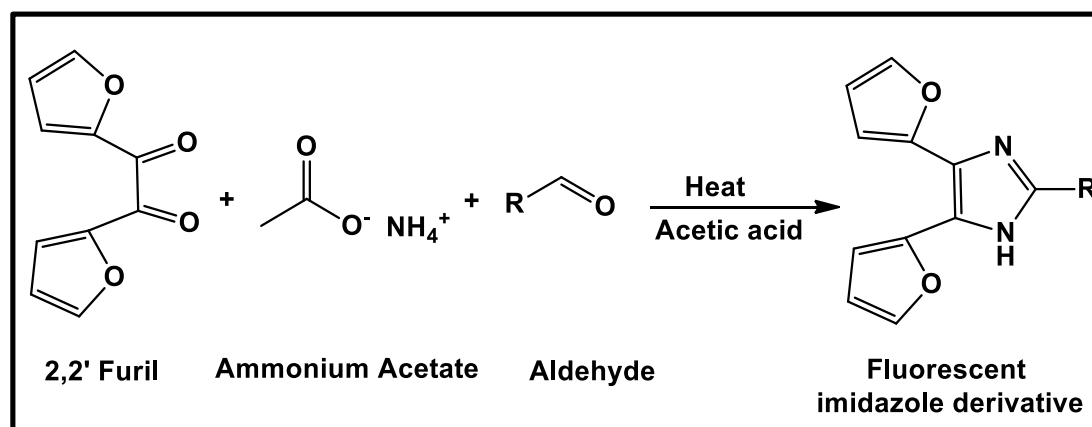


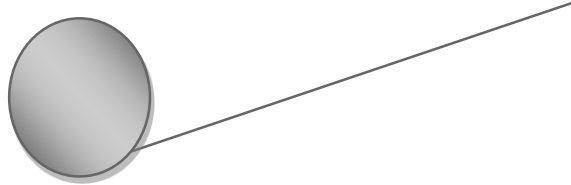
Fig. 2.2: Scheme for the fluorogenic derivatization reaction of the target aldehydes with 2,2'-furyl and ammonium acetate.

2-2. Experimental

2-2-1. Materials and reagents

All reagents were of analytical grade and used as received. ACR monomer (90%, w/v) and 2,2'-furil were obtained from Tokyo Chemical Industries (Tokyo, Japan). GO (40%, w/v) and MDA tetrabutylammonium salt (96%, w/w) were supplied from Sigma Aldrich (St. Louis, MO, USA). HNE (1%, w/v) was purchased from Cayman Chemical Company (Ann Arbor, MI, USA). Ammonium acetate, citric acid monohydrate and phosphate buffer saline (PBS) powder were purchased from Wako Pure Chemical Industries (Osaka, Japan). Methanol (HPLC grade) was obtained from Kanto Chemical Company (Tokyo). Glacial acetic acid and di-sodium hydrogen phosphate dodecahydrate were purchased from Nacalai Tesque (Kyoto, Japan). The used water was purified by a Simpli Lab UV (Millipore, Bedford, MA, USA).

Stock solutions of GO, ACR, MDA and HNE (5.0 mM) were separately prepared in methanol. A mixed standard solution containing the four aldehydes (200.0 μ M of each aldehyde) was prepared by diluting the stock solutions with methanol then diluted with the same solvent as needed to obtain the required concentrations. 8.0 mM 2,2'-Furil and 3.0 M ammonium acetate were prepared in methanol and glacial acetic acid, respectively. 0.01 M PBS was prepared in water. All solutions were kept in the refrigerator at 4 °C except for the HNE stock solution and the mixed standard solution containing the four aldehydes were kept at -80 °C.



2-2-2. Instrumentations and chromatographic conditions

The HPLC system (Fig. 2.3) consisted of two Shimadzu LC-20AD pumps (Kyoto), a Rheodyne injector (Cotati, CA, USA) with a 20 μ L sample loop, a Cosmosil 5C₁₈-MS II column (250 mm \times 4.6 mm i.d., 5 μ m particle size) from Nacalai Tesque, a Shimadzu RF-20AXS fluorescence detector and an EZ Chrom Elite chromatography data acquisition system (Scientific software, Pleasanton, CA, USA). Analysis was performed at ambient temperature. Gradient elution was performed using two mobile phases; A: methanol-citrate phosphate buffer (5.0 mM; pH 5.0) (48:52, v/v %) and B: methanol-citrate phosphate buffer (5.0 mM; pH 5.0) (80:20, v/v %) were pumped at a flow rate of 1.0 mL/min in the following gradient elution mode: 0% B (0-22.0 min), 0% B to 100% B linearly (22.0-32.0 min) and 100% B (32.0-40.0 min). The fluorescence detector wavelengths were set at 355 nm for emission and 250 nm for excitation.

The fluorescence spectra were recorded on a Shimadzu RF-1500 spectrofluorophotometer. Horiba F22 pH-meter was used to adjust the pH of the buffer. The samples were centrifuged using Himac CR 15 refrigerated centrifuge (Hitachi Koki Co., Ltd., Tokyo). Yamato HF-41 heating block (Tokyo) was used in the derivatization process. The solutions were evaporated in Eyela CVE-3100 solvent centrifugal evaporator (Tokyo Rikakikai Co., Ltd., Tokyo).

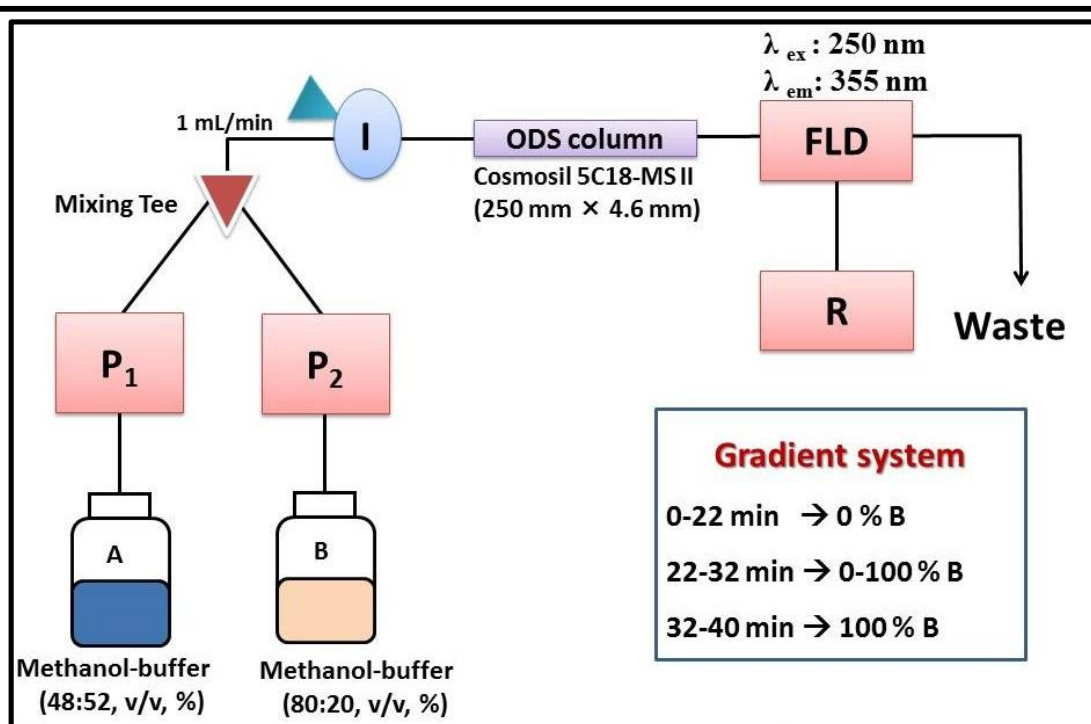
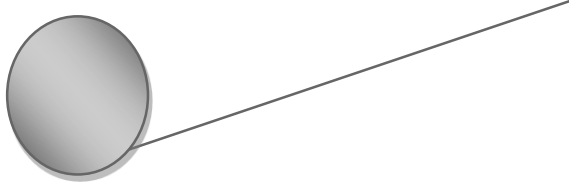


Fig. 2.3: Schematic diagram of the HPLC-FL system

P₁: pump 1, P₂: pump 2, I: injector, ODS column: Cosmosil 5C₁₈-MS II column (250 mm × 4.6 mm i.d., 5 μm particle size), FLD: fluorescence detector, R: read out, buffer: citrate phosphate buffer (pH 5.0; 5.0 mM)

2-2-3. Clinical samples

The present experiments were approved by the Ethics Committee of the School of Pharmaceutical Sciences, Nagasaki University, Japan, and performed in accordance with the established guidelines. Serum samples from 6 diabetic patients (2 females and 4 males; mean age 53.2±10.7) and 6 rheumatoid arthritis patients (3 females and 3 males; mean age 56.7±15.3) in addition to a control group of 6 healthy subjects (2 females and 4 males; mean age 52.0±7.5) were supplied by Sasebo Chuo Hospital (Nagasaki, Japan) and stored at -80 °C until analyzed.



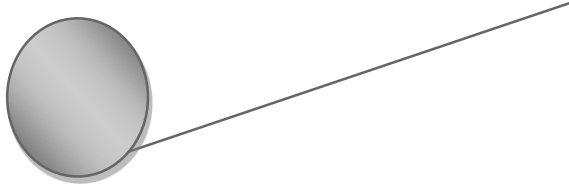
2-2-4. Assay procedure for LPRRAs in human serum

To 50 μL of human serum, spiked with the targeted aldehydes, 950 μL of methanol was added to denature proteins. The mixture was mixed for 30 seconds then centrifuged at $2200\times g$ for 5 min at 4°C . A 500 μL portion of the supernatant was transferred to a screw-capped vial followed by 400 μL of 8.0 mM 2,2'-fural and 150 μL of 3.0 M ammonium acetate. The mixture was heated at 90°C for 30 min then cooled. The solution was evaporated and the residue was reconstituted with 100 μL of the mobile phase then mixed for 1 min and filtered through 0.45 μm cellulose acetate membrane filter. An aliquot of 20 μL was injected into the HPLC system. Blank experiment and analysis of pattern of aldehydes in healthy and diseased human subjects were carried out using unspiked serum. For preparation of reagent blank and standard mixture chromatograms, the previous procedure was adopted with replacing serum with 50 μL of PBS.

2-2-5. Validation procedure

Validation of the proposed method was performed following U.S. Guidance for Industry on Bioanalytical Method Validation (Food and Drug Administration, FDA) ⁶⁶. Calibration curves for the four LPRRAs were constructed in human serum using six concentrations for each aldehyde. The limits of detection (LOD) were calculated as the concentrations with a signal-to-noise ratio (S/N) of 3.

Accuracy of the proposed method was evaluated by the closeness of the mean test results obtained by the proposed method to the true concentration of the analytes. Serum samples spiked with a standard mixture of aldehydes at three different concentrations were analyzed for the assessment of accuracy. Percentage recoveries were expressed as follows:



% Recovery = [(amount found/amount spiked) x100].

To evaluate the intra- and inter-day precision of the proposed method; five replicates of three sets of human serum samples spiked with standard mixture of LPRRAs at three concentration levels were analyzed on five successive times within the same day and on five successive days, respectively.

2-2-6. Statistical analysis

The data are presented as mean \pm standard error (SE) for the number of experiments. In order to compare the levels of the four targeted aldehydes in the three studied groups (healthy subjects, diabetic, and rheumatoid arthritis patients), Kobayashi decision tree⁶⁷ was employed. Bartlett's test was used as a test for the equality of k variances. It was found that the k sampled populations have unequal variances and Steel's Dwass test for comparing all pairs was used⁶⁷. All the statistical tests were two-sided at a significant level of $\alpha=0.05$.

2-3. Results and discussion

2-3-1. Fluorescence characteristics of the products

2,2'-Furil has been proven as a selective reagent for aldehydes. Also it is stable and safe compared to other fluorescence derivatizing agents such as hydrazine reagents⁶⁵. 2,2'-Furil reacts with the target aldehydes in the presence of ammonium acetate in glacial acetic acid at 90°C converting them to highly fluorescent difurylimidazole derivatives (Fig. 2.2). The formed derivatives exhibited high fluorescence intensity at 355 nm after excitation at 250 nm (Fig. 2.4). Both 2,2'-furil and ammonium acetate exhibit no native fluorescence, however fluorescence was observed in the blank free from aldehydes. This is probably due to incorporation of short chain

aliphatic aldehydes from the reagents, solvents or from the air ⁶⁸. Additionally, 2,2'-furyl was reported to react with ammonium acetate in the presence of glacial acetic acid, in the absence of any aldehydes, producing trifurylimidazole fluorescent product ⁶⁹.

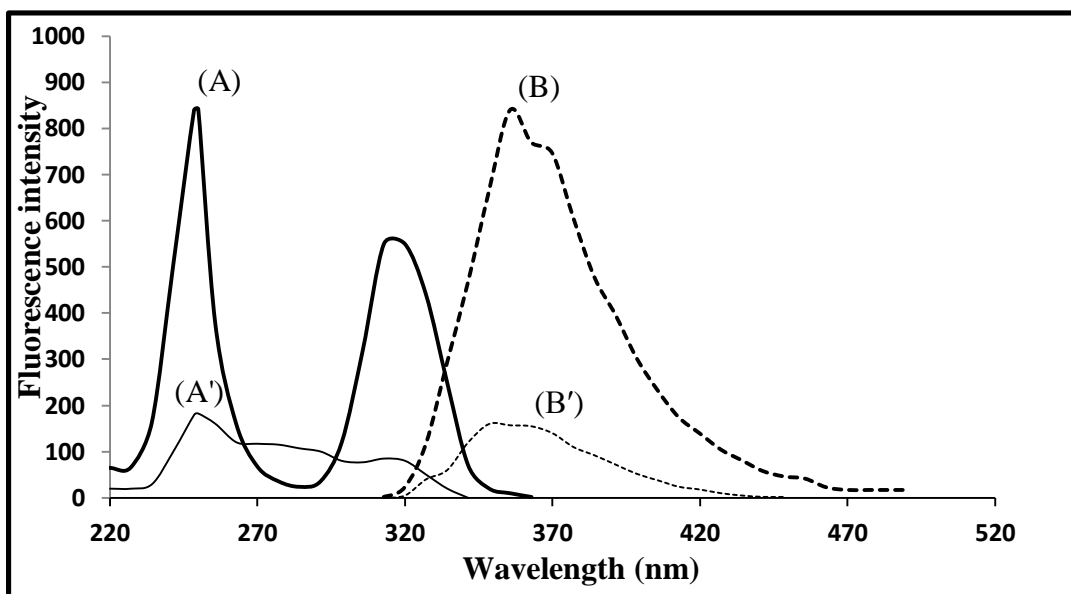
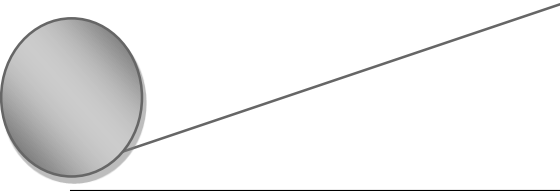


Fig. 2.4: Fluorescence spectra of MDA-2,2'-furyl derivative and reagent blank, where; (A), (B): excitation and emission spectra of MDA-2,2'-furyl derivative, respectively, (A'), (B'): excitation and emission spectra of reagent blank, respectively.

2-3-2. Optimization of chromatographic conditions

Initially, isocratic separation of the four analytes was investigated. We first used an isocratic HPLC system to separate the four aldehydes' derivatives but this was not possible due to the different natures of the analytes since GO, ACR and MDA are hydrophilic (C₂, C₂ and C₃ aldehydes, respectively) while, HNE is lipophilic (C₉ aldehyde). Using a mobile phase consisting of methanol-citrate phosphate buffer (5mM; pH 5.0) (48:52, v/v %), the derivatives of GO, ACR and MDA were well separated, but no peak for HNE derivative appeared up to 2 h. Increasing the ratio of methanol in the mobile phase resulted in co-elution of GO, ACR and MDA. Hence, a gradient elution



mode was adopted for separation of the analytes within a reasonable time. Two mobile phases; A: methanol-citrate phosphate buffer (5 mM; pH 5.0) (48:52, v/v) and B: methanol-citrate phosphate buffer (5mM; pH 5.0) (80:20, v/v %) were pumped at a flow rate of 1.0 mL/min in the gradient elution mode mentioned earlier (section 2-2-2.).

The influence of pH of the mobile phase on the separation of the four derivatives was studied using buffer solutions of different pH values (3.2-7.0). pH 5.0 was found to be the optimum for best peak symmetry and resolution, at pH values higher than 5.0, peak broadening was observed specially for ACR peak, meanwhile at pH values less than 5.0 the resolution decreased and complete overlapping between the peaks of GO, ACR and MDA occurred at pH 4.0. The influence of ionic strength of buffer was also investigated over the range of 2.5-10.0 mM and it was found to exhibit a negligible effect on the resolution, shape and symmetry of the peaks. 5.0 mM buffer was used in this study.

Different columns including monomeric Cosmosil 5C₁₈-MS II (250 mm × 4.6 mm i.d., 5µm particle size), polymeric Cosmosil 5C₁₈-AR II (250 mm × 4.6 mm i.d., 5µm particle size) and Cosmosil 5C₈-MS (150 mm × 4.6 mm i.d., 5µm particle size) were also tested. The optimum separation was accomplished on a Cosmosil 5C₁₈-MS II column (250 mm × 4.6 mm i.d., 5µm particle size).

Typical chromatograms for a standard mixture of the four LPRRAs derivatives and reagent blank are shown in Fig. 2.5. Baseline resolution of the four LPRRAs derivatives was achieved with the retention times (t_R) of 3.1, 8.0, 19.8 and 36.9 min for GO, ACR, MDA and HNE, respectively and a total chromatographic run was completed with less than 40 min.

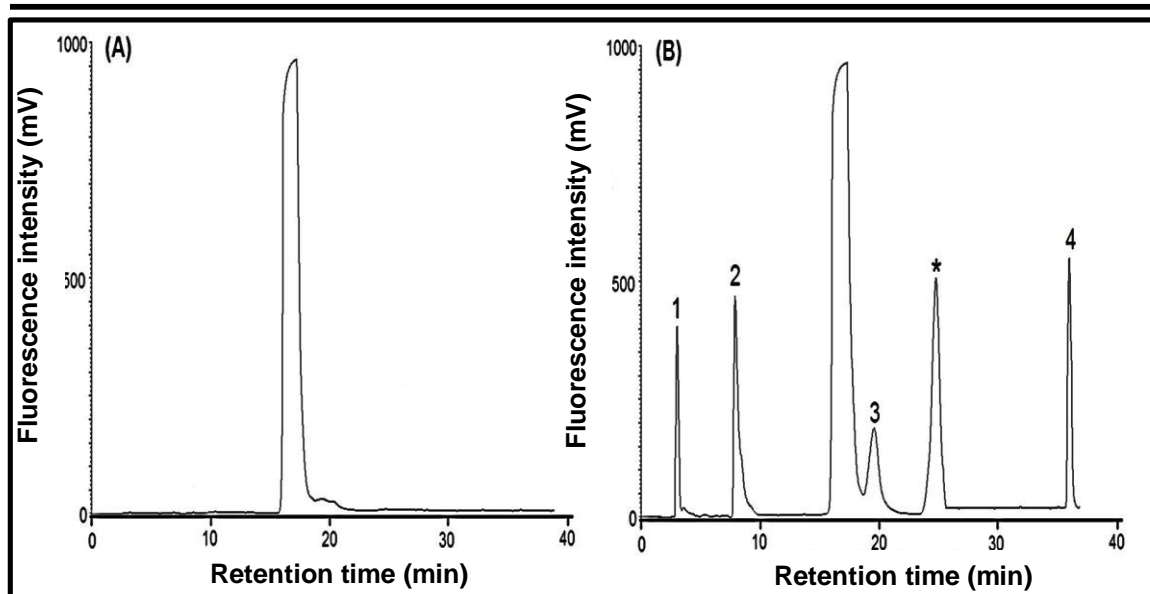


Fig. 2.5: Representative chromatograms of (A) reagent blank, (B) standard mixture of the studied aldehydes (5 nmol/mL each), where: 1=GO, 2=ACR, 3=MDA, 4=HNE, * acrolein dimer.

A blank peak was observed in all chromatograms, this might be attributed to the presence of short chain aliphatic aldehydes as impurities⁶⁸ or from the reaction of 2,2'-fural with ammonium acetate in the presence of glacial acetic acid as we discussed earlier⁶⁹. Meanwhile, when injecting ACR following derivatization, two peaks were observed at t_R of 8.0 and 24.8 min. This might be attributed to the presence of ACR dimer as an impurity in the standard solution⁷⁰ which reacts with 2,2'-fural giving a fluorescent derivative at t_R of 24.8 min. Nevertheless, this peak did not interfere with the peaks of the target analytes proving selectivity of the proposed method.

2-3-3. Optimization of derivatization conditions

In order to obtain the highest sensitivities, derivatization conditions including reagent concentrations, heating temperature and time were optimized using a standard

mixture of the four LPRRAs (5.0 nmol/mL each) spiked to human serum. The influence of 2,2'-fural concentration was investigated over the range of 0.4-12.0 mM, where increasing the concentration of the reagent produced a corresponding increase in the peak areas of the formed derivatives with maximum response obtained using 8.0 mM (Fig. 2.6).

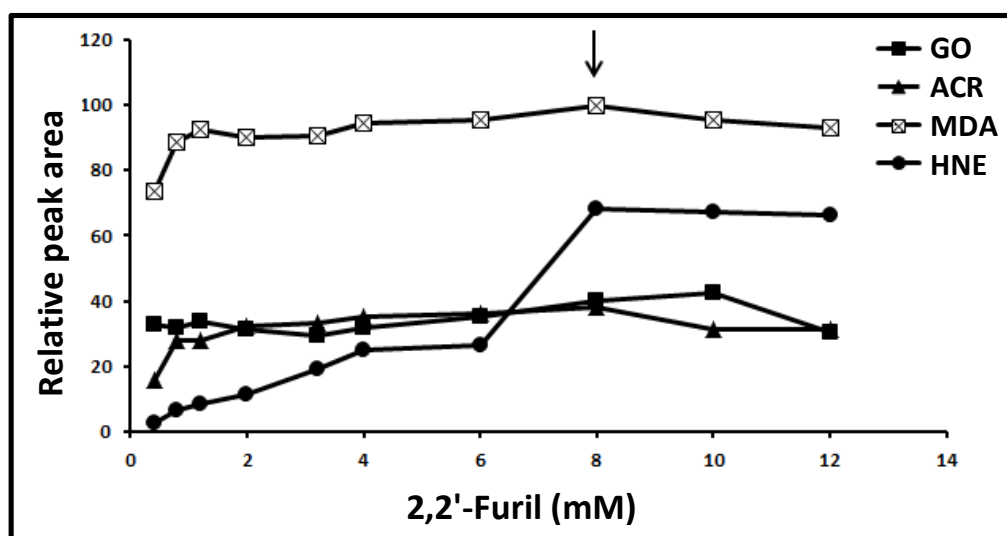


Fig. 2.6: Effect of 2,2'-fural concentration on the relative peak area of the studied aldehydes derivatives (5.0 nmol/mL).

Also, the effect of ammonium acetate concentration was studied from 0.5 to 4.0 M. Increasing the concentration of ammonium acetate resulted in proportional increase in the peak areas of ACR and MDA derivatives with minor effects on the peak areas of GO and HNE derivatives. The optimum concentration was found to be 3.0 M ammonium acetate giving maximum and constant peak areas for all aldehydes derivatives (Fig. 2.7).

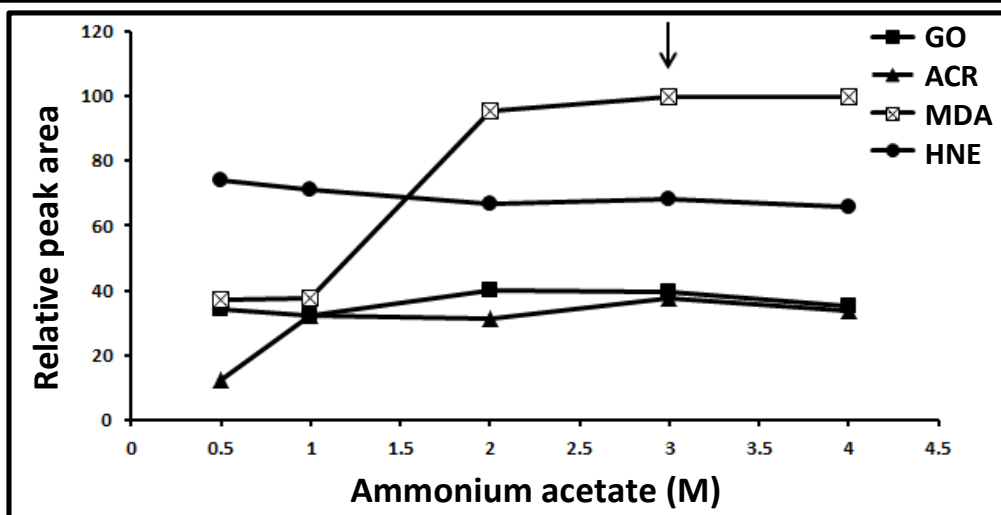


Fig. 2.7: Effect of ammonium acetate concentration on the relative peak area of the studied aldehydes derivatives (5.0 nmol/mL).

The effect of heating temperature was also investigated, where it was found that increasing the temperature gave rise to a corresponding increase in the peak areas up to 90 °C after which further increase in the temperature resulted in a gradual decrease in the analytical response for all of the studied aldehydes except MDA (Fig. 2.8) which may be attributed to the instability of their reaction product at higher temperatures. Thus, 90 °C was used as the optimum heating temperature for performing the reaction.

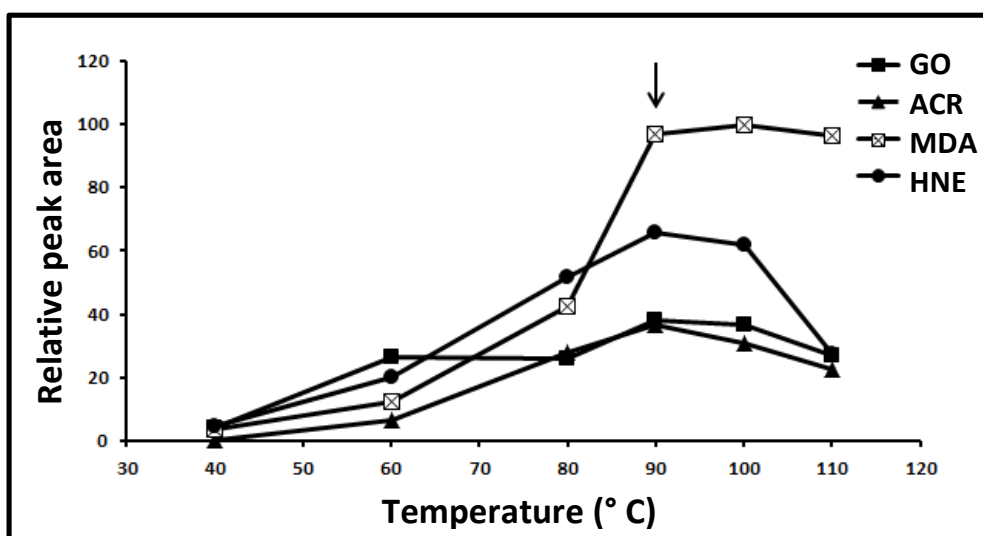


Fig.2.8: Effect of reaction temperature on the relative peak area of the studied aldehydes derivatives (5.0 nmol/mL).

The influence of heating time on the derivatization reaction was also investigated where; maximum peak areas were obtained upon heating for 30 min after which a slight decrease of the peak areas was observed (Fig. 2.9).

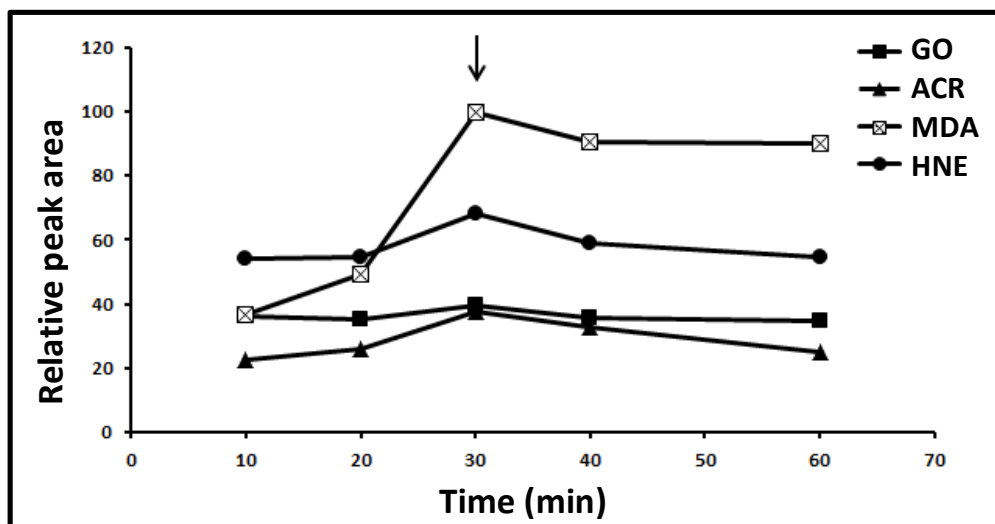


Fig.2.9: Effect of reaction time on the relative peak area of the studied aldehydes derivatives (5.0 nmol/mL).

2-3-4. Validation of the proposed method

Results of the validation study of the proposed method agree well with the Guidance for Industry on Bioanalytical Method Validation⁶⁶. A linear dependence of the concentration on the average peak areas was achieved for each of the studied analytes with correlation coefficients ranged from 0.997 to 0.9998. The LOD (S/N = 3) were ranged from 0.030 to 0.11 nmol/mL. Calibration ranges, regression equations, correlation coefficients, and LOD of the four LPRRAs are summarized in Table 2.1.

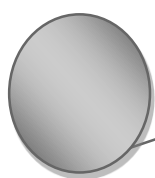


Table 2.1 Calibration ranges, regression equations, correlation coefficients and detection limits for the target aldehydes in spiked serum

Compound	Range, nmol/mL	Regression equation ^a , $n = 3$	r ^b	LOD ^c , nmol/mL (pmol/injection)
GO	0.100–5.00	$Y = 3.10 \times 10^5 + 8.40 \times 10^5 X$	0.997	0.030 (0.60)
ACR	0.200–10.0	$Y = 11.5 \times 10^5 + 6.50 \times 10^5 X$	0.999	0.060 (1.2)
MDA	0.200–40.0	$Y = 62.2 \times 10^5 + 10.3 \times 10^5 X$	0.999	0.050 (1.0)
HNE	0.400–10.0	$Y = -6.20 \times 10^5 + 16.9 \times 10^5 X$	0.9998	0.11 (2.2)

^a Y= peak area, X= aldehyde concentration (nmol/mL).

^b Correlation coefficient.

^c S/N= 3.

The accuracy and precision of the proposed method were also examined using three concentration levels for each aldehyde. It was found that the accuracy of the determinations was ranged from 95.5 to 103%. The % RSD values for intra-day ($n = 5$) and inter-day ($n = 5$) precision were 0.50–5.0% and 1.1–6.2%, respectively. Results of accuracy and precision studies are summarized in Table 2.2. These results indicate that the proposed method enables precise and accurate analysis of the targeted four LPRRAs in human serum.

Table 2.2 Accuracy and precision of the proposed method for the determination of the target aldehydes in spiked serum

Aldehyde	Spiked amount (nmol/mL)	Intra-day (<i>n</i> = 5)			Inter-day (<i>n</i> = 5)		
		Found amount (nmol/mL)	Accuracy (%)	Precision (% RSD)	Found amount (nmol/mL)	Accuracy (%)	Precision (% RSD)
		GO	0.200	0.191	95.5	4.60	0.193
	2.00	1.91	95.5	5.00	1.91	95.5	5.30
	5.00	4.91	98.2	1.70	4.90	98.0	4.10
ACR	0.500	0.498	99.6	0.500	0.516	103	6.20
	5.00	4.91	98.2	1.80	4.91	98.2	2.00
	10.0	9.88	98.8	1.10	9.92	99.2	1.20
MDA	0.500	0.481	96.2	3.90	0.494	98.8	2.10
	15.0	14.8	98.7	1.70	14.8	98.7	1.40
	30.0	29.8	99.3	0.900	29.7	99.0	1.10
HNE	1.00	0.993	99.3	1.50	0.962	96.2	3.60
	5.00	4.88	97.6	2.50	4.92	98.4	1.50
	10.0	9.92	99.2	0.900	9.73	97.3	3.90

2-3-5. Application to the analysis of serum samples from healthy and diseased human subjects

The proposed HPLC-FL method was applied to the determination of the four LPRRAs in the sera of healthy and diseased human subjects. Fig. 2.10 shows typical chromatograms of spiked serum and serum samples from healthy control subjects, diabetic and rheumatoid arthritis patients determined by the proposed method. Although several peaks that are attributed to the biological components other than the reagent blank

were detected in the chromatogram of serum samples, the peaks of the studied LPRRAs could be clearly separated and detected without any interference.

The levels of the target LPRRAs were compared between control group, diabetic and rheumatoid arthritis patients using Steel's Dwass test ⁶⁷ for comparing each pair and the results are abridged in Table 2.3. The statistical tests were two-sided at a significant level $\alpha = 0.05$. The level of the LPRRAs in healthy subjects were found to be 1.04 ± 0.060 , 1.26 ± 0.28 , 15.1 ± 0.52 and 0.960 ± 0.060 for GO, ACR, MDA and HNE, respectively, and these values show good agreement with other previous reports ^{49,71-74}.

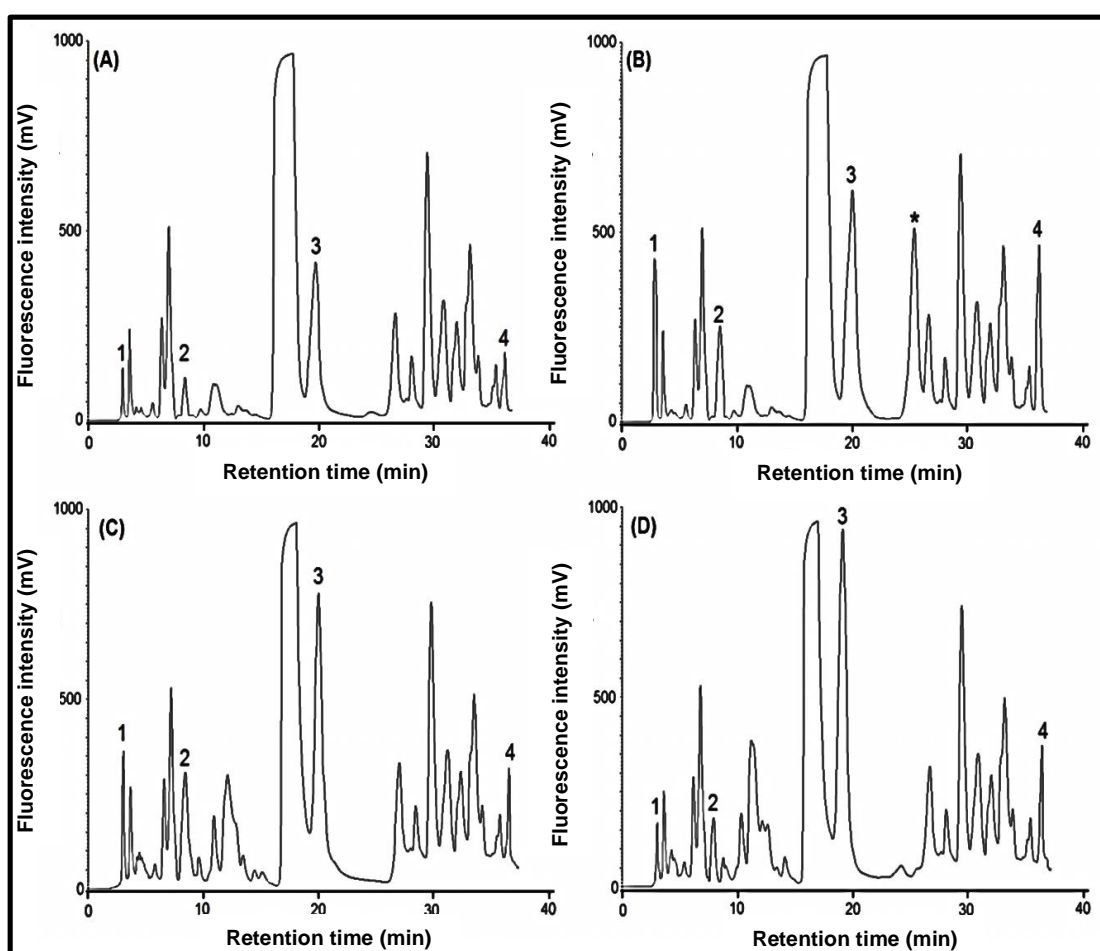


Fig. 2.10: Chromatograms of (A) healthy human serum, (B) human serum spiked with a standard mixture of the studied aldehydes (5.0 nmol/mL each), (C) diabetic patient serum, and (D) rheumatoid arthritis patient serum; where peaks 1-4: as in Fig. 2.5.

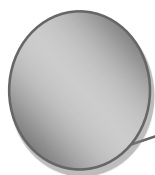


Table 2.3 Statistical analysis of the results for determination of the target aldehydes in healthy, diabetic and rheumatic patients' sera.

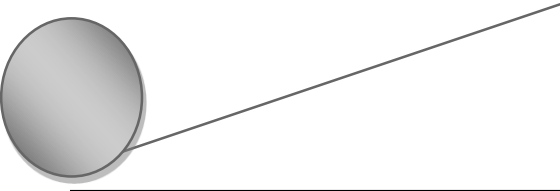
Groups (n=6)	Parameters	LPRRAs data				
		GO	ACR	MDA	HNE	
control	Range (nmol/mL)	0.900-1.26	0.660-2.18	13.4-16.6	0.780-1.14	
	Mean ± SE	1.04±0.060	1.26 ±0.28	15.1±0.52	0.960±0.060	
diabetic patients	Range (nmol/mL)	1.68-4.04	4.60-9.29	21.1-30.5	1.19-1.36	
	Mean ± SE	2.75 ±0.34	6.35 ±0.71	25.6±1.8	1.27±0.030	
rheumatic patients	Range (nmol/mL)	0.700-2.06	2.29-3.71	35.2-39.6	1.37-2.47	
	Mean ± SE	1.34 ±0.18	2.92 ±0.20	36.95±0.62	1.78±0.17	
Statistical analysis	Bartlett	(p)	0.00400 ^a	0.0178 ^a	0.0328 ^a	0.00180 ^a
	Control vs Diabetic	(p) ^b	0.0141 ^a	0.0141 ^a	0.0141 ^a	0.0141 ^a
	Control vs Rheumatic	(p) ^b	0.281 ^c	0.0141 ^a	0.0141 ^a	0.0141 ^a
	Diabetic vs Rheumatic	(p) ^b	0.0349 ^a	0.0141 ^a	0.0141 ^a	0.0141 ^a

^a P < 0.05.

^b Steel's Dwass test.

^c Non-significant.

Statistical analysis revealed the presence of significantly higher concentration of GO, ACR, MDA and HNE in diabetic patients when compared to healthy controls, which is in accordance with previous reports^{21,26,29,54,55,61}. The increased level of MDA and HNE in diabetic patients is attributed to the catalysis of lipoperoxidation by free glucose and glycosylated collagen⁷⁵. It had also been demonstrated that oxidation of the glycation products can release dicarbonyls such as GO and short chain aldehydes such as ACR. This process of glycooxidation takes place when there is an extra amount of glucose

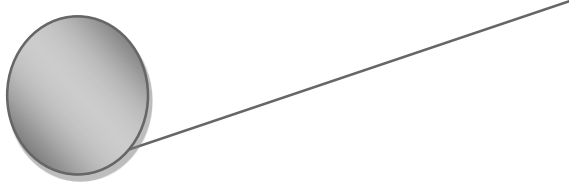


coupled with high levels of oxidants, and this is the case in diabetes⁸. Also, GO may arise from enzymatic and non-enzymatic degradation of glucose⁷⁶.

On the other hand, the levels of ACR, MDA and HNE were found to be significantly higher in the sera of rheumatoid arthritis patients compared to the healthy controls, which is similar to previously reported results^{27,55}. Meanwhile, there was no significant difference in the concentration of GO in the two groups. The elevated levels of MDA and HNE in rheumatoid arthritis patients are probably due to high level of ROS produced by activated polymorphonuclear cells and injury resulting from ischemia and reperfusion in the inflamed joints⁷⁷. Besides oxidative stress and increased lipoperoxidation, the presence of ACR at a significantly higher concentration in rheumatic group might be also attributed to the oxidative deamination of polyamines⁷⁸ which were previously detected in high levels in rheumatic patients' urine samples⁷⁹.

Comparing the levels of the four LPRRAs in rheumatic and diabetic groups, HNE and MDA were found to be present in significantly higher levels in rheumatic sera than in diabetic sera. Since the main source of these two aldehydes is lipid peroxidation^{22,77}, we could conclude that the rates of oxidative stress and lipid peroxidation are relatively higher in rheumatic condition than in hyperglycemic one. On the other hand, the concentrations of GO and ACR were found to be significantly higher in serum of diabetic group than in rheumatic one. This might be due to the increase of glycation and glycoxidation processes in diabetic patients^{8,28}.

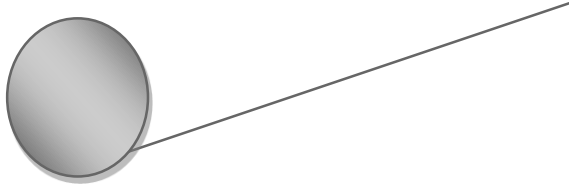
It is worth noting that the present work is the first study that explores and compares the patterns of the most harmful LPRRAs (GO, ACR, MDA and HNE) in these two diseased conditions. However, there are some reports that determine these



compounds in different biological, environmental or lipid matrices^{11,48–53,56–60,62–64}, none of these methods simultaneously determine these LPRRAs in human serum.

2-3-6. Comparison of the analytical performance of the proposed method and published literature

The proposed method was found to be about 10, 59 and 1.5 times more sensitive than the reported GC-flame ionization detection⁴⁹ and HPLC-FL methods^{50,51} for GO, respectively, 2.5 times more sensitive than the reported HPLC-FL method for ACR⁵² and the HPLC-CL method for MDA⁵⁷ and 1.5 and 6.5 times more sensitive than HPLC-FL methods^{53,54} for ACR, respectively. On the other hand, the proposed method showed comparable sensitivity to the reported HPLC-FL⁶¹ and HPLC-UV⁶⁰ methods for HNE, yet these methods involved time consuming^{60,61} and tedious extraction procedure⁶⁰. Even though some of the published literature for LPRRAs exhibits higher sensitivity than the present method, but they either entail the use of sophisticated very expensive instrumentation^{48,62–64} or instruments that are unavailable in many laboratories⁵⁹ or the use of a non-selective derivatizing agent such as hydrazine based reagents^{55,62–64} which are also unstable, flammable, and irritant⁶⁵ and thiobarbituric acid⁵⁸ that probably yields false high results due to likely interference from other thiobarbituric acid-reactive compounds including reducing sugars, pyrimidine and prostaglandin endoperoxides⁵⁹. 2,2'-Furil was proven as a stable derivatization reagent which is relatively safe compared with hydrazine reagents and highly selective relative to thiobarbituric acid.



2-4. Conclusions

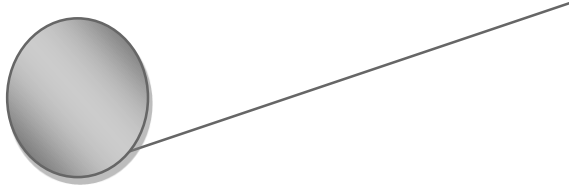
A sensitive, reliable and accurate HPLC method with fluorescence detection was developed and validated for the simultaneous determination of four LPRRAs including GO, ACR, MDA and HNE using 2,2'-furyl as a sensitive and selective fluorogenic derivatizing reagent employing a gradient elution mode. The proposed method allowed monitoring the levels of such aldehydes in human serum with the aim of evaluating the oxidative status in healthy subjects and in patients suffering from diabetes and rheumatoid arthritis. The proposed method permitted the simultaneous determination of the patterns of LPRRAs in both healthy and diseased conditions. Using the proposed method, a significant increase in the levels of GO, ACR, MDA and HNE was detected in diabetic patients' sera relative to healthy sera, while significantly elevated levels of ACR, MDA and HNE were detected in sera of rheumatoid arthritis patients compared to the healthy sera. In addition, a comparison of the levels of these aldehydes in sera of diabetic and rheumatic patients revealed significant elevation in the levels of HNE and MDA in rheumatic conditions than in diabetic ones, and elevated levels of ACR and GO in diabetic conditions than in rheumatic ones.

Chapter III

9,10-Phenanthrenequinone as a mass-tagging reagent for ultra-sensitive liquid chromatography tandem mass spectrometry assay of aliphatic aldehydes in human serum

Mahmoud H. El-Maghrabey, Naoya Kishikawa, Naotaka Kuroda, Journal of Chromatography A, 1462 (2016) 80–89.

DOI: 10.1016/j.chroma.2016.07.082



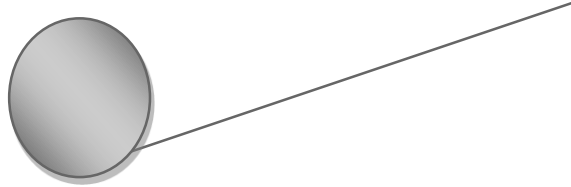
3-1. Introduction

The *in vivo* lipid peroxidation process is associated with degenerative free radical propagation reactions which are involved in the production of many carbonyl compounds. Saturated aliphatic aldehydes (C₃-C₁₀) are produced by lipid peroxidation together with α,β -unsaturated aldehydes, dialdehydes, and other carbonyl compounds⁸⁰. Aldehydes are relatively more stable than free radicals and can spread inside or out of the cell attacking sites far from the original place of free radical-initiated actions⁸¹.

Elevated levels of hexanal, nonanal and decanal in plasma of haemodialysis patients compared to control group suggested the contribution of these aldehydes to the intoxication caused by increased lipid peroxidation in these patients. *n*-Alkanals have higher affinity for amino group than other types of aldehydes, which explains the highest negative correlation found only between the residual amino groups and total *n*-alkanals⁸².

Additionally, propanal, butanal, pentanal, hexanal and nonanal have been proven to have cytotoxic effect on rat and human hepatocytes, which was increased by increasing the length of carbon chain. However, these *n*-alkanals have intrinsic genotoxic activity on rat hepatocytes only, with no effect on human hepatocytes⁸³.

Saturated aliphatic aldehydes have been analyzed in different matrices by HPLC, mostly with UV or FL detection, following derivatization. The most widely used derivatizing agents for aldehydes are those based on hydrazine nucleus including 2,4,6-trichlorophenylhydrazine (TCPH)⁸⁴, *N*-methyl-4-hydrazino-7-nitrobenzo-furazan (MNBDH)⁸⁵, DNPH⁸⁶⁻⁹¹, dansylhydrazine (DNSH)⁹², DBD-H⁹³ and 1,3,5,7-tetramethyl-8-aminozide-difluoroboradiaza-s-indacene (BODIPY-aminozide)⁹⁴. Some

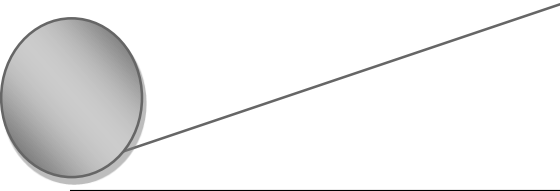


hydrazine-based reagents have also been used in combination with MS detection such as DNPH^{64,95}, and DNSH⁹⁶. Despite the large number of analytical methods depend on them; hydrazine-based reagents have some inevitable drawbacks such as poor selectivity that probably introduces interferences from other carbonyl compounds *e.g.* ketones and small carboxylic acids. In addition, the formation of stereoisomeric hydrazone derivatives as reaction products may cause analytical errors. As well, hydrazine reagents are irritant, flammable, and unstable⁹⁷.

Some other reagents that are not based on hydrazine nucleus were utilized for aldehyde derivatization such as *O*-2,3,4,5,6-(penta-fluorobenzyl)hydroxylamine (PFBHA)^{98,99}, and 1,3-cyclohexanedione (CHD)^{100,101}. However, these reagents exhibited some disadvantages such as poor selectivity^{98,99}, need for long derivatization time¹⁰⁰ and poor sensitivity^{100,101}. Interestingly, 2,2'-fural has been used in our laboratory as a safe, stable, selective and sensitive fluorogenic derivatizing agent for aliphatic aldehydes⁶⁵.

Additionally, some reagents have been used for derivatization of aldehydes to improve their ionization characters prior MS detection *e.g.* 4-(2-(trimethylammonio)ethoxy)benzenaminium halide (4-APC)⁶⁸, 4-(2-((4-bromophenethyl)dimethylammonio)ethoxy)benzenaminium dibromide⁴⁷, CHD-based reagents^{102,103} and d₀/d₃-4-(1-methyl-1*H*-phenanthro[9,10-*d*]imidazol-2-yl) phenlamine (d₀/d₃-MPIA)¹⁰⁴. Though, these methods suffer from some shortcomings such as long reaction time of 3 hours^{47,68,102-104}, lower sensitivity^{47,68,102,103}, and poor selectivity¹⁰⁴.

In Chapter II, we used the α,β -diketo derivatizing agent, 2,2'-fural, for quantification of LPRRAs (GO, ACR, MDA and HNE) in biological fluids with high



selectivity by HPLC-FL detection. The same reagent has also been used in our laboratory for derivatization of C₅-C₁₀ aldehydes prior HPLC-FL detection ⁶⁵. The inspiring chemical and analytical characteristics of the formed imidazole derivatives motivated us to utilize this reaction as a model to design a LC electrospray ionization tandem mass spectrometry (LC/ESI-MS/MS) method with high selectivity and sensitivity for the screening of aliphatic aldehydes (C₃-C₁₀) in human serum.

LC/MS is currently considered the most specific and selective technique for metabolites determination, where it combines the separation efficiency of LC and the specificity and sensitivity of MS. LC-MS/MS is a powerful technique with superior sensitivity and specificity relative to LC/MS. ESI is most commonly used for metabolites analysis due to its ability to cover a wide diversity of compounds than other atmospheric pressure ionization methods, *e.g.* atmospheric pressure chemical ionization ¹⁰⁵. The poor ionization and fragmentation properties of aldehydes made their direct analysis by LC-MS/MS impossible; hence derivatization is an efficient solution to enhance the MS detectability of aldehydes as well as improving their chromatographic behavior and sensitivity of the assay ⁴⁶.

In this study, several α,β -diketo reagents were evaluated to select the most proper one for aldehydes derivatization in terms of sensitivity and selectivity. 9,10-Phenanthrenequinone (PQ) was our reagent of choice that enables MS detection of the aldehydes selectively in the low picomolar levels. Fig.3.1 illustrate the reaction between PQ and aldehydes in presence of ammonium acetate. A study on the screening of C₃-C₁₀ aldehydes in human serum was conducted to demonstrate the applicability of the method in biological samples.

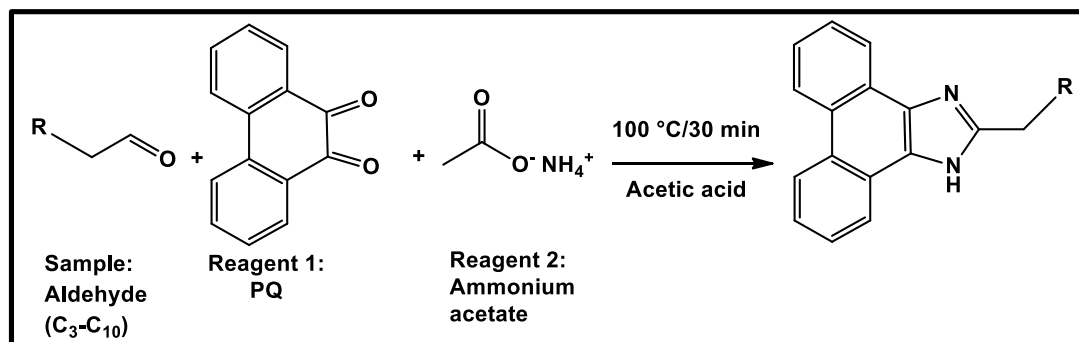
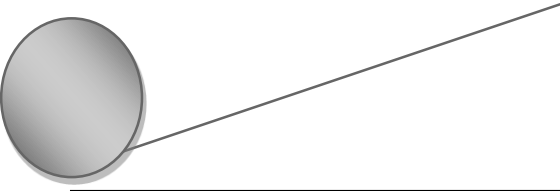


Fig. 3.1: Reaction pathway of the mass tagging of the target aliphatic aldehydes with PQ and ammonium acetate.

3-2. Experimental

3-2-1. Chemicals and reagents

Analytical grade reagents were used in this study and solvents were of LC/MS grade. PQ, 2,2'-pyridil, 4,4'-dimethoxybenzil (*p*-anisil), 1,10-phenanthroline-5,6-dione (PAD), ammonium acetate, and nonanal were obtained from Sigma Aldrich. Butanal, pentanal, hexanal, heptanal, octanal, decanal, glacial acetic acid, formic acid, and ultrapure water (LC/MS grade) were obtained from Wako Pure Chem. Ind. Propanal, benzil, and sodium chloride were from Nacalai Tesque. Methanol and acetonitrile (LC/MS grade) were from Kanto Chem. Co. 3-Phenylpropanal (internal standard, IS) and 2,2'-furil were purchased from Tokyo Chem. Ind., while ammonium formate was obtained from Kishida Chem. Co. (Osaka). 4-Dimethylaminobenzil (DMAB) was synthesized in our laboratory in two steps; first we synthesized 4-dimethylaminobenzoin as reported by Levi and Hauser¹⁰⁶ then it was converted to DMAB using Fehling's solution¹⁰⁷.



Stock solutions of the target aliphatic aldehydes (10.0 mM) were individually prepared in acetonitrile. Accurate volumes from the stock solutions of the eight aldehydes were mixed together and diluted with acetonitrile to obtain a mixed standard solution containing 4.0 μM of each aldehyde. Dilution of this solution was made as needed to obtain the required concentration levels. 3-Phenylpropanal (IS) solution (8.0 μM) was also prepared in acetonitrile. PQ solution (4.0 mM) was prepared in acetonitrile and ammonium acetate (2.0 M) was prepared in glacial acetic acid. The mixed standard solution and IS solution were stored at $-30\text{ }^{\circ}\text{C}$, while all other solutions were stored at $4\text{ }^{\circ}\text{C}$ in the refrigerator.

3-2-2. Instrumentation and LC/ESI-MS/MS conditions

The LC system (Fig. 3.2) employed for the separation of the studied aldehydes consisted of a Waters 2695 separation module (Waters Co., Milford, MA, USA) with a Cosmosil 3C₁₈-AR-II column (100 mm x 4.6 mm i.d., 3 μm particle size) from Nacalai Tesque operated at $25\text{ }^{\circ}\text{C}$. Gradient elution was employed with a mobile phase mixture of methanol (A) and ammonium formate buffer (20 mM, pH 4.0) (B). For the first 3 min of the run, the percentage of A was increased linearly from 70% to 100%. For the next 7 min the proportion of A was maintained at 100%. The initial composition of the mobile phase was re-established for 5 min before starting a new run. The flow rate of mobile phase was set at 0.5 mL/min and the sample injection volume was 20 μL . MS analysis was accomplished by a Quattro microTM triple-quadrupole mass spectrometer (Waters Co.) fitted with an ESI source. Acquisition of positive-ion ESI-MS data was done at a capillary voltage of 5 kV, source temperature of $120\text{ }^{\circ}\text{C}$, desolvation gas temperature of $350\text{ }^{\circ}\text{C}$ and flow rate of 500 L/h, and cone gas flow rate of 40 L/h. Table 3.1 illustrates the cone voltage, collision voltage, precursor and product ions for the studied aldehydes

(C₃-C₁₀) and IS. The PQ-aldehyde derivatives were detected using the multiple reaction monitoring (MRM) mode. This strategy was considered to detect a specific product ion (m/z value of 231.9) by collision induced dissociation (CID).

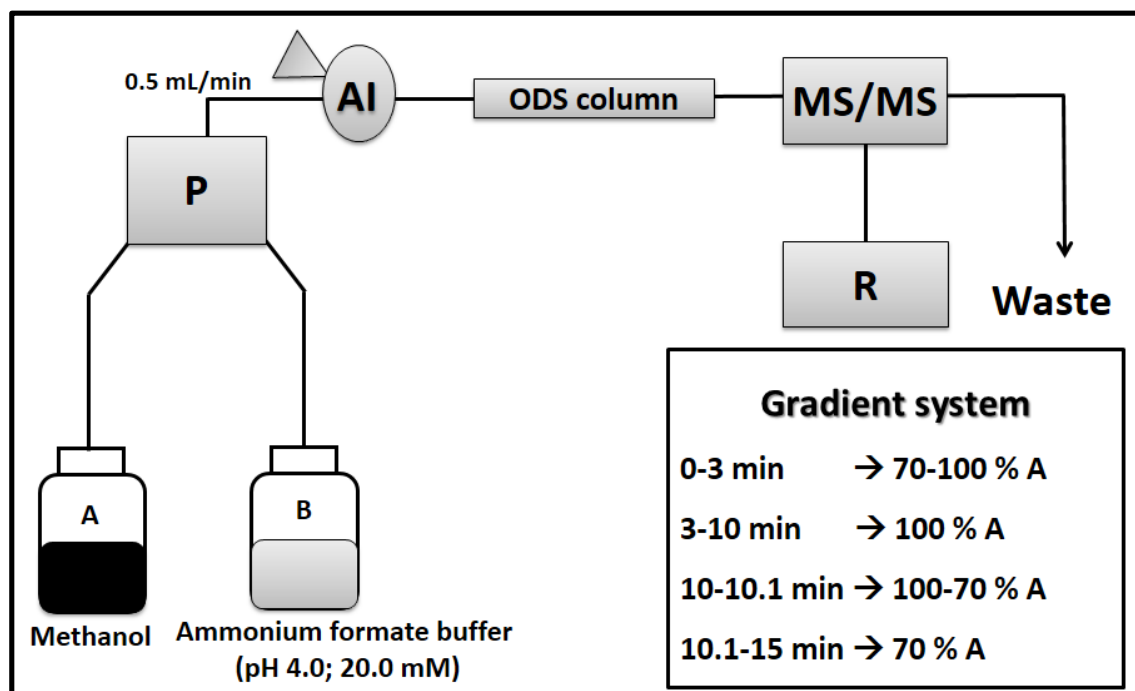
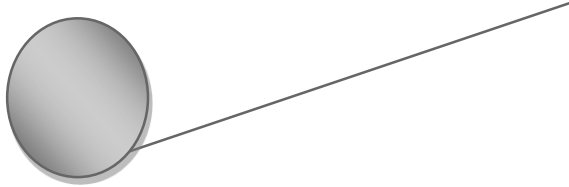


Fig. 3.2: Schematic diagram of the LC/ESI-MS/MS system

P: pump, AI: auto injector, ODS column: Cosmosil 3C₁₈-AR II column (100 mm × 4.6 mm i.d., 3 μ m particle size), MS/MS: triple quadrupole ESI-MS/MS detector, R: read out.

Table 3.1 Optimum MS/MS conditions for the analysis of PQ derivatives of the studied aliphatic aldehydes

Aldehyde	Cone voltage (V)	Collision voltage (V)	Precursor ion	Product ion
Propanal	35	30	247.0	231.9
Butanal	40	30	261.0	231.9
Pentanal	45	30	275.0	231.9
Hexanal	50	30	289.0	231.9
Heptanal	50	30	303.0	231.9
Octanal	50	35	317.1	231.9
Nonanal	50	35	331.1	231.9
Decanal	50	35	345.0	232.0
3-Phenylpropanal (IS)	40	30	322.9	231.9



3-2-3. Clinical samples

All conducted studies were approved by the Ethics Committee of the School of Pharmaceutical Sciences, Nagasaki University. Serum samples from 14 healthy human volunteers (10 males and 4 females, mean age of 38.4 ± 13.1 years) were provided by Sasebo Chuo Hospital. Serum samples were kept at $-80\text{ }^{\circ}\text{C}$ and gently thawed before analysis.

3-2-4. Derivatization procedure

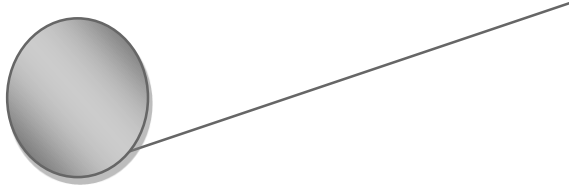
Aliquots of $50\text{ }\mu\text{L}$ PQ solution (4.0 mM) and $100\text{ }\mu\text{L}$ of ammonium acetate (2.0 M) were mixed with $150\text{ }\mu\text{L}$ of aldehydes standard solution in a screw-capped vial, then heated for 30 min at $100\text{ }^{\circ}\text{C}$. After cooling, the solution was filtered with cellulose acetate membrane filter ($0.45\text{ }\mu\text{m}$) and $20\text{ }\mu\text{L}$ of the samples were injected to the LC/ESI-MS/MS *via* the auto injector. A reagent blank was prepared simultaneously.

3-2-5. Serum samples treatment by salting out liquid-liquid extraction (LLE)

A volume of $200\text{ }\mu\text{L}$ of serum was mixed with $10\text{ }\mu\text{L}$ IS, $390\text{ }\mu\text{L}$ acetonitrile, and 0.2 g NaCl followed by centrifugation for 5 min at $3000\times g$. $150\text{ }\mu\text{L}$ of the supernatant was taken and the derivatization procedure was performed in the same way as for the standard solution.

3-2-6. Validation procedure

The Guidance for Industry on Bioanalytical Method Validation ⁶⁶ was followed. The validation procedure included determination of calibration curves, limit of quantification (LOQ), LOD, accuracy, precision, recovery, and stability study.



Calibration curves were generated for the eight studied aldehydes (C₃-C₁₀) by spiking serum at six concentration levels (including the LOQ) for each aldehyde and plotting the relative peak area (peak area of analyte/peak area of IS) *versus* concentration (nM). The LOQ was also determined for the eight aldehydes as the minimum concentration in the calibration curves which can be determined with satisfactory accuracy (80-120%) and precision (% RSD of $\leq 20\%$)⁶⁶. In addition, the LOD was calculated as the concentration corresponding to S/N = 3.

The method was also evaluated regarding accuracy and precision by replicate analyses of serum samples spiked with the analytes at three concentrations within the working linearity ranges (0.5, 5.0, and 50 nM for each aldehyde). Each concentration was measured five times and the average was calculated. The difference of the average from the exact value expresses the accuracy. The intra-day precision was calculated as the % RSD for the peak areas of five injections per concentration within one day, and the inter-day precision was also measured as the % RSD for the peak areas of replicate determinations on five successive days for each concentration⁶⁶.

Recovery studies were conducted to evaluate the efficiency of the extraction method. The recovery was calculated for the studied aldehydes at three concentration levels for each aldehyde (0.5, 5.0, and 50.0 nM) according to the following equation:

$$\% \text{ Recovery} = \frac{\text{relative peak area of aldehyde extracted from serum samples}}{\text{relative peak area of aldehyde in un-extracted standard solution}} \times 100$$

Evaluation of the stability of aldehydes and IS solutions was conducted at room temperature for 6 h and at 4 °C for 1 week. Additionally, the stability of the mass tagging reagent PQ was tested at 4 °C up to 2 months. Also, the stability of the derivatized aldehydes and IS was also determined over the anticipated resident time in the

autosampler, *i.e.* up to 48 h at 4 °C. All of the stability studies were performed by comparison of the results obtained for old solutions with those for newly prepared ones.

3-3. Results and discussion

3-3-1. Preliminary screening for candidate derivatizing agents

Aldehydes are small hydrophilic molecules that cannot be retained or separated on common reversed-phase LC columns resulting in weak or no signals at the MS detector. Chemical derivatization has been long applied to improve stability, MS detectability, and chromatographic behavior of aldehydes.

As we discussed in Chapter II, the α,β -diketo compounds react with aldehydes in the presence of ammonium acetate in a one-pot reaction catalyzed by acetic acid at 90–100 °C forming a stable imidazole derivative⁶⁵. In this study, we initially screened several α,β -diketo reagents for selective and sensitive derivatization of the target aldehydes (C₃–C₁₀). The reagents investigated were PQ, PAD, 2,2'-pyridil, benzil, DMAB, *p*-anisil and 2,2'-fural (Fig. 3.3).

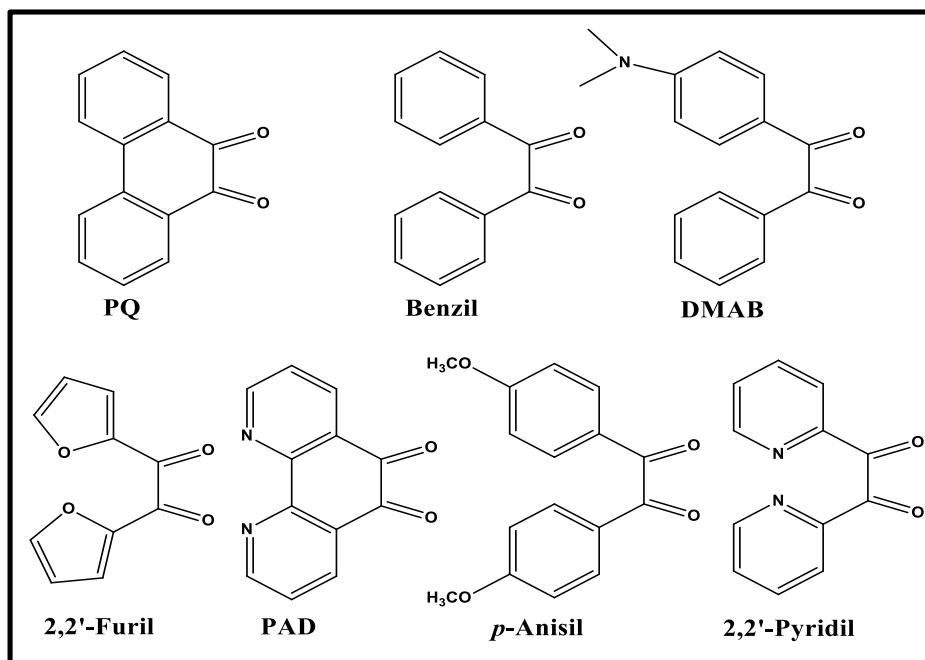
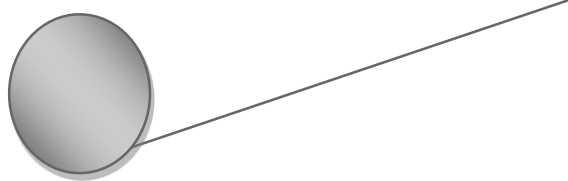


Fig. 3.3: Structures of the initially screened α,β -diketo reagents for the derivatization of the target aldehydes.



We conducted the preliminary screening using both positive-ion and negative-ion ESI-MS/MS modes and heptanal as a representative aldehyde. The MS conditions, precursor and product ions for all reagents are summarized in Table 3.2. The product ion spectra for the reagents-heptanal derivatives are shown in Fig. 3.4-3.10.

Table 3.2 The optimum MS/MS conditions for the studied α,β -diketo reagents

Reagent (ESI mode)	Capillary voltage (kV)	Cone voltage (V)	Collision voltage (V)	Precursor ion	Main product ion
PQ (+)	5.0	50	30	303.0	231.9, 164.9
PQ (-)	-3.0	-50	-30	301.0	230.0
Anisil (+)	5.0	55	30	365.1	350.1
Anisil (-)	-3.5	-40	-35	362.9	333.0
Benzil (+)	5.0	50	30	305.0	194.0
Benzil (-)	-3.5	-50	-30	303.2	232.1
DMAB (+)	5.0	50	50	348.0	222.0
DMAB (-)	-4.5	-35	-35	346.0	330.2
Furil (+)	5.0	40	35	285.0	185.0
Furil (-)	-3.5	-40	-35	282.9	183.0
Pyridil (+)	5.0	50	45	307.1	235.9
PAD (+)	3	50	35	305.0	233.8
PAD (-)	-3	-50	-30	303.0	232.0

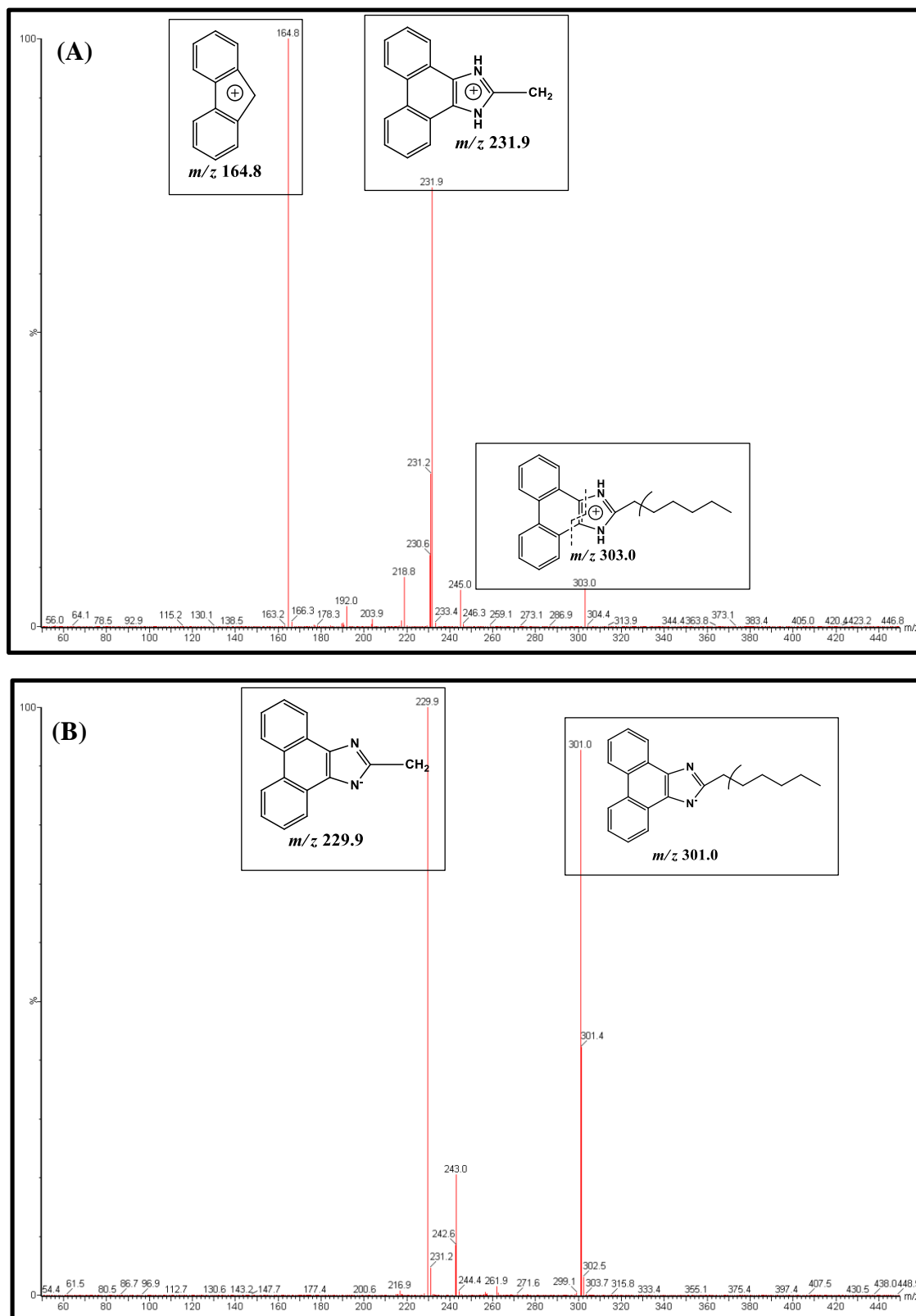


Fig. 3.4: Product ion spectra of heptanal derivatives of PQ using (A) ESI⁺ mode and (B) ESI mode

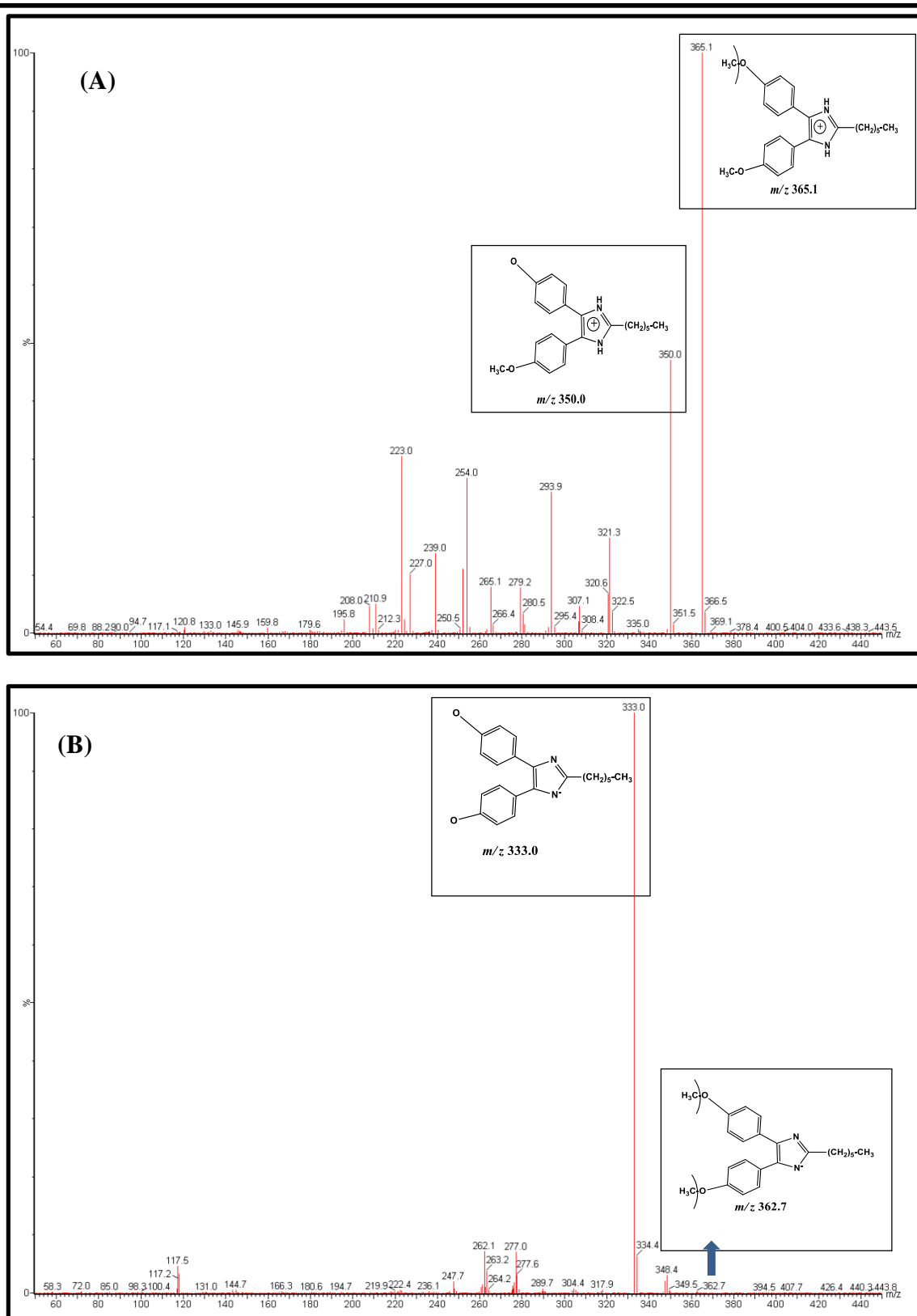


Fig. 3.5: Product ion spectra of heptanal derivatives of *p*-anisil using (A) ESI⁺ mode and (B) ESI⁻ mode

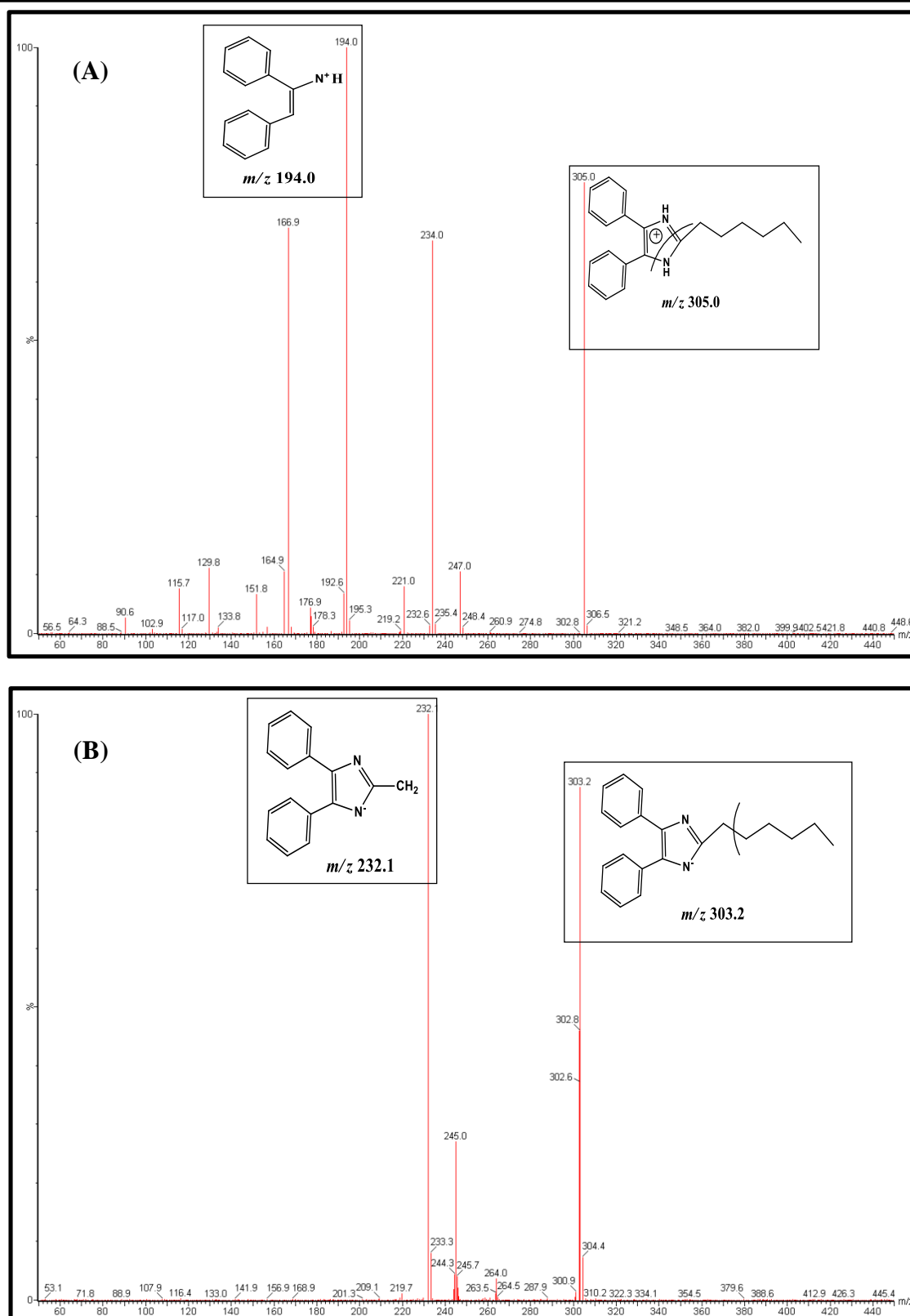


Fig. 3.6: Product ion spectra of heptanal derivatives of benzil using (A) ESI⁺ mode and (B) ESI mode

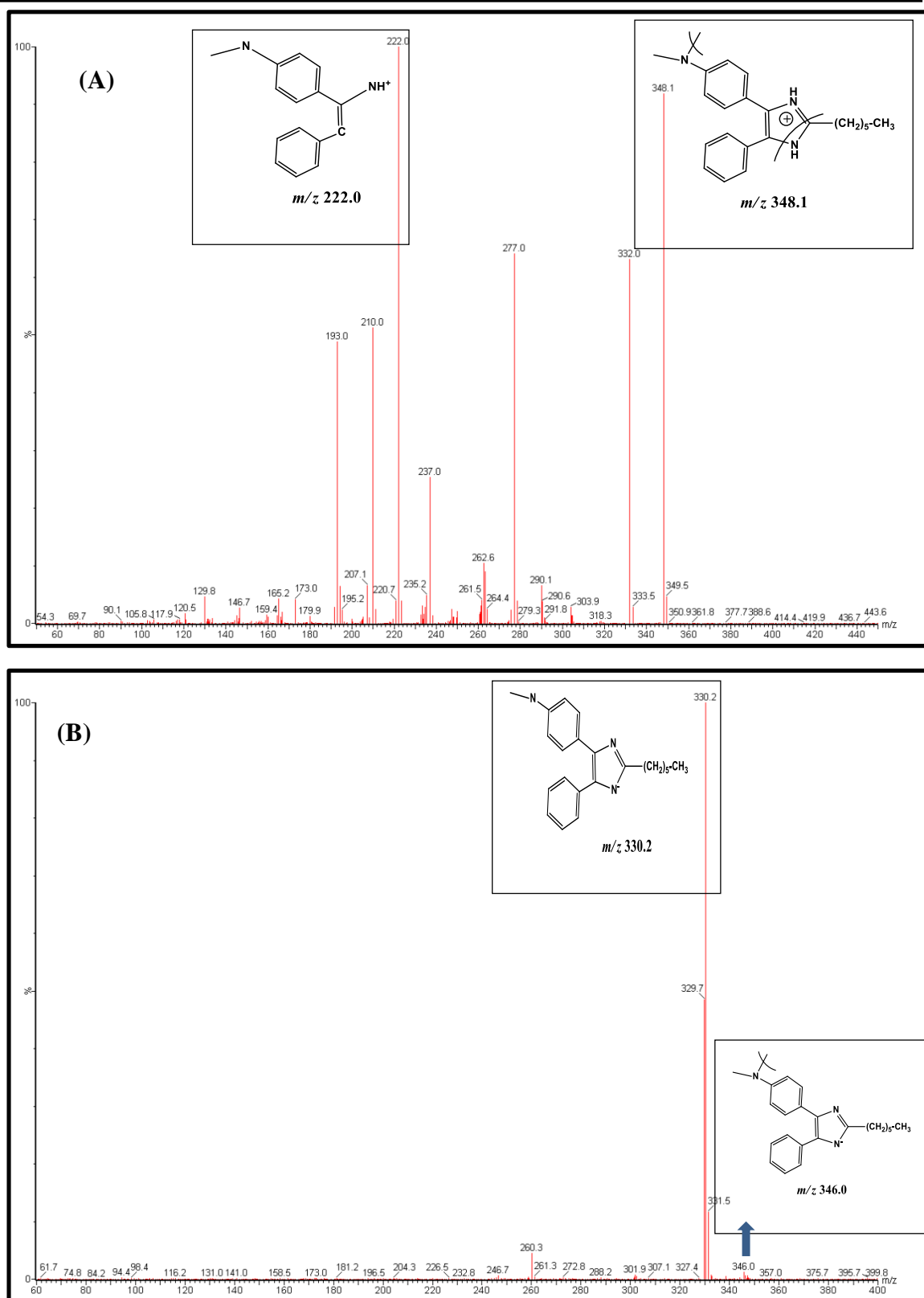
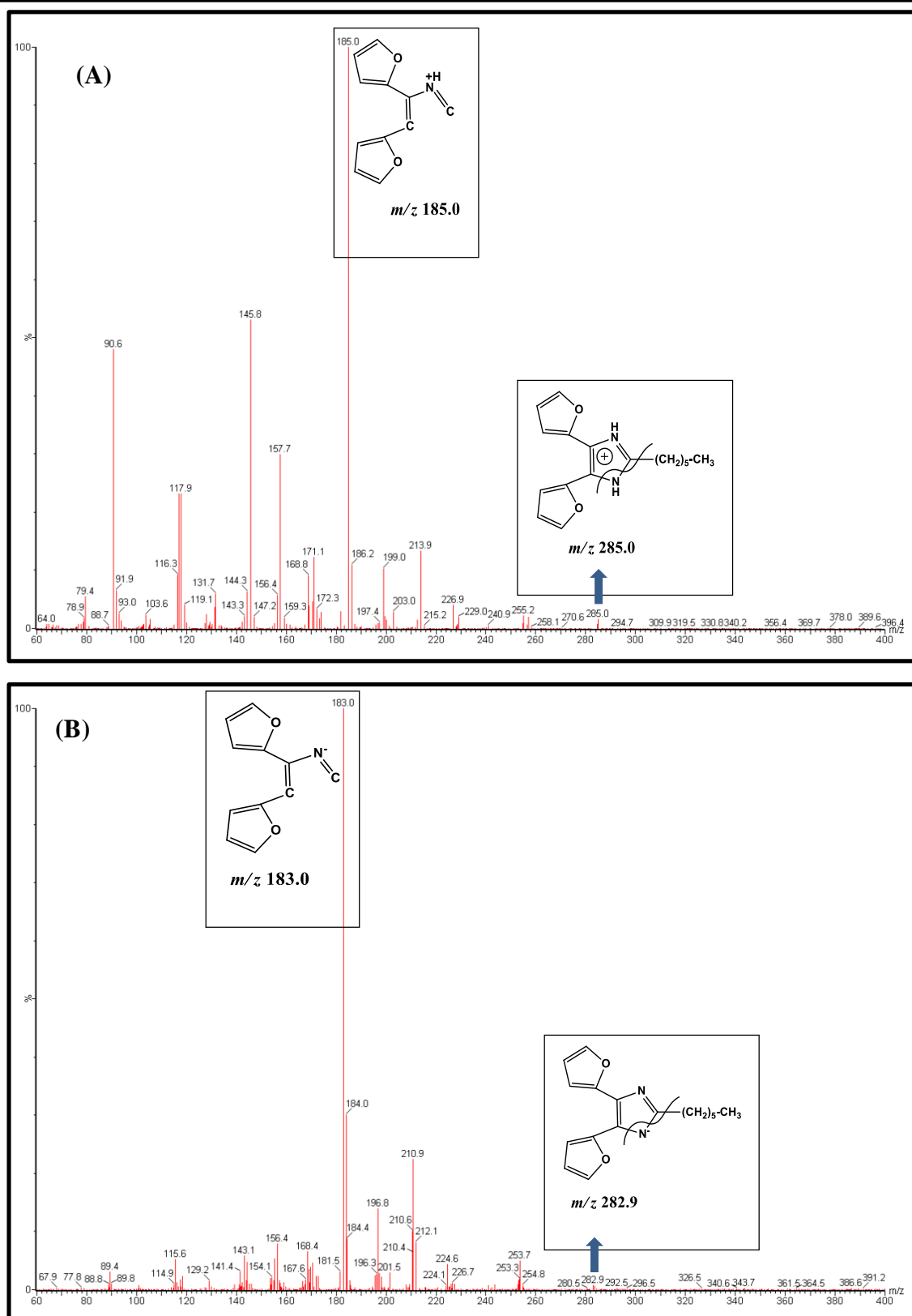


Fig. 3.7: Product ion spectra of heptanal derivatives of DMAB using (A) ESI⁺ mode and (B) ESI⁻ mode



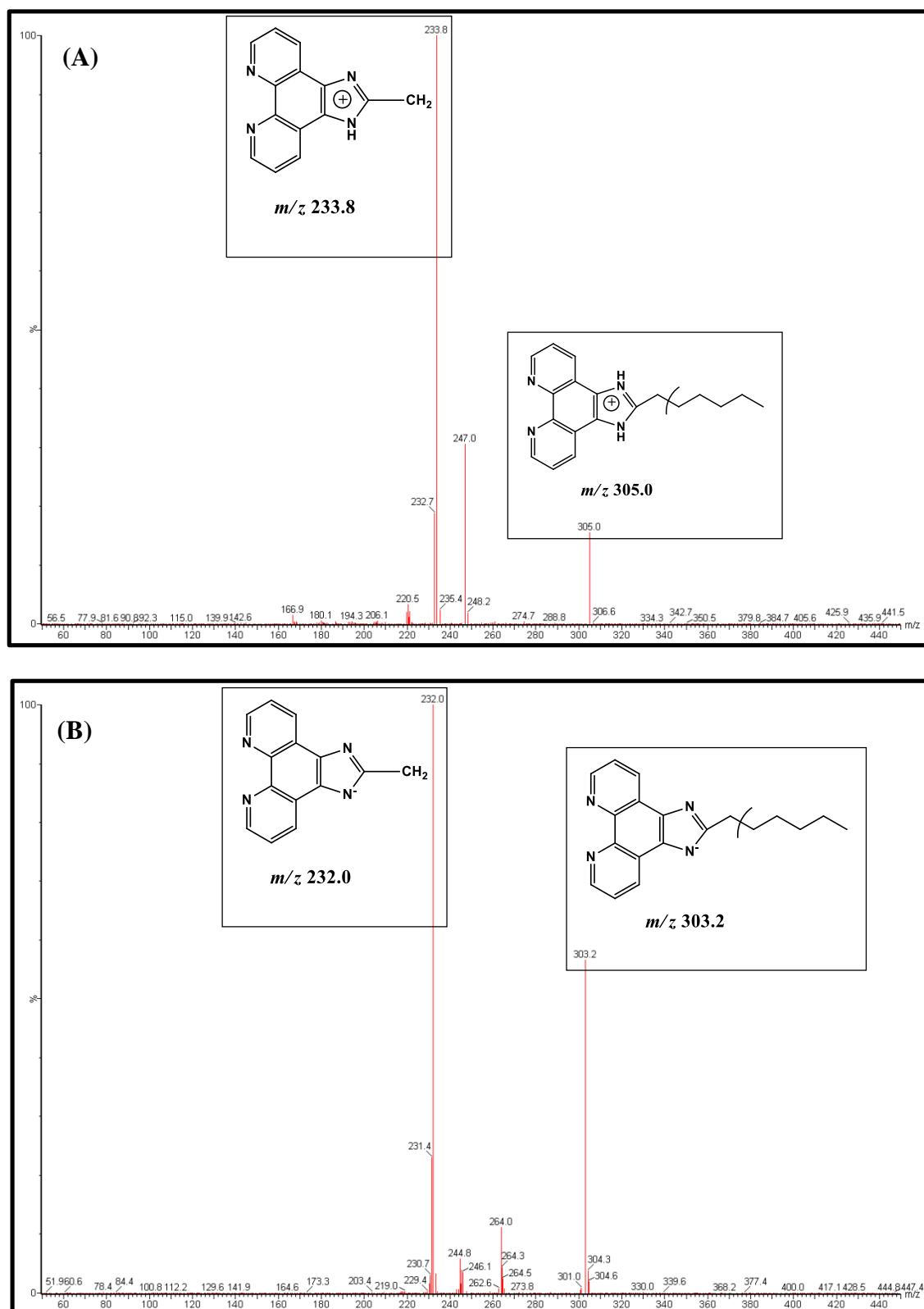


Fig. 3.9: Product ion spectra of heptanal derivatives of PAD using (A) ESI⁺ mode and (B) ESI⁻ mode

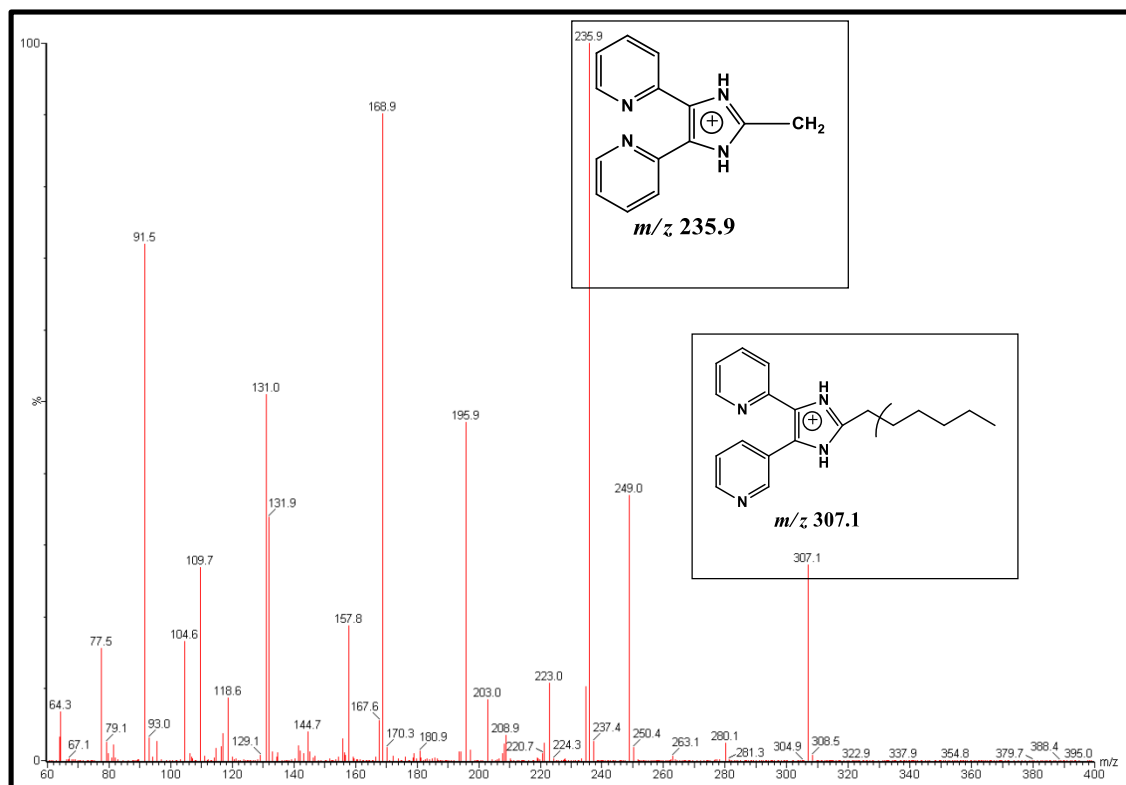


Fig. 3.10: Product ion spectrum of heptanal derivative of 2,2'-pyridil using ESI⁺ mode

For all of the reagents, the positive-ion mode showed better response than the negative-ion mode. Yet, the 2,2'-pyridil-heptanal derivative showed no distinct molecular ion peak in the negative-ion mode (Fig. 3.11). The PQ-heptanal derivative has the simplest and clearest product ion spectra among the tested reagents-heptanal derivatives (Figures 3.4-3.10), in addition it afforded the highest sensitivity in the positive-ion mode (Figure 3.11). Hence, PQ was selected as the best derivatizing agent for further experiments.

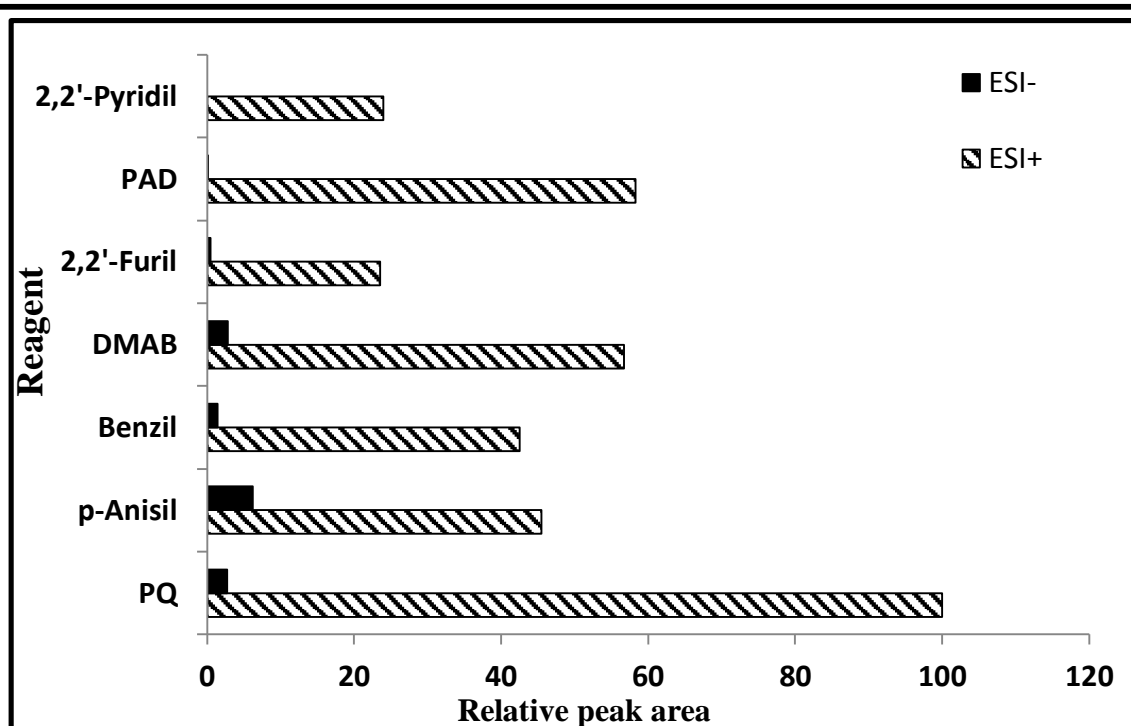


Fig. 3.11: Relative peak areas of heptanal derivatives of the studied reagents using ESI⁺ and ESI⁻ modes.

3-3-2. The MS/MS fragmentation pattern of PQ-aldehydes derivatives

PQ has been used as a fluorogenic reagent for guanidino group in alkaline solution¹⁰⁸. It has also been used as a complexing agent for the determination of many metals such as ruthenium(III), rhodium(III)¹⁰⁹, copper (II)^{110,111}, iron (III), Ni(II) and Co(II)¹¹¹. The use of PQ as a mass tagging agent for aliphatic aldehydes has not been previously reported, indicating the novelty of the proposed method. The suggested mechanism of the reaction of the α,β -diketo reagent PQ with aldehydes in the presence of ammonium acetate is shown previously in Fig. 3.1.

It is noteworthy that, all of the PQ-aldehydes derivatives gave the corresponding $[M+H]^+$ as well as two major common product ions with m/z values at 231.9 and 164.8 (Fig. 3.4) which were assigned to 2-methyl-1*H*-phenanthro[9,10-*d*]imidazole and

fluorene moieties, respectively, produced by the cleavage of the PQ-aldehyde derivative during the CID (Fig. 3.12). Although the product ion of m/z 164.8 has a higher response (1.3 times) than that of m/z 231.9, the later has better S/N. So, the MRM acquisitions were performed at the product ion with m/z value of 231.9.

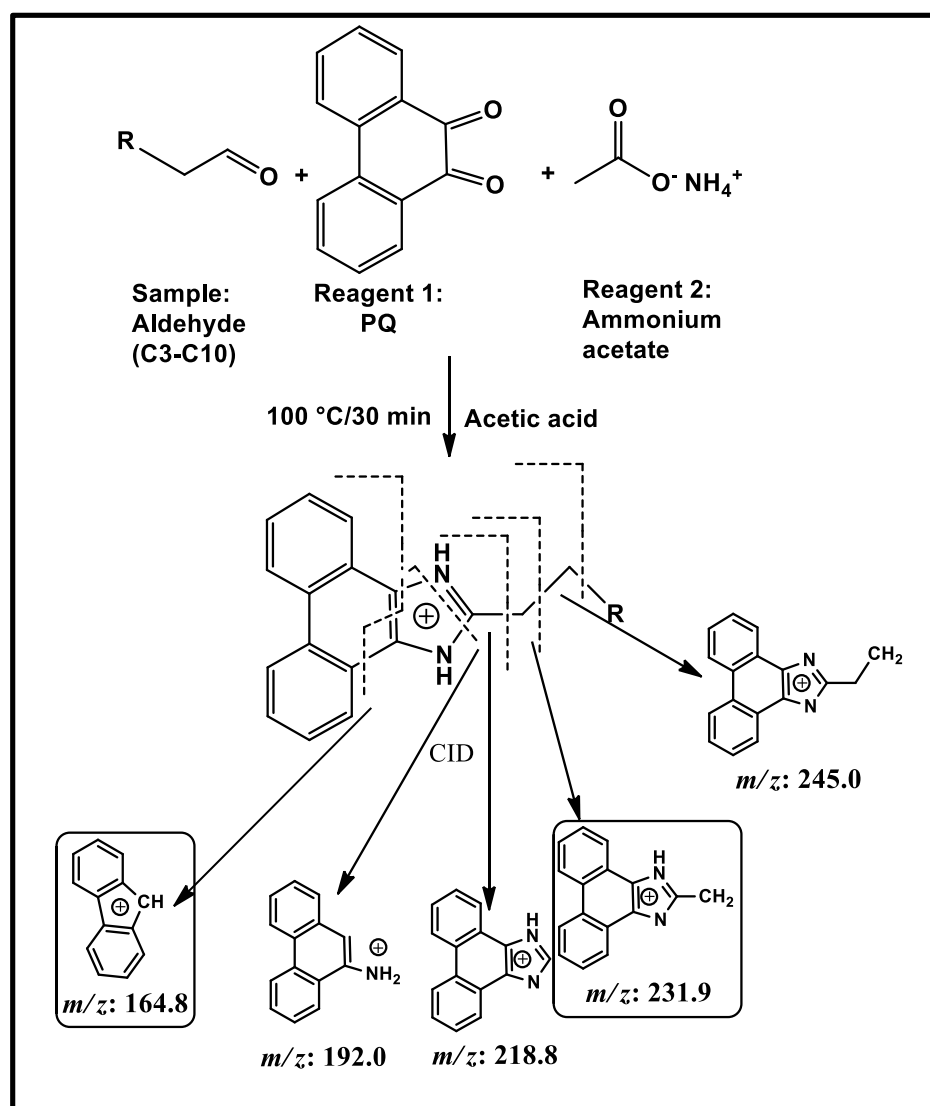
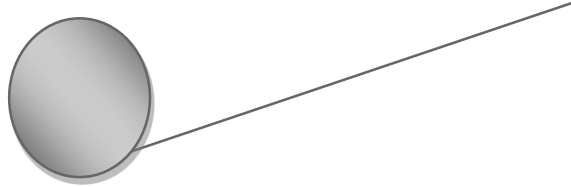


Fig. 3.12: The MS/MS fragmentation pattern of the formed product from the reaction of target aldehydes and PQ.



3-3-3. PQ selectivity for aldehydes

In order to monitor the selectivity of PQ for aldehydes in the presence of their isomers (ketones), we conducted the same reaction using acetone as a representative ketone. Then, we compared the obtained total ions spectrum of propanal (Fig. 3.13 A) and that of its ketone isomer (acetone) (Fig. 3.13 B). As illustrated in Fig. 3.13 A, in addition to the reagent peak at about m/z 209, a distinct precursor ion of PQ-propanal derivative is shown at m/z 247, while in Fig. 3.13 B, only the reagent peak appeared with no any precursor ion corresponding to acetone derivative of PQ. This finding conformed with the results obtained by our group which assured the selectivity of α,β -diketo compound to aldehydes in presence of acetone and 2-hydroxyacetophenone⁶⁵. Also, carboxylic acid didn't interfere also. Acetic acid is used as a catalyst for this type of reaction and conducting the reaction in the presence of it without any aldehyde did not produce any products. In Fig. 3.13 B where the reaction occur in presence of acetone (non-reactive substance toward our reaction as mentioned previously) and acetic acid (as a catalyst) we couldn't detect a precursor ion at 233 (if the carbonyl and hydroxyl group converted to diamine) or 249 (if only the carbonyl group reacted as in case of aldehydes). This confirmed the selectivity of PQ for aldehydes in presence of ketones and carboxylic acids, which is a very attractive advantage since most of the reported derivatizing reagents for aldehydes lack the selectivity^{64,84-96,98,99,104}.

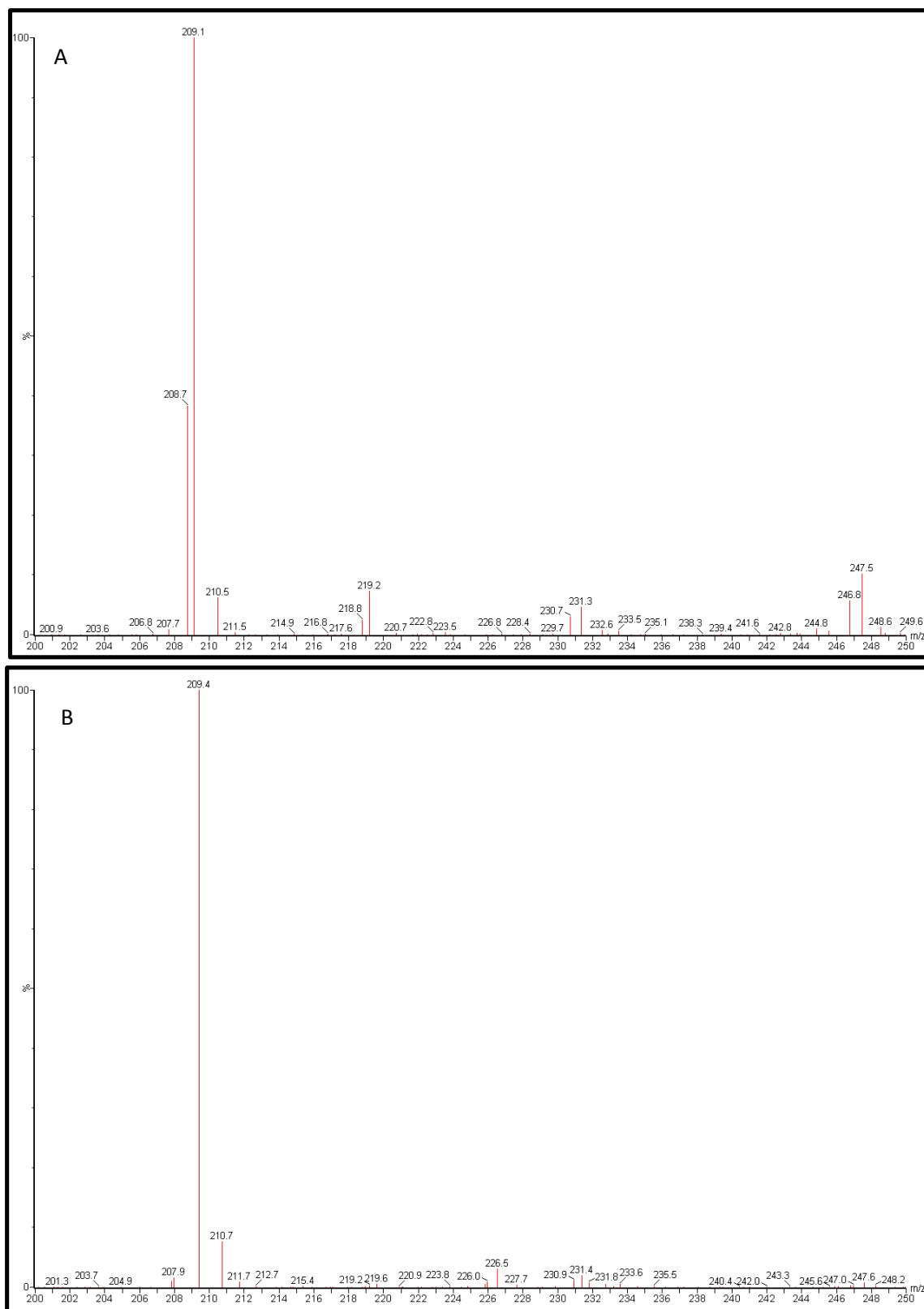


Fig. 3.13: Total ion spectra of (A) propanal derivative resulted from the reaction of propanal with PQ and ammonium acetate in presence of acetic acid and (B) reaction mixture of acetone with PQ and ammonium acetate in presence of acetic acid using ESI⁺.

3-3-4. Optimization of the derivatization conditions

Different derivatization conditions were investigated in order to obtain the highest derivatization efficiency. First, the effect of PQ concentration on the relative peak areas was studied using concentrations ranged from 1.0 to 12.0 mM. Constant response was obtained using 4.0 mM PQ, and further increase of the reagent concentration over this concentration did not affect the relative peak areas (Fig. 3.14). Further, the influence of the solvent used for preparation of PQ was evaluated using methanol and acetonitrile. Higher signal was obtained using acetonitrile as a solvent, so 4 mM PQ solution in acetonitrile was used in further experiments.

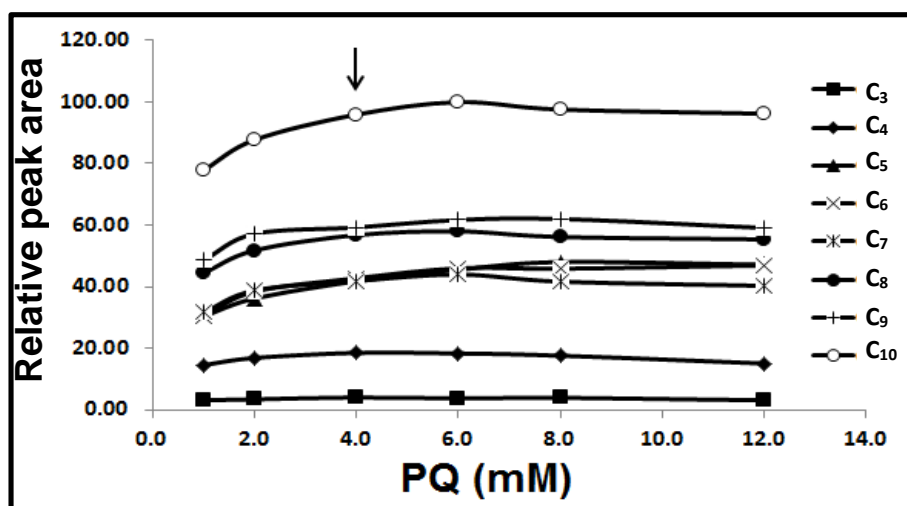


Fig. 3.14: Effect of PQ concentration on the relative peak area of the studied aldehydes derivatives (50.0 nM)

The effect of the concentration of ammonium acetate was also investigated from 0.1 to 4.0 M. The highest relative peak areas were obtained using 1.5 M ammonium acetate then a plateau was reached up to 4.0 M where a slight decrease in the response was observed (Fig. 3.15). Therefore, in this study 2.0 M of ammonium acetate was selected as the best concentration.

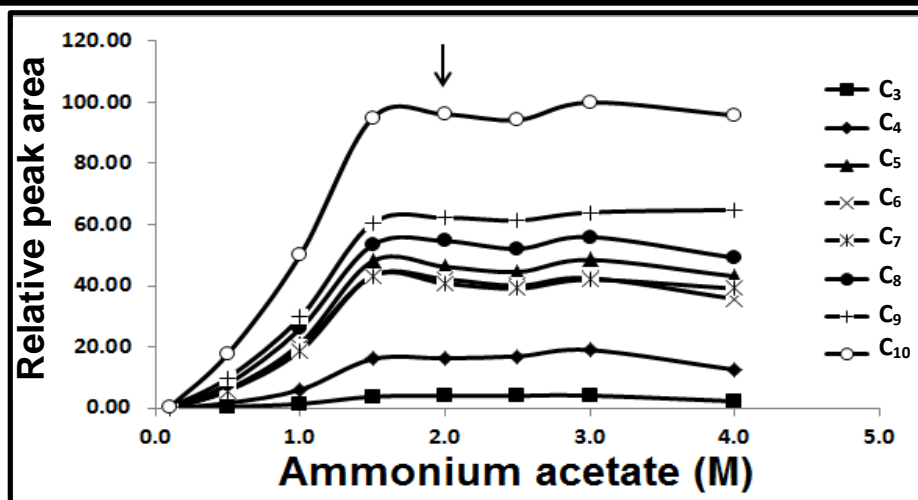


Fig. 3.15: Effect of ammonium acetate concentration on the relative peak area of the studied aldehydes derivatives (50.0 nM)

The reaction temperature was also studied from 40 to 110 °C, and the best response was obtained at 100 °C (Fig. 3.16). Additionally, the derivatization time was investigated from 5 to 60 min. Increasing the reaction time produced a corresponding increase in the analytical response up to 30 min, after which no further increase was obtained indicating that the reaction is completed (Fig. 3.17). Hence, the reaction was conducted at 100 °C for 30 min.

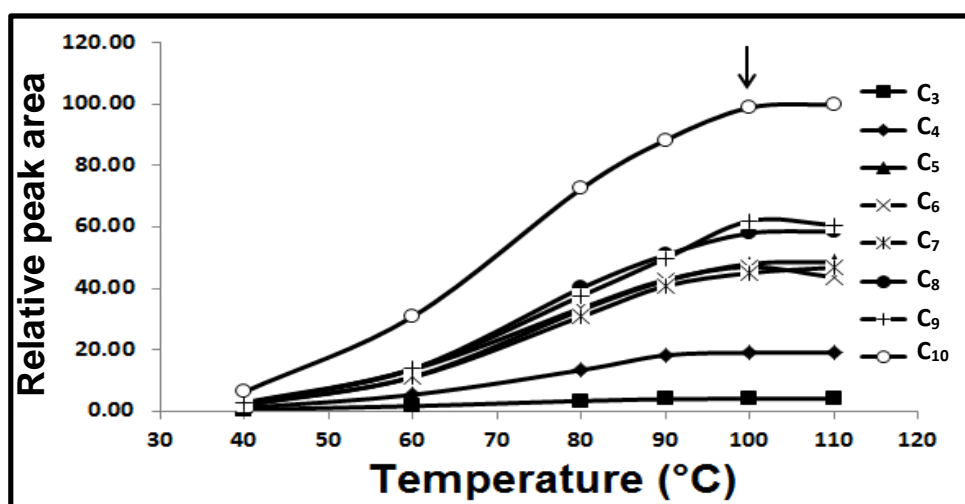


Fig. 3.16: Effect of reaction temperature on the relative peak area of the studied aldehydes derivatives (50.0 nM)

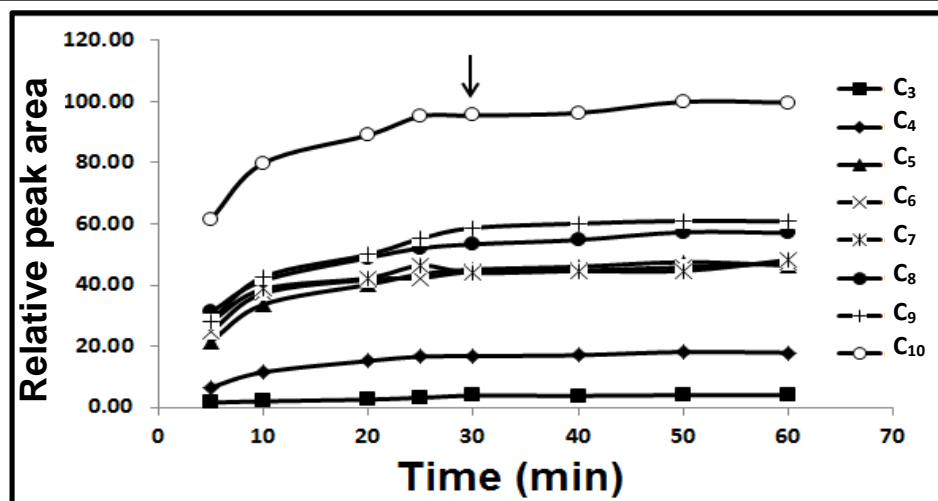


Fig. 3.17: Effect of reaction time on the relative peak area of the studied aldehydes derivatives (50.0 nM)

3-3-5. Optimization of HPLC separation and MS/MS monitoring

The LC/ESI-MS/MS operational conditions were optimized. 3-Phenylpropanal was selected as the IS since its chromatographic behavior ($t_R = 7.3$ min for IS and 6.3-9.2 min for the eight aldehydes) and extraction efficiency (102% for IS and 92.6-110.8% for the eight aldehydes) are similar to and perfectly matched with the studied aldehydes. Additionally, 3-phenylpropanal is a non-physiological aldehyde with derivatization reactivity approximate to our target analytes. As well, 3-phenylpropanal has the same fragmentation pattern and product ion (m/z 231.9) like the studied aldehydes. Full scan product ion spectrum of the PQ-IS derivative is shown in Fig. 3.18. The mass parameters including the cone and collision voltages were optimized to obtain the maximum response for the eight analytes. Table 3.1 illustrates the optimum parameters selected for each analyte and IS.

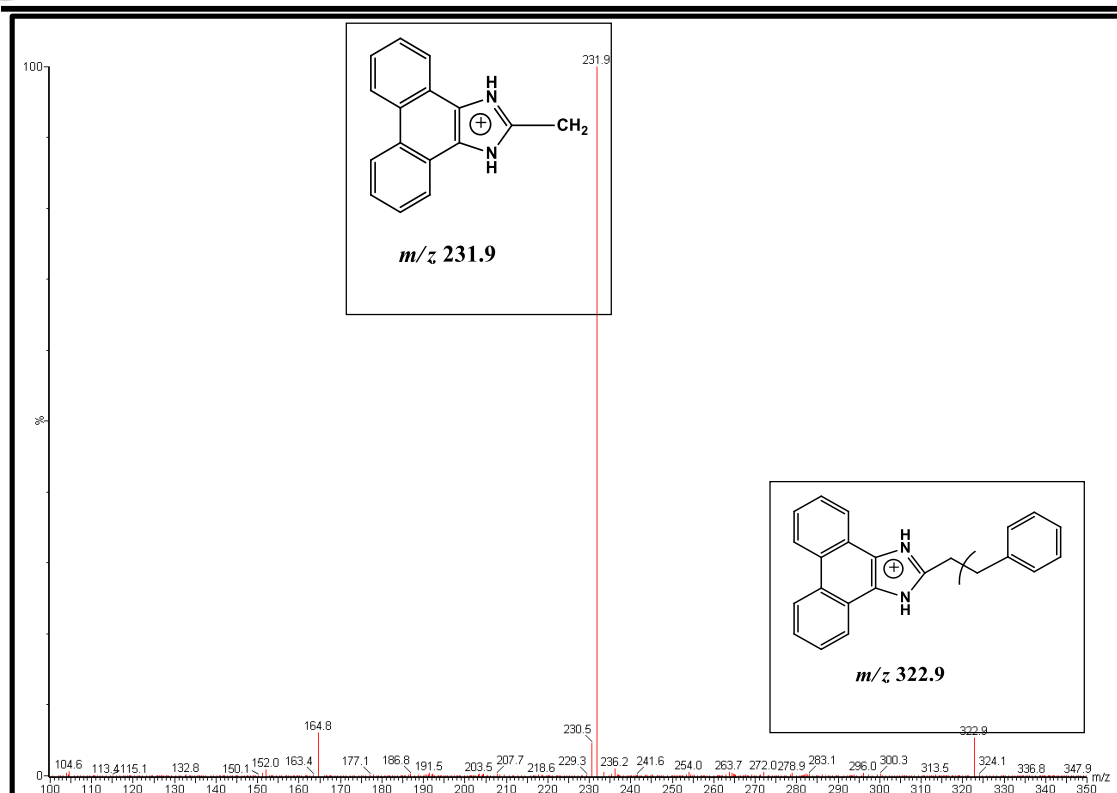
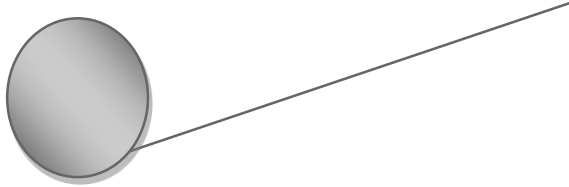


Fig. 3.18: Product ion spectrum of PQ-IS derivative

Besides, the mobile phase was optimized carefully to attain the best chromatographic behavior. In initial experiments, a mobile phase composed of 0.1% formic acid in methanol: 0.1% formic acid in water (8:2, v/v) was isocratically eluted with a 3C₁₈ column (100 mm x 4.6 mm i.d. 3 μ m particle size). Under these conditions, the separation of the eight analytes was not possible and there was a strong distortion of the peak shape for the eight aldehydes. Using the same mobile phase with a 5C₁₈ column (250 mm x 4.6 mm i.d., 5 μ m particle size) improved the peak shape for C₃-C₈ aldehydes to some extent, while no separation could be achieved between C₃-C₇ aldehydes.

Isocratic elution with a mobile phase consisted of methanol: ammonium formate buffer (20 mM, pH 4.0) (9:1, v/v) and a 3C₁₈ column (100 mm x 4.6 mm i.d., 3 μ m particle size) produced a substantial enhancement of the peak shape, yet, propanal and butanal were not efficiently separated. As well, the run time was long (22 min). Consequently,



we decided to investigate gradient elution with methanol as solvent A and ammonium formate buffer (20 mM, pH 4.0) as solvent B. The initial concentration of solvent A was studied from 60 to 90% and its final concentration was similarly studied from 90 to 100%. The gradient time was also studied from 1 to 5 min. Finally, based on resolution, sensitivity, and run time, we employed the gradient system described earlier in section “3-2-2.” for separation of the eight aldehydes. After method optimization, the target aldehydes were separated within 10 min (propanal was eluted at $t_R = 6.3$ min, butanal at $t_R = 6.7$ min, pentanal at $t_R = 7.0$ min, hexanal at $t_R = 7.5$ min, heptanal at $t_R = 7.8$ min, octanal at $t_R = 8.3$ min, nonanal at $t_R = 8.7$ min, decanal at $t_R = 9.2$ min, and the IS at 7.3 min).

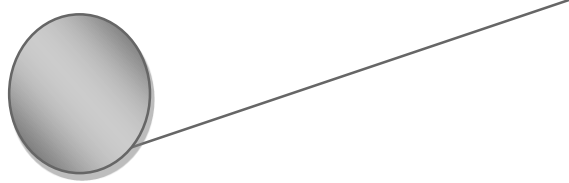
3-3-6. Validation study

Validation of the developed LC/ESI-MS/MS method was established following Guidance for Industry on Bioanalytical Method Validation⁶⁶. Calibration functions were fitted by a linear model:

$$Y = b + mX$$

Where: Y = relative peak area, X = aldehyde concentration spiked to serum in nM, m = slope of the regression line, and b = intercept of the regression line.

Excellent correlation coefficients (> 0.999) were obtained for the eight studied aldehydes (Table 3.3). The LOQ was also calculated for the target aldehydes and found to be ranged from 0.01 to 0.25 nM with accuracy ranged from -6.0 to 9.4% and precision $\leq 17.3\%$. In addition, the LOD was determined for the studied aldehydes and found to be within the range of 0.004-0.1 nM (Table 3.3). Such results indicated the linearity, high



sensitivity, and applicability of the method for quantification of trace levels of aldehydes in biological fluids.

Table 3.3 Collective regression data, LOD, LOQ, accuracy and precision at LOQ for the studied aldehydes in serum

Compound	LOD ^a , nM (fmol/injection)	LOQ ^b (nM)	Accuracy at LOQ (%)	Precision at LOQ (% RSD)	Range (nM)	Regression equations ^c , <i>n</i> = 3	<i>r</i> ^d
Propanal	0.100 (2.0)	0.25	6.2	12.5	0.25-200	Y= 0.0017+0.0010X	0.9997
Butanal	0.050 (1.0)	0.10	9.4	17.3	0.1-200	Y= 0.0125+0.0044X	0.9995
Pentanal	0.013 (0.26)	0.05	-5.5	11.4	0.05-100	Y= 0.0590+0.0110X	0.9991
Hexanal	0.027 (0.54)	0.05	7.3	8.6	0.05-100	Y= 0.0869+0.0100X	0.9991
Heptanal	0.010(0.20)	0.05	-2.2	9.9	0.05-100	Y= 0.0120+0.0112X	0.9997
Octanal	0.012 (0.24)	0.05	-4.9	6.9	0.05-100	Y= 0.0193+0.0143X	0.9991
Nonanal	0.018 (0.36)	0.05	1.7	16.3	0.05-100	Y=0.0268+0.0151X	0.9991
Decanal	0.004 (0.08)	0.01	-6.0	12.7	0.01-50.0	Y= 0.0108+0.0254X	0.9993

^a S/N= 3.

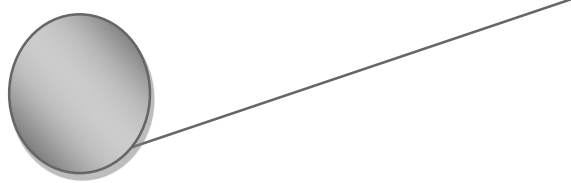
^b S/N \geq 5.

^c Y= relative peak area (IS: 100 nM 3-phenylpropanal), X= aldehyde concentration (nM).

^d Correlation coefficient.

Results for the study of accuracy, stated as the deviation of the mean values from the true values, and precision (% RSD) are illustrated in Table 3.4. As can be seen, the proposed method exhibited acceptable accuracy (-13.8 to 9.0%) and satisfactory precision (% RSD ranged from 0.1 to 11.7% in case of intra-day precision and from 1.4 to 13.4% for inter-day precision).

The recovery of the target aldehydes was estimated by comparing the response of extracted serum and un-extracted standard (denotes 100% recovery) at three concentrations (0.5, 5.0, and 50.0 nM). The recoveries were found to be ranged from 92.6 to 110.8% (Table 3.5).



The stability of the aldehydes and IS solutions was evidenced at room temperature up to 6 h, and at 4 °C up to 1 week. No significant variation was observed in both cases in respect to the response of fresh solutions. Additionally, the PQ solution showed high stability at 4 °C up to 2 months. The stability of the derivatized aldehydes kept in sealed vials at 4 °C was demonstrated for 48 h which guarantees the stability of the processed samples during the resident time in the auto sampler.

The results of validation study agreed well with the requirements of the Guidance for Industry on Bioanalytical Method Validation⁶⁶ proving the suitability of the proposed method to screen the studied aldehydes in human serum.

Table 3.4 Accuracy and precision of the proposed method for the determination of the studied aliphatic aldehydes in spiked serum samples.

Aldehydes	Spiked Conc. (nM)	Intra-day (<i>n</i> = 5)			Inter-day (<i>n</i> = 5)		
		Found conc. (nM)	Accuracy (%)	Precision (% RSD)	Found conc. (nM)	Accuracy (%)	Precision (% RSD)
Propanal	0.5	0.488	-2.4	7.2	0.521	4.2	10.5
	5	4.74	-5.2	6.0	5.01	0.2	3.2
	50	50.3	0.6	2.2	51.0	2.0	5.1
Butanal	0.5	0.488	-2.4	6.8	0.542	8.4	11.3
	5	4.94	-1.2	5.2	5.05	1.0	2.7
	50	50.2	0.4	1.9	50.7	1.4	4.2
Pentanal	0.5	0.431	-13.8	11.7	0.536	7.2	7.3
	5	5.05	1.0	7.1	5.00	0.0	1.9
	50	54.5	9.0	2.1	52.9	5.8	5.4
Hexanal	0.5	0.479	-4.2	7.7	0.532	6.4	6.9
	5	4.35	-13.0	10.6	4.94	-1.2	7.8
	50	50.5	1.0	0.5	50.1	0.2	1.7
Heptanal	0.5	0.505	1.0	5.2	0.507	1.4	10
	5	5.04	0.8	1.8	5.08	1.6	1.4
	50	49	-2.0	0.3	49.4	-1.2	1.9
Octanal	0.5	0.524	4.8	4.8	0.527	5.4	6.5
	5	5.07	1.4	3.4	5.22	4.4	1.7
	50	48.9	-2.2	0.6	52.4	4.8	8.2
Nonanal	0.5	0.496	-0.8	4.3	0.489	-2.2	13.4
	5	5.18	3.6	7.5	5.06	1.2	2.7
	50	49.7	-0.6	0.8	50.4	0.8	10.7
Decanal	0.5	0.544	8.8	9.4	0.497	-0.6	13.2
	5	4.99	-0.2	2.0	4.98	-0.4	4.1
	50	50.2	0.4	0.1	54.5	9.0	11.1

Table 3.5 Results of recovery study of the target of aliphatic aldehydes from spiked serum samples after salting out LLE.

Spiked				Spiked			
Aldehyde	Conc. (nM)	% Recovery	SD	Aldehyde	Conc. (nM)	% Recovery	SD
Propanal	0.5	97.2	14.5	Heptanal	0.5	96.6	5.8
	5	103.8	3.0		5	98.8	2.1
	50	110.8	2.0		50	96.6	2.7
Butanal	0.5	99.8	4.3	Octanal	0.5	98.6	8.8
	5	102.4	5.5		5	100.0	3.0
	50	103.8	2.9		50	99.2	1.6
Pentanal	0.5	106.2	4.5	Nonanal	0.5	96.8	3.3
	5	102.2	11.5		5	92.6	2.5
	50	98.2	3.0		50	95.8	0.7
Hexanal	0.5	96.8	6.2	Decanal	0.5	98.0	7.6
	5	104.6	6.9		5	99.2	3.2
	50	100.8	1.4		50	100.8	0.3

3-3-7. Application of the proposed LC/ESI-MS/MS method to determination of the target aldehydes in human serum

For application of the developed LC/ESI-MS/MS method to the quantitation of the target aliphatic aldehydes (propanal, butanal, pentanal, hexanal, heptanal, octanal, nonanal, and decanal) in human serum, a key factor to be considered is the choice and optimization of an efficient extraction procedure. In the course of this study, different extraction techniques were investigated including protein precipitation (PPT) with methanol, sub-zero temperature LLE with acetonitrile, and salting out LLE using

acetonitrile/NaCl. The best recoveries for the eight analytes ($\geq 92.6\%$) with accurate and reproducible results were attained using the salting out LLE method (Figure 3.19).

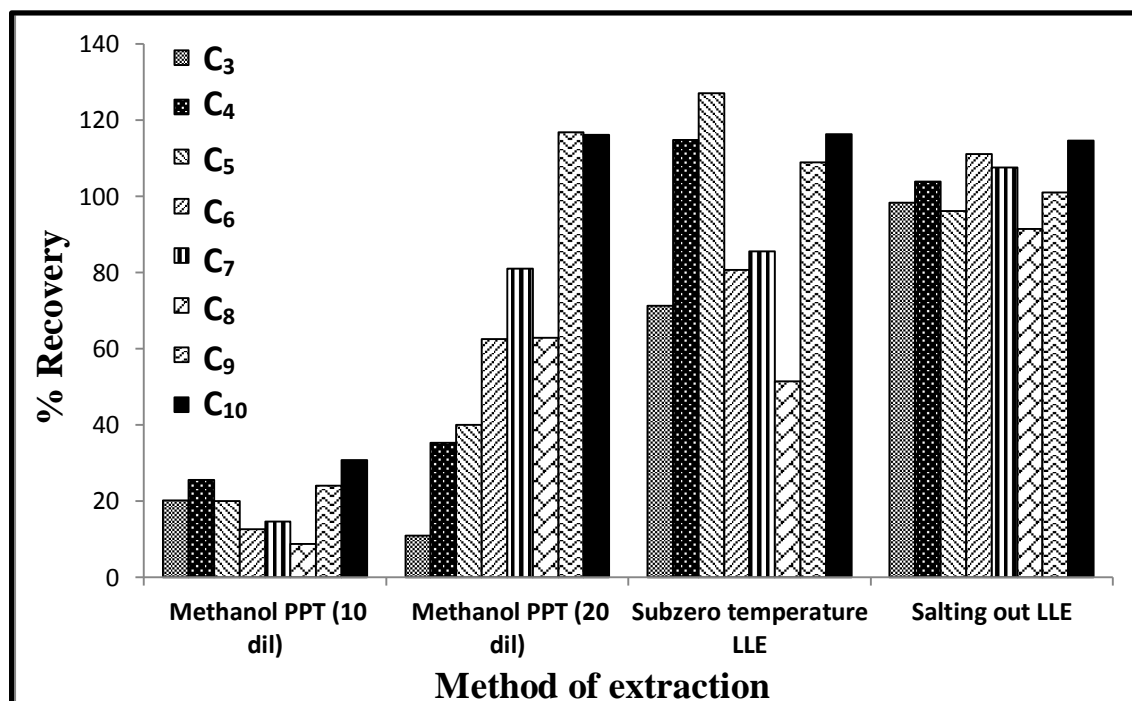
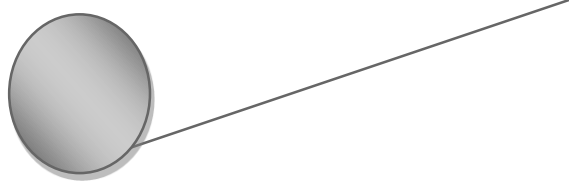


Figure 3.19: Recovery of the studied aldehydes from serum after PPT with methanol (10 or 20 folds dilution of serum), subzero-temperature LLE and salting out LLE.

Hence, the levels of the target aldehydes (C₃-C₁₀) were determined in the serum of 14 healthy volunteers using the developed method (Table 3.6). The eight target aldehydes were detected and quantified in all serum samples. Figure 3.20 shows a MRM chromatogram of the aldehydes detected in serum of a healthy volunteer. The levels of the aldehydes found in the serum using the proposed method are in accordance with those reported in the literature (Table 3.6).^{65,94,95}

**Table 3.6** Levels of the target aliphatic aldehydes in healthy human serum

Aldehydes	Range, nM ^a	Mean \pm SD, nM ^a	Previously reported level, nM ^{65,94,95}	Ref
Propanal	7.2-68.8	26.2 \pm 4.6	34.0	94
Butanal	21.7-40.0	27.7 \pm 1.4	35.0	94
Pentanal	41.2-88.4	60.7 \pm 3.5	37.0	94
Hexanal	1.8-21.7	11.0 \pm 1.6	1.8 - 15.2	65,95
Heptanal	0.1-11.6	3.5 \pm 0.9	1.1 - 15.2	65,95
Octanal	0.1-11.9	2.6 \pm 0.9	1.7 $>$	65,94
Nonanal	0.2-73.6	27.2 \pm 6.7	1.0 \geq - 25.0	65,94
Decanal	0.1-2.1	1.1 \pm 0.2	0.8 \geq - 1.5	65

^a n=14, 10 Males + 4 Females, age = 38.4 \pm 13.1 years.

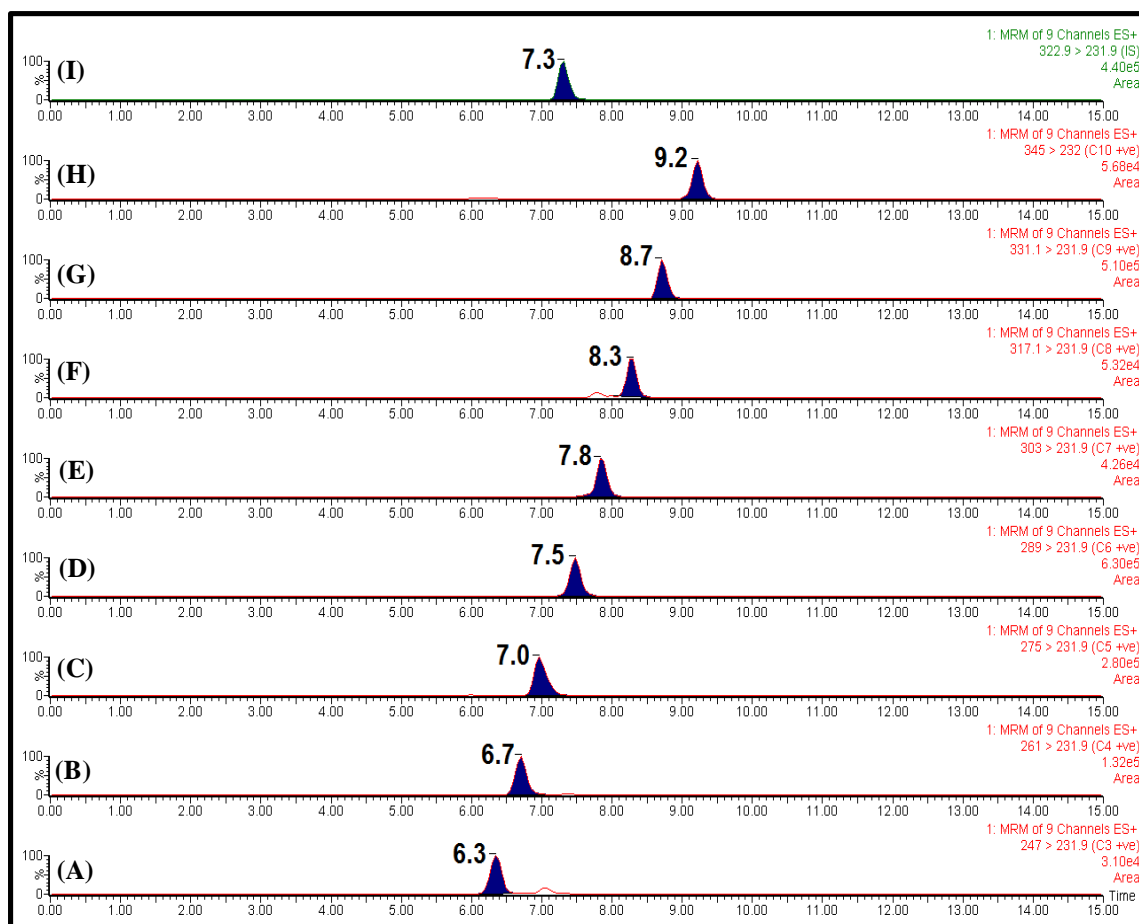
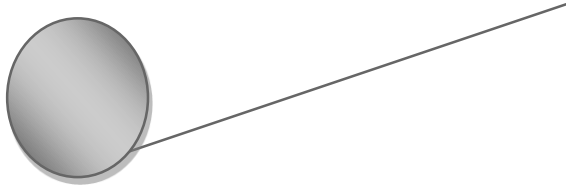


Fig. 3.20: Representative chromatograms of the target aliphatic aldehydes and IS in serum after derivatization with PQ where (A) propanal, (B) butanal, (C) pentanal, (D) hexanal, (E) heptanal, (F) octanal, (G) nonanal, (H) decanal, and (I) IS (100 nM)



3-3-8. Comparison of the developed method and reported methods for aldehydes determination in biological fluids

For evaluation of the newly developed LC/ESI-MS/MS method, we compared it with the methods found in the literature for determination of aldehydes in biological fluids (Table 3.7). Our method has much lower LODs than the reported methods^{47,64,65,68,89–91,94–96,99,102,103} yielding high sensitivity of about 19 to 1000 folds. This high sensitivity made the proposed method well-suited for trace quantification of aldehydes in biological fluids at low picomolar concentration levels (4.0 to 100 pM) .

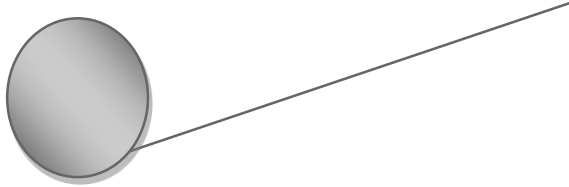
Additionally, the novel derivatizing agent PQ allows highly selective MS/MS detection of the aldehydes without any interference from other carbonyl compounds. This advantage overcame the problem of selectivity associated with the use of hydrazine-based derivatizing reagents^{64,89–91,95,96}. As well, the derivatization reaction is rapid and simple one-pot reaction giving a stable water-soluble reaction product does not require either extraction or evaporation/reconstitution steps prior analysis with LC/ESI-MS/MS. Additional advantages associated with the use of PQ reagent are its commercial availability and stability. Furthermore, the product ion spectra of PQ derivatives of aldehydes were clear and simple.

In spite that our main target matrix is human serum, it is worth noting that the developed method exhibited superior sensitivity to most of the reported methods for determination of aldehydes in environmental samples like air and water^{85–88,92,98}. Although our method has a comparable sensitivity to the LC-MS/MS method of Sun et al.,¹⁰⁴ our method is better than this one regarding rapidness, selectivity and commercial availability of the derivatizing agent.

Table 3.7 Comparison of the proposed and reported methods for determination of aldehydes in biological fluids

Analyte/matrix	Derivatization conditions		Analytical method	LOD, nM	% Recovery	Ref.
	Reagent	Temp °C/ time (min)				
C ₆ ,C ₇ /human blood	DNPH	40/20	HPLC-UV	0.79-0.8	75.2-101.1	89
C ₆ ,C ₇ /human blood	DNPH	40/10	HPLC-UV	7.9-2.34	67.84-70.28	90
C ₆ ,C ₇ /human plasma	DNPH	N/A ^a	HPLC-UV	2.4-3.6	83-87	91
C ₁ -C ₁₂ /human serum	BODIPY-aminozide	60/30	HPLC-FL	0.43-0.69	95-105	94
C ₆ ,C ₇ ,C ₉ , malondialdehyde, α,β -unsaturated aldehydes/exhaled breath condensate	DNPH	RT/60	LC/APCI-MS/MS	1 (for C ₆ ,C ₇ ,C ₉)	N/A ^a	64
C ₆ ,C ₇ /human blood	DNPH	N/A ^a	LC/APCI-MS/MS	0.076-0.17	94-110	95
aldehydes and ketones/mice plasma	DNSH	RT/240	LC/ESI-MS/MS	0.2-4	70.3-111.8	96
C ₆ ,C ₇ , acetone/human serum	PFBHA	40/8	GC/MS	0.24-0.32	88-92	99
C ₆ -C ₁₀ /human serum	2,2'-Furil	100/30	HPLC-FL	0.25-0.5	88-105	65
C ₅ -C ₁₀ , malondialdehyde, trans-2-pentanal/human urine	4-ACP	10/180	LC-MS/MS	3.0	N/A ^a	68
C ₆ -C ₁₀ , alkenals, hydroxyalkenals/human plasma	CHD	60/60	LC-MS/MS	(10-100 Pg)	N/A ^a	102
C ₃ -C ₁₀ /human serum	PQ	100/30	LC-MS/MS	0.004-0.1 (0.01-0.1 pg)	92.6-110.8	Proposed method

^a N/A: Not available



3-4. Conclusions

We optimized and validated an ultra-sensitive, selective, and rapid LC/ESI-MS/MS method for the monitoring of aliphatic aldehydes (C₃-C₁₀) as lipid peroxidation biomarkers in human serum. It has been shown that aldehydes are readily derivatized with PQ forming imidazole derivatives that can be easily determined by ESI-MS/MS in the positive ionization mode with LOD values within the range of 4 to 100 pM. Aldehyde derivatization followed by LC/ESI-MS/MS yielded higher sensitivity and selectivity than existing HPLC-FL or UV detection methods. As well, our newly developed LC/ESI-MS/MS method is superior to other LC-MS/MS methods for aldehyde quantification with regard to sensitivity, selectivity and rapidness. Thus, the developed method proved to be ideal for analyzing aldehydes in human serum. Based on the obtained results, we believe that our newly developed mass-tagging reagent PQ is very useful and superior to other available reagents for establishing the level of low and medium chain aliphatic aldehydes (C₃-C₁₀) in biological fluids.

Chapter IV

**Development of an isotope-coded derivatization
LC/ESI-MS/MS assay for reactive aldehydes in
human serum using $^{14}\text{N}/^{15}\text{N}$ ammonium acetate
and 9,10-phenanthrenquinone**

4-1. Introduction

HNE is the foremost 4-hydroxy-2-alkenals end-product, produced by decomposition of ω -6 PUFAs¹⁰, while HHE is a main 4-hydroxy-2-alkenal resulted from the oxidative damage to ω -3 PUFAs, e.g. docosahexaenoic acid and eicosapentaenoic acid⁴⁶. Both of HNE and HHE are very reactive compounds since they contain three functional groups (Fig. 4.1): (i) C₂=C₃ double bond which can react *via* Michael additions with biomolecules containing nucleophilic moieties such as thiols, primary and secondary amines or undergo reduction or epoxidation, (ii) C₁ carbonyl group which can give acetal/thioacetal or can undergo Schiff-base formation, oxidation, or reduction, and (iii) 4-hydroxyl group which can be oxidized to a ketone^{46,112}.

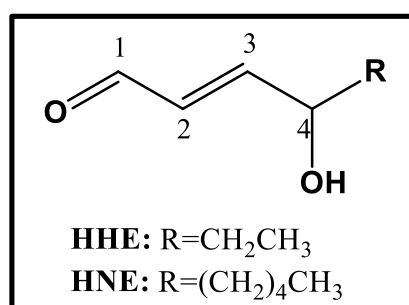
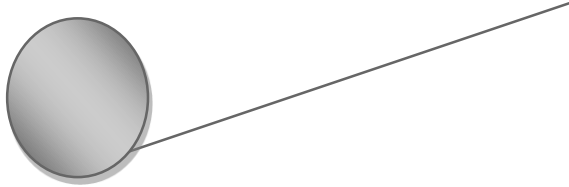


Fig. 4.1: Structures of HNE and HHE.

A May, 2016 PubMed search for “4-hydroxynonenal or 4-hydroxy-2-nonenal” retrieved 4153 articles, while a search for “4-hydroxyhexenal or 4-hydroxy-2-hexenal” identified 132 articles only. Though it is not well studied like HNE, HHE is biologically important in systems rich in ω -3 PUFAs such as the central nervous system and retina. Both of HHE and HNE have common properties but there are important differences between them, particularly with respect to adduction targets and detoxification routes⁴⁶.

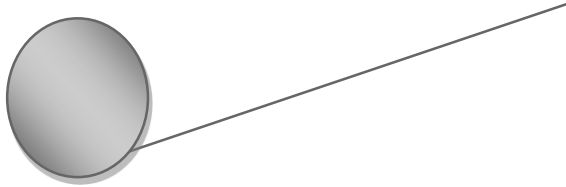
The *in vivo* experiments using ³H-HHE revealed that it bounds hepatic proteins but not DNA or RNA¹¹³. Despite that, HHE, like HNE, is genotoxic, but the mechanism of its genotoxicity is not yet clear^{114,115}. Additionally, the levels of HHE-



phosphatidylethanolamine adducts were 2 folds greater than those of HNE-phosphatidylethanolamine adducts in retina isolated from diabetic rats ¹¹⁶. As well, the experiments revealed that HHE and HNE have different protein targets in the primary cerebral cortical neurons due to the difference in their lipophilicity ¹¹⁷.

HHE was found to be 20-30 folds more reactive towards glutathione metabolism than HNE in the lipid-rich brain tissue ^{118,119} due to the higher lipophilicity of HNE allowing it to diffuse into the lipophilic microenvironment with less capacity to interact with glutathione than HHE ⁴⁶. As well, the enzyme aldehyde dehydrogenase 5A utilized HNE more than HHE ¹¹⁷ since the carbon tail of HNE is necessary for positioning at the enzyme active site ¹²⁰.

As we discussed in Chapter II, some analytical methods are reported for the determination of HNE in different matrices ^{11,60-63}. As well, some methods were also developed for the simultaneous quantification of HHE and HNE. Two GC/MS methods were applied for the simultaneous determination of HHE and HNE either alone or among other aldehydes after derivatization with PFBHA in copper-oxidized human LDL ¹²¹ and in the liver of mice intraperitoneally injected with bromobenzene ¹²². Also, a HPLC-UV ¹²³ and a LC-MS/MS ¹²⁴ methods were used for determination of HHE and HNE in oil samples following derivatization with DNPH. Additionally, HHE and HNE were determined with other aldehydes in biological fluids by LC-MS/MS after derivatization with DNPH ⁶⁴, CHD ¹⁰² or DNSH ⁹⁶. These methods suffered from some drawbacks such as the need for unavailable deuterated ISs which necessitates time consuming and tedious synthesis procedure ¹²¹, and long derivatization time ^{64,96,102,122-124}. As well, derivatization with DNPH ^{63,64,123,124} and DNSH ⁹⁶ involves many shortcomings such as poor selectivity, likely interferences from ketones and carboxylic acids and the formation of two



stereoisomeric hydrazone derivatives. In addition, DNPH is a flammable, unstable and irritant reagent ⁶⁵.

The development of a valid analytical method for determination of these two highly reactive 4-hydroxy-2-alkenals in biological samples is very important in order to evaluate their role in different diseases onset and progression. To the best of our knowledge, the scientific literature lacks a reliable and rapid analytical method with high sensitivity enough to allow simultaneous determination of HHE and HNE in human serum under normal and pathological conditions. This fact encouraged us to develop and validate a highly sensitive isotope-coded derivatization (ICD) LC/ESI-MS/MS method for the simultaneous determination of HHE and HNE in human serum.

LC/ESI-MS/MS is a powerful method that enables rapid analysis with outstanding sensitivity. Yet, matrix effects caused by co-existing substances often occur while analyzing metabolites by LC-MS/MS. In addition, the ion abundance may differ from run to run, even for the same analyte, due to instrumental drift or technical troubles. As a result, IS is required to keep accuracy of the quantification. A stable isotope-labeled analogue of the analyte is appropriate for this purpose. However, the number of commercially available isotope-labeled analogues is restricted and their synthesis in the laboratory is a laborious and expensive process. Hence, ICD has been recently introduced to overcome this problem. For ICD, a stable isotope moiety is introduced to the analyte and the formed derivative can be used instead of isotope-labeled analogue of the analyte ¹⁰⁵. In ICD, the sample is derivatized with a light reagent (¹H, ¹²C or ¹⁴N-coded reagent), while the standard is derivatized with a heavy reagent (²H, ¹³C or ¹⁵N coded reagent). Then, the two derivatives are combined and submitted to LC-MS/MS. The two isotopes

are eluted at the same retention time in the same run and their ionization is estimated to be the same ¹⁰⁵.

In Chapter III, saturated aliphatic aldehydes (C₃-C₁₀) were derivatized with PQ/ammonium acetate and determined by LC/ESI-MS/MS. In this work, we extend this reaction to develop a convenient and practical ICD LC/ESI-MS/MS for determination of HHE and HNE simultaneously in human serum using ¹⁴N/¹⁵N-ammonium acetate as ICD reagent (Fig.4.2). The use of ¹⁴N/¹⁵N-ammonium acetate is very advantageous from commercial availability and cost-effectiveness point of view. In addition, it will avoid the chromatographic isotopic effect that emerges upon using hydrogen/deuterium isotope pairs ¹²⁵. Another aim of this work is to apply the developed method for monitoring and comparing the levels of HHE and HNE in serum of healthy controls and human subjects with different diseased conditions including diabetes mellitus, rheumatoid arthritis and cardiac disorders.

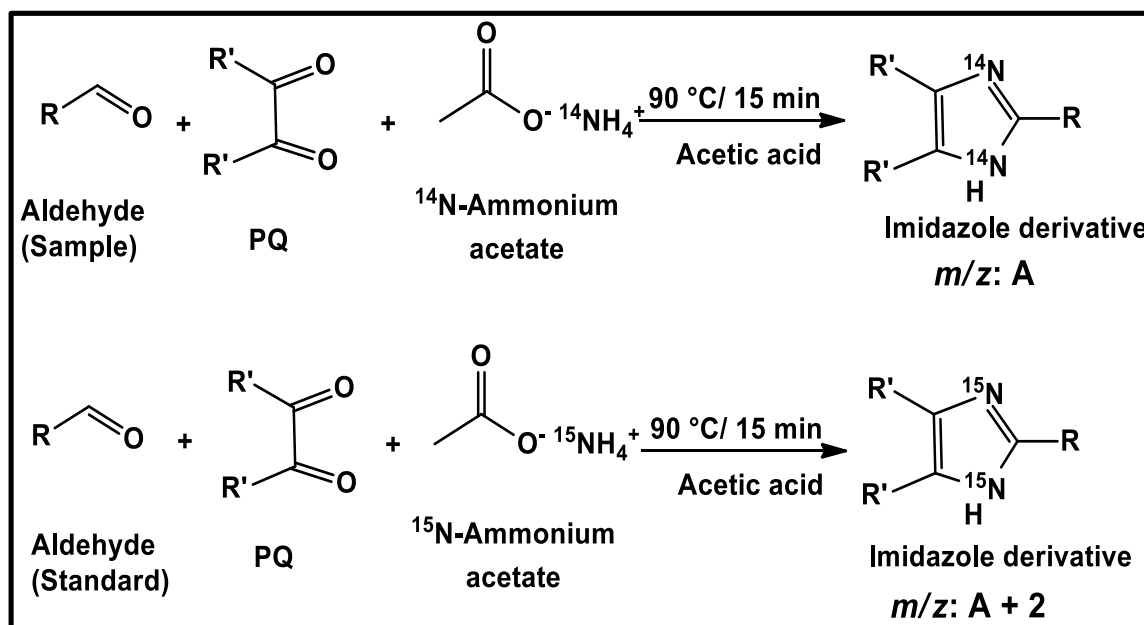
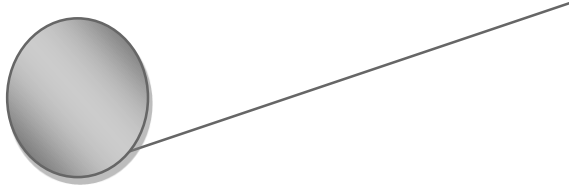


Fig. 4.2: Reaction pathway of the target aldehydes with PQ and ¹⁴N/¹⁵N ammonium acetate



4-2. Experimental

4-2-1. Materials and reagents

^{15}N ammonium acetate was obtained from Sigma Aldrich. HHE (1%, w/v) and HNE (1%, w/v) were obtained from Cayman Chemical Co. All other chemicals were as described in Chapter III under section “3-2-1.”

Stock solutions of HHE and HNE (200.0 μM) were separately prepared in acetonitrile. A mixed aldehydes standard solution containing 4.0 μM of each aldehyde was prepared daily in acetonitrile. Dilution of this solution was made as needed to obtain the required concentration levels. In addition, a mixed standard solution (4.0 μM HHE + 0.8 μM HNE) was prepared in water. All aldehydes solutions were stored at $-80\text{ }^\circ\text{C}$. PQ solution (22.0 mM) was prepared in acetonitrile. Solutions of ^{14}N and ^{15}N ammonium acetate (3.0 M) were prepared in glacial acetic acid. Reagents solutions were stored at $4\text{ }^\circ\text{C}$.

4-2-2. Instrumentation and LC/ESI-MS/MS conditions

Specifications of the LC/ESI-MS/MS system were the same as described in Chapter III under section “3-2-2.” A Cosmosil 3C₁₈-AR-II (100 mm \times 4.6 mm i.d., 3 μm particle size) was operated at $25\text{ }^\circ\text{C}$ and gradient elution was employed using mobile phase (A): methanol and mobile phase (B): ammonium formate buffer (20 mM, pH 4.0). For the first 30 S, the amount of mobile phase (A) was linearly increased from 95 to 100%, from 0.5 to 7 min the amount of mobile phase (A) was kept at 100%. The initial composition of the mobile phase was re-established for 5 min before starting a new run. The flow rate was 0.5 mL/min.

ESI⁺-MS/MS data acquisition was done at a capillary voltage of 5.0 kV, source temperature of 120 °C, desolvation gas temperature of 350 °C and flow rate of 500 L/h, and cone gas flow rate of 40 L/h. MRM mode was used for detection of the formed derivatives by CID. A summary of the cone voltage, collision voltage, precursor ions and product ions for the studied analytes is illustrated in Table 4.1.

Table 4.1 Optimum MS/MS conditions for the analysis of PQ derivatives of the studied aldehydes

Aldehyde	Cone voltage (V)	Collision voltage (V)	Precursor ion	Product ion
HHE-PQ-¹⁴N	40	25	303.2	231.3
HHE-PQ-¹⁵N	40	30	305.2	233.3
HNE-PQ-¹⁴N	40	30	345.2	231.3
HNE-PQ-¹⁵N	40	35	347.2	233.3

4-2-3. Clinical samples

All experiments conducted with human subjects were approved by the Ethics Committee of the School of Pharmaceutical Sciences, Nagasaki University. Sasebo Chuo Hospital kindly supplied us with 34 human serum samples including 16 healthy control (9 males and 7 females; mean age 39.3±12.3), 8 rheumatic patients (one male and 7 females; mean age 67.5±8.8), 5 diabetic patients (2 males and 3 females; mean age 52.6±16.2) and 5 cardiac disorder patients (2 males and 3 females; mean age 77.0±6.5). All serum samples were kept at -80 °C until analyzed.

4-2-4. Derivatization procedure for elucidation of product ion spectra

Aliquots of 150 μL of aldehydes standard solutions were mixed with 50 μL of 22.0 mM PQ and 100 μL of 3.0 M $^{14}\text{N}/^{15}\text{N}$ ammonium acetate in a screw capped vial. The mixture was heated at 90 $^{\circ}\text{C}$ for 15 min then cooled and filtered with 0.45 μm cellulose acetate membrane filter. The solutions were injected to ESI-MS/MS system *via* syringe pump to elucidate product ion spectra.

4-2-5. Assessment of ICD technique for relative quantification

The suitability of the developed ICD method for relative quantification was evaluated according to Dai et al. ¹²⁶ by applying the following methods: (i) specific concentrations of analytes (0.25, 0.5 and 1.0 μM) were individually labeled with PQ- ^{14}N ammonium acetate (light labeling) and analytes with concentration of 0.5 μM were labeled with PQ- ^{15}N ammonium acetate (heavy labeling). The aldehyde-PQ- ^{14}N and aldehyde-PQ- ^{15}N derivatives were mixed in equal volumes. Mixtures containing aldehyde-PQ- ^{14}N /aldehyde-PQ- ^{15}N derivatives in the ratios of 1:2, 1:1 and 2:1 were analyzed by LC/ESI-MS/MS to study the signal intensity of aldehyde-PQ- ^{14}N and aldehyde-PQ- ^{15}N derivatives. (ii) Aldehydes standards were individually labeled with PQ- ^{14}N ammonium acetate and PQ- ^{15}N ammonium acetate. Then, the aldehyde-PQ- ^{14}N and aldehyde-PQ- ^{15}N were mixed in different ratios (1:10, 1:5, 1:2, 1:1, 2:1, 5:1 and 10:1) and analyzed by LC/ESI-MS/MS.

4-2-6. Serum samples treatment and ICD protocol

A salting out LLE procedure was used for extraction of HHE and HNE from serum samples. Aliquots of 200 μL of serum samples were mixed with 400 μL acetonitrile and 0.15 g NaCl then centrifuged at 7500 $\times g$ for 10 min. A volume of 150 μL of the supernatant was subjected to the derivatization procedure mentioned in section "4-2-4"

using light labeling by PQ and ^{14}N ammonium acetate (Solution A). Aqueous aldehydes mixed standard solution ($4.0\ \mu\text{M}$ HHE + $0.8\ \mu\text{M}$ HNE) was similarly extracted by salting out LLE followed by derivatization using heavy labeling with PQ and ^{15}N ammonium acetate (solution B). The two solutions were cooled and filtered with $0.45\ \mu\text{m}$ cellulose acetate membrane filter. Solutions A and B were mixed in 3:1 ratio, respectively and analyzed by the LC/ESI-MS/MS (Fig. 4.3).

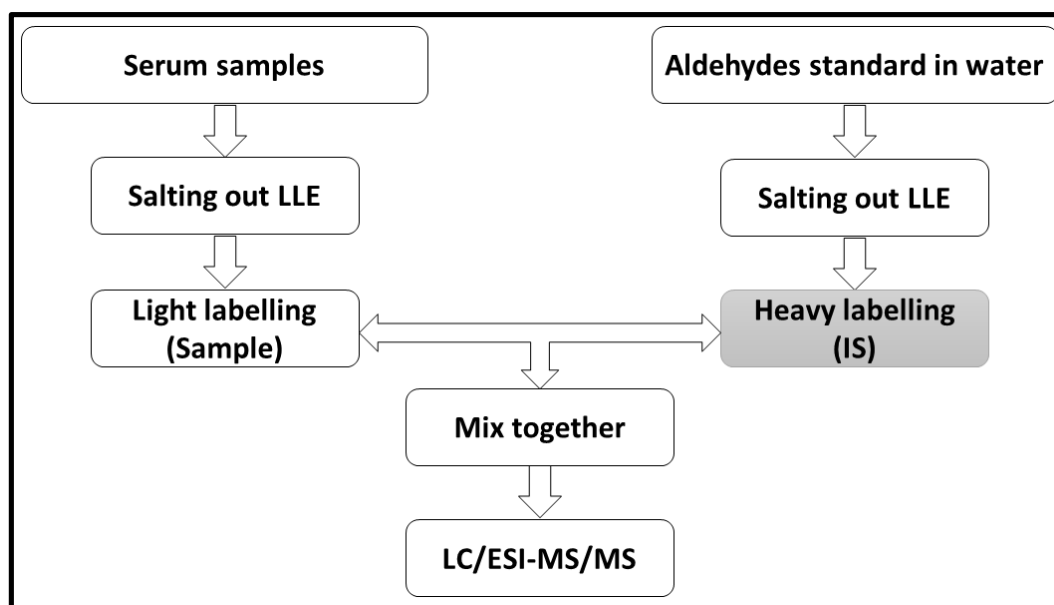
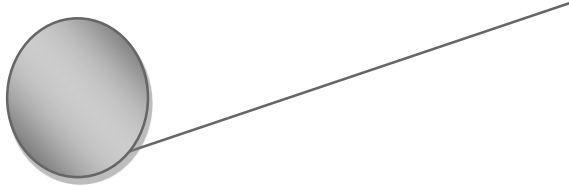


Fig. 4.3: Scheme of the quantification procedure based on ICD.

4-2-7. Validation procedure

For validation of the developed method, we followed the Guidance for Industry on Bioanalytical Method Validation ⁶⁶. Calibration curves were conducted for HHE and HNE using serum samples spiked at six concentration levels, including the LOQ, for each aldehyde. Then the spiked serum samples were treated as mentioned in section "4-2-6". The average relative peak areas were plotted *versus* concentrations (nM). The LOQ was calculated as the lowest concentration in the calibration curve that was determined with



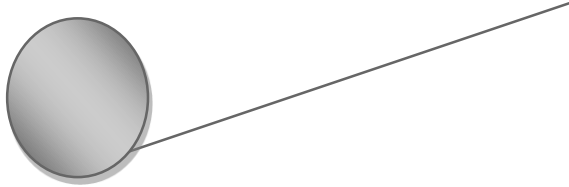
accuracy of 80-120% and precision (% RSD) of $\leq 20\%$. The LOD was also calculated at $S/N = 3$.

Accuracy and precision of the method were also examined by analysis of serum samples spiked with the studied analytes at three concentration levels for five determinations per each concentration. The accuracy was calculated as the variation of the mean calculated value from the true value. As well, the intra-day precision was determined as the % RSD for five determinations, at each concentration, in the same day. The inter-day precision was also determined as the % RSD for five determinations, at each concentration, on five consecutive days.

The stability of aldehydes solutions was also studied at -80°C up to 2 months and at room temperature up to 6 h. In addition, the stability of PQ and $^{14}\text{N}/^{15}\text{N}$ ammonium acetate solutions was examined over 2 months. We also checked the stability of the derivatized aldehydes at 4°C for 48 h which is the conditions of the auto sampler. The response in every condition was compared to that of freshly prepared solution.

4-2-8. Statistical analysis

The data are presented as mean \pm SE for the number of experiments. In order to compare the levels of HHE and HNE in the four studied groups (healthy subjects, diabetic, rheumatic, and cardiac disorders patients), Kobayashi decision tree ⁶⁷ was employed. Bartlett's test was used as a test for the equality of k variances. For HHE, it was found that the k sampled populations have unequal variances and Steel's Dwass test for comparing all pairs was used ⁶⁷. For HNE, it was found that the k sampled populations have equal variances and Anova test was used to compare mean of different groups. The four groups have different means from each other, thus the post hoc Tukey's multiple comparison test



was used for comparing all pairs⁶⁷. All the statistical tests were two-sided at a significant level of $\alpha=0.05$.

4-3. Results and discussion

4-3-1. The MS/MS fragmentation of PQ-aldehydes derivatives

The aldehydes were derivatized by PQ-¹⁴N/¹⁵N ammonium acetate giving imidazole derivative (Fig. 4.2). The derivatization reaction was accomplished within 15 min at 90 °C in the presence of glacial acetic acid.

The HHE-PQ-¹⁴N and HNE-PQ-¹⁴N derivatives gave precursor ions [M+H]⁺ at m/z of 303.2 and 345.2, respectively, which provided the same product ion at m/z of 231.3 by CID. The product ion was assigned for 2-methyl-1*H*-phenanthro[9,10-*d*]imidazole formed by the cleavage of the C=C double bond of the side chain attached to the imidazole ring. The HHE-PQ-¹⁵N and HNE-PQ-¹⁵N derivatives have a similar fragmentation pattern (m/z 305.2 \rightarrow m/z 233.3 and m/z 347.2 \rightarrow m/z 233.3, respectively). Figures 4.4 and 4.5 illustrate the product ion spectra of the target aldehydes derivatives.

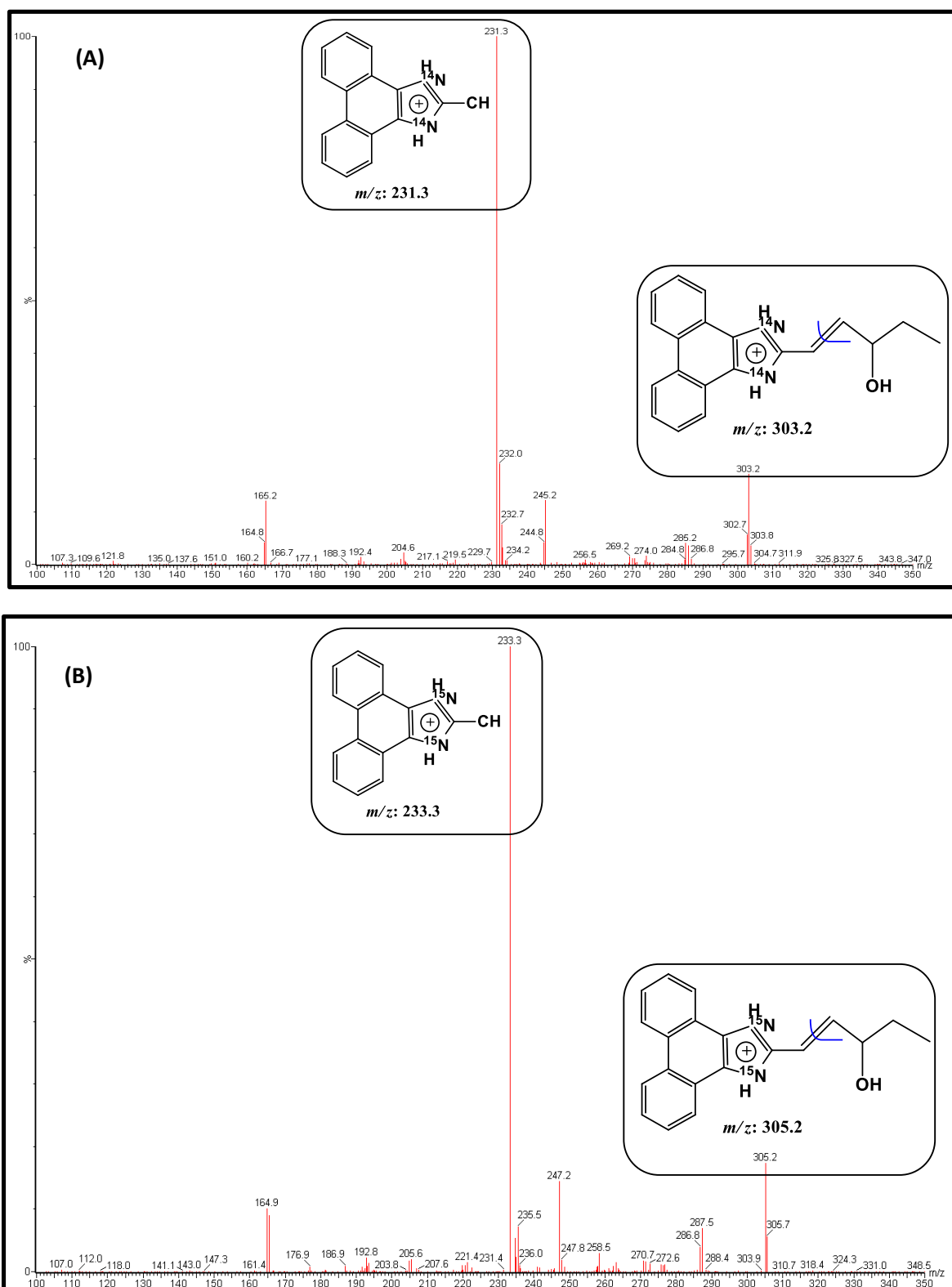


Fig. 4.4: Product ion spectra of (A) HHE-PQ- ^{14}N and (B) HHE-PQ- ^{15}N derivatives

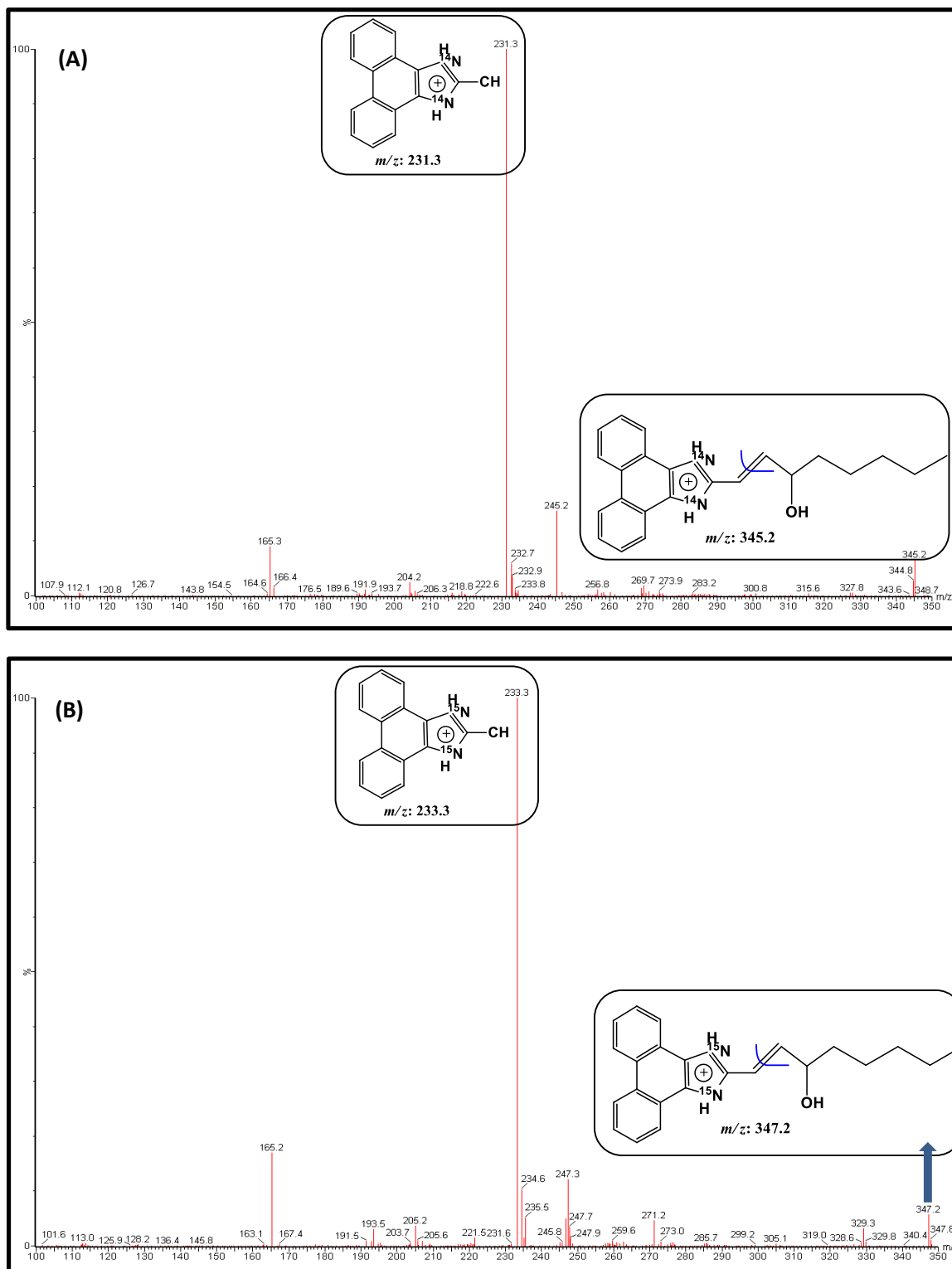


Fig. 4.5: Product ion spectra of (A) HNE-PQ-¹⁴N and (B) HNE-PQ-¹⁵N derivatives

4-3-2. Optimization of derivatization conditions

Derivatization conditions were optimized to attain the highest sensitivities. The effect of PQ concentration was investigated over the range of 0.1 to 28 mM. Increasing the concentration of PQ resulted in an increase of the signal intensity up to 22.0 mM and further increase has insignificant effect on the response (Fig. 4.6). Hence, for the best sensitivity, 22.0 mM PQ was chosen as the optimum reagent concentration.

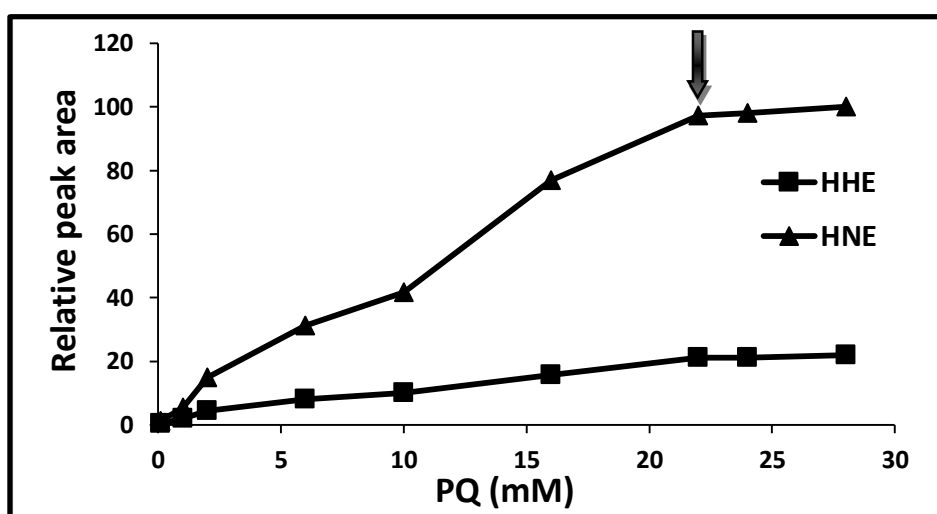


Fig. 4.6: Effect of PQ concentration on the relative peak area of the studied aldehydes derivatives (100.0 nM)

The influence of ammonium acetate concentration on the signal intensity was also studied in the range of 0.5-4.0 M. The highest signal intensity was obtained upon using 3.0 M ammonium acetate and further increase of the concentration beyond this level has no effect on the signal intensity (Fig. 4.7). Thus, 3.0 M was selected as the optimum ammonium acetate concentration in further experiments.

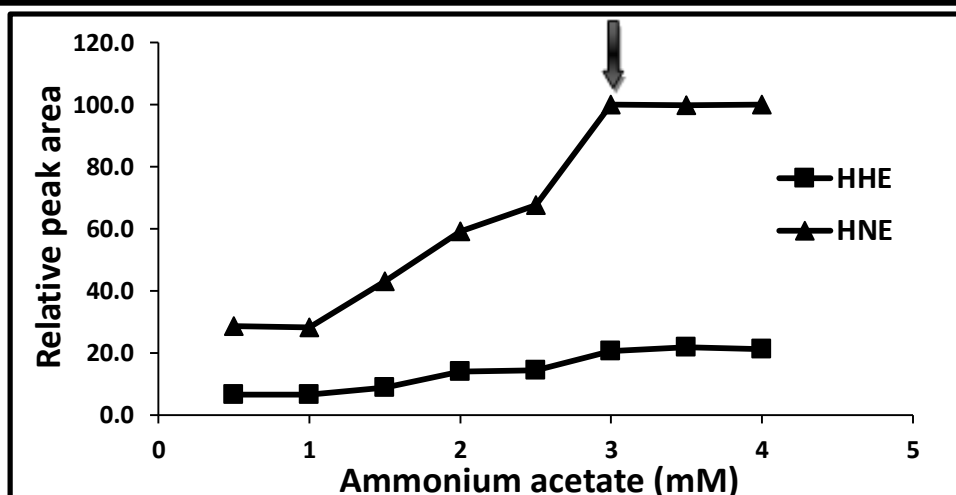


Fig. 4.7: Effect of ammonium acetate concentration on the relative peak area of the studied aldehydes derivatives (100.0 nM)

The derivatization temperature and time were also tested. The temperature was studied from 40 to 110 °C and the highest sensitivity was attained at 90 °C. Further increase in the temperature resulted in a slight decrease in the signal (Fig. 4.8).

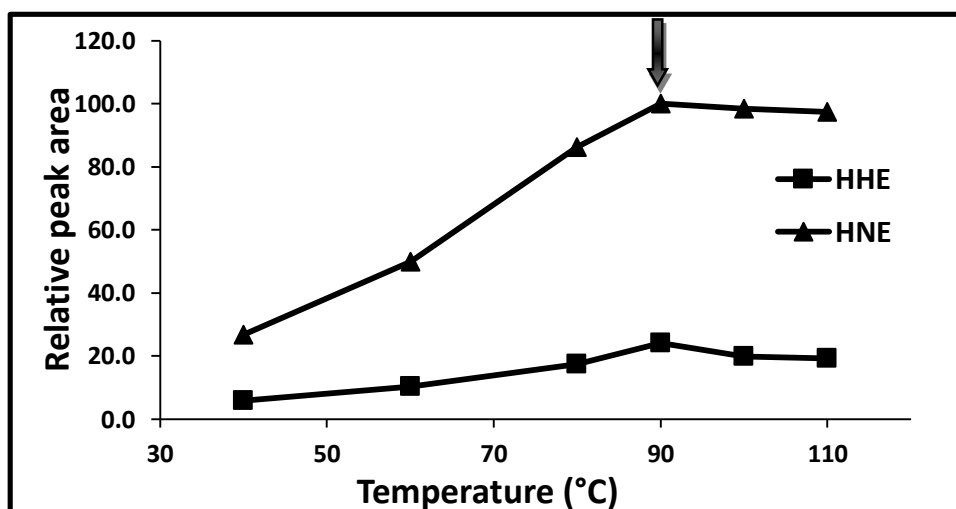


Fig. 4.8: Effect of reaction temperature on the relative peak area of the studied aldehydes derivatives (100.0 nM)

The derivatization time was examined from 5 to 60 min. The best sensitivity was obtained after 15 min, prolonged heating after that caused a slight decrease in the signal

in case of HNE-derivative without a significant effect on HHE-derivative (Fig. 4.9). Thus, heating for 15 min at 90 °C was selected.

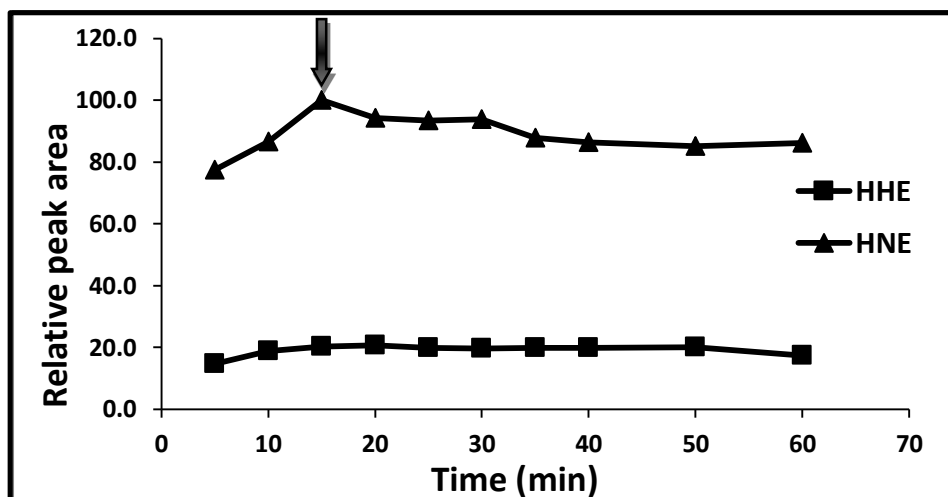
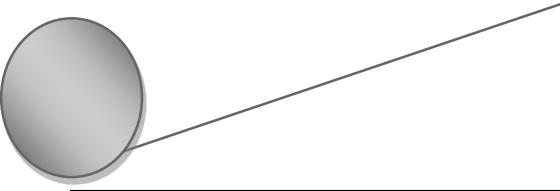


Fig. 4.9: Effect of reaction time on the relative peak area of the studied aldehydes derivatives (100.0 nM)

4-3-3. Optimization of HPLC separation and MS/MS monitoring

The LC/ESI-MS/MS operational conditions were optimized. The mass parameters including the cone and collision voltages were optimized to obtain the maximum response for the four PQ-aldehyde derivatives. Table 4.1 illustrates the optimum parameters selected for each analyte and its isotope IS.

Moreover, the mobile phase was carefully studied to achieve the best chromatographic performance. In preliminary investigations, mobile phases consisted of 0.1% formic acid in methanol: 0.1% formic acid in water in the ratios of 9:1 and 8:2, v/v were tested adopting isocratic elution mode using a 3C₁₈ column (100 mm x 4.6 mm i.d., 3µm particle size). Yet, the peaks for the target aldehydes were strongly distorted. Hence, isocratic elution with a mobile phase consisted of methanol: ammonium formate buffer



(20 mM, pH 4.0) (95:5, v/v) was tried with the same column and a significant improvement of the peaks shape was observed but it needs a long run time. Accordingly, we investigated gradient elution with methanol as solvent A and ammonium formate buffer (20 mM, pH 4.0) as solvent B. The initial concentration of solvent A was varied from 70 to 95% and its final concentration was kept in all cases at 100%. The gradient time was also studied from 0.5 to 3 min. Finally, for best resolution, sensitivity, and shortest run time, the gradient system described under section “4-2-2.” was used for separation of HHE and HNE derivatives in less than 5 min (HHE derivatives were eluted at $t_R = 3.36$ min and HNE derivatives at $t_R = 3.98$ min).

4-3-4. Results of the assessment study of ICD technique for relative quantification

Evaluation of the developed ICD method for relative quantification according to Dai et al. ¹²⁶ showed its practicability. The aldehydes-PQ-¹⁴N and aldehydes-PQ-¹⁵N derivatives were found in the same run at the same retention time ($t_R = 3.36$ min for HHE-PQ-¹⁴N/HHE-PQ-¹⁵N pair and $t_R = 3.98$ min for HNE-PQ-¹⁴N/HNE-PQ-¹⁵N pair) (Fig. 4-10 A and B). The difference in m/z values is attributed to the replacement of two ¹⁴N with ¹⁵N and same concentrations showed nearly the same relative abundance (Fig. 4.10 C and D). The ratios of MS signals of aldehyde-PQ-¹⁴N/aldehyde-PQ-¹⁵N pairs prepared in the ratios of (1:2, 1:1, and 2:1) are approximately 0.5 (ranged from 0.5 to 0.51), 1 (ranged from 0.97 to 1.05) and 2 (ranged from 2.0-2.07), respectively (Fig. 4.11 A and B). The MS signal ratios of the aldehyde-PQ-¹⁴N/aldehyde-PQ-¹⁵N pairs prepared in the ratios of (1:10, 1:5, 1:2, 1:1, 2:1, 5:1 and 10:1) showed excellent linearity ($r = 0.9999$) (Fig. 4-11 C and D) indicating that relative quantification can be accomplished by the developed ICD method.

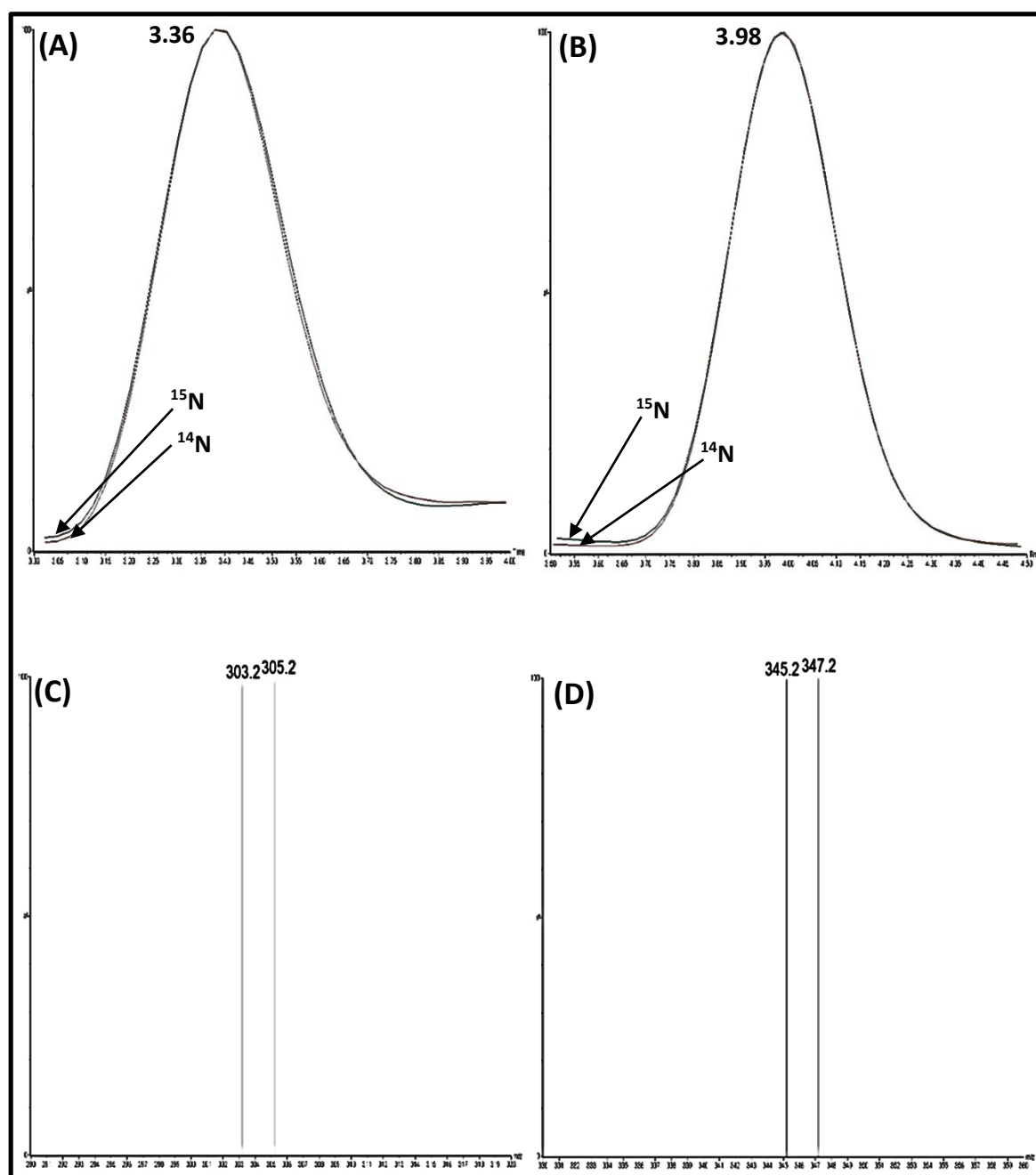


Fig. 4.10: Chromatograms of ^{14}N and ^{15}N labeled aldehydes for (A) HHE and (B) HNE; mass spectrum of the ion pair of ^{14}N and ^{15}N labeled aldehydes for (C) HHE and (D) HNE.

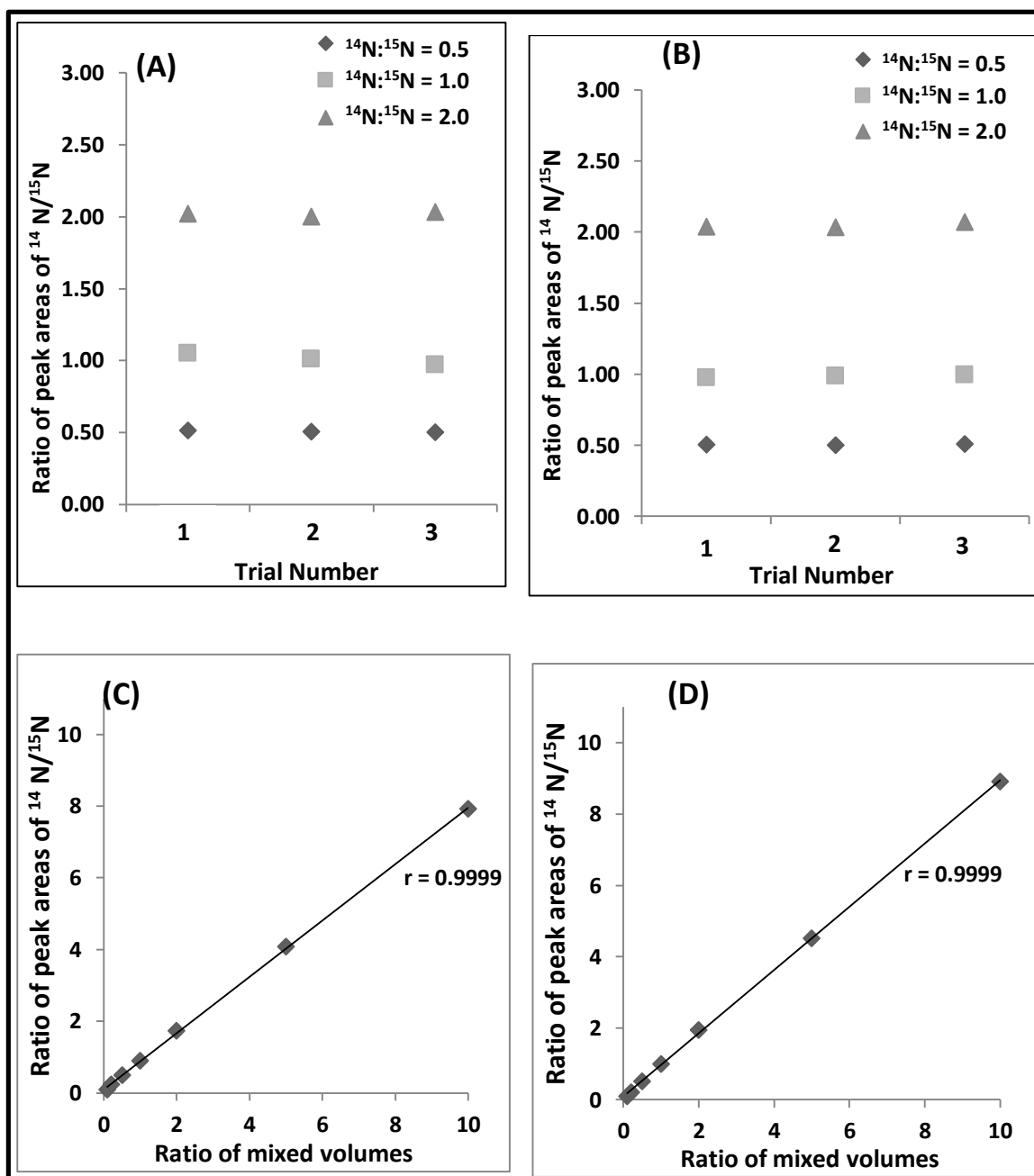
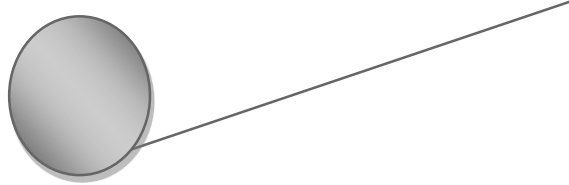


Fig. 4.11: MS intensity ratios of ^{14}N and ^{15}N labeled HHE (A) and HNE (B) with the amount of 1:2, 1:1, and 2:1; and ion pairs of ^{14}N and ^{15}N labeled HHE (C) and HNE (D) in 1:10, 1:5, 1:2, 1:1, 2:1, 5:1 and 10:1 mixed solutions showed a good linear regression.



4-3-5. Validation of the method

The calibration curve was established for each aldehyde and the linearity was approved by the values of the correlation coefficient ($r \geq 0.999$). The LOQ and LOD were also calculated for the two aldehydes. Table 4.2 illustrates the linearity data, LOQ and LOD of the studied analytes by the proposed method. The values of LOD (0.05 and 0.01 nM for HHE and HNE, respectively) indicated the high sensitivity of the proposed method and its suitability for determination of the two aldehydes at trace concentration levels in human serum. A comparison between the sensitivity of the proposed method and the previously reported ones will be discussed later.

Table 4.2 LOD, LOQ, calibration ranges, regression equations and correlation coefficients for the target aldehydes in spiked serum

Compound	LOD ^a , nM (fmol/injection)	LOQ ^b (nM)	Accuracy at LOQ (%)	Precision at LOQ (% RSD)	Range (nM)	Regression equations ^c , $n = 3$	r ^d
HHE	0.05 (1.0)	0.2	8.3	4.4	0.2-500	$Y=0.0010+0.0021X$	0.999
HNE	0.01 (0.2)	0.05	5.0	6.0	0.05-100	$Y=-0.0004+0.0100X$	0.9996

^a S/N= 3.

^b S/N \geq 5.

^c Y= relative peak area (IS: heavy labeled 500 nM HHE & 100 nM HNE), X= aldehyde concentration (nM).

^d Correlation coefficient.

Accuracy of the proposed method for the determination of HHE and HNE in human serum was expressed as % variation of the mean from the exact value and it was found within the range of -5.4 to +5% (Table 4.3). The % RSD for the intra-day precision of the proposed method ranged from 0.7 to 6.3 and that for the inter-day precision ranged from 1.7 to 8.1 (Table 4.3). These values indicated the accuracy and precision of the proposed method.

Table 4.3 Accuracy and precision of the proposed method for the determination of the target aldehydes in spiked serum

Aldehyde	Spiked amount (nM)	Intra-day (<i>n</i> = 5)			Inter-day (<i>n</i> = 5)		
		Found amount (nM)	Accuracy (%)	Precision (% RSD)	Found amount (nM)	Accuracy (%)	Precision (% RSD)
HHE	1.0	1.04	4.0	6.3	1.04	4.0	5.9
	50.0	49.7	-0.6	3.4	50.4	0.8	1.7
	500.0	501.5	0.3	2.5	492.7	-1.5	2.4
HNE	0.20	0.20	0.0	2.9	0.20	0.0	3.6
	10.0	10.5	5.0	4.1	9.46	-5.4	8.1
	100.0	100.5	0.5	0.7	95.8	-4.2	4.3

The aldehydes standard solutions were found to be stable at -80 °C over the estimated time period of 2 months and stable at room temperature up to 6 h. The reagents solutions (PQ and ¹⁴N/¹⁵N ammonium acetate) were also stable up to 2 months at 4 °C. Additionally, the derivatized aldehydes were found to be stable at 4 °C for 48 h indicating their stability while residing in the auto sampler.

The results of the validation study confirmed the agreement of the method with the Guidance for Industry on Bioanalytical Method Validation ⁶⁶.

4-3-6. Selection and optimization of the extraction procedure and recovery study

Different extraction methods were studied to select the most efficient method for extraction of HHE and HNE from serum samples. First, PPT method was attempted using either methanol or acetonitrile. Additionally, subzero-temperature LLE with acetonitrile and LLE using methanol:chloroform mixture (2:1, v/v) were tested. Also, salting out LLE method using acetonitrile was attempted. SPE was also studied using Oasis hydrophilic-lipophilic balance (HLB, 1 CC/30 mg) cartridge preconditioned with 500 µL methanol

and equilibrated with 500 μL water, followed by loading of 200 μL of aldehydes solution and elution with 400 μL methanol. The best % recoveries for the two aldehydes were obtained using salting out LLE method using acetonitrile (Fig. 4.12).

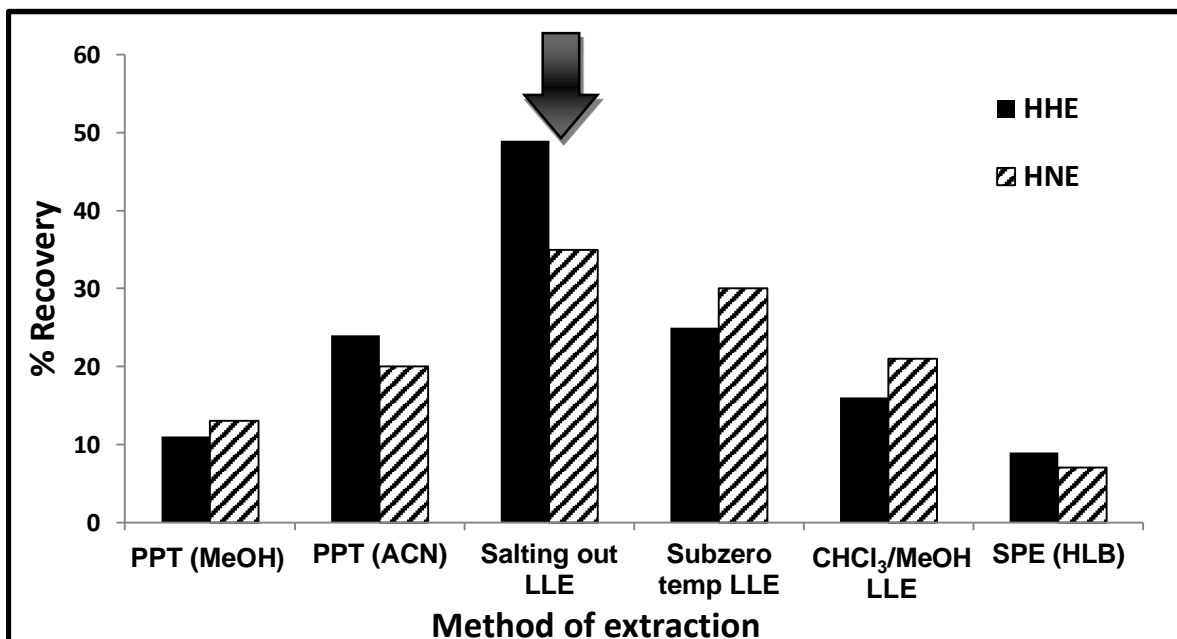


Fig. 4.12: Recovery of the studied aldehydes from serum after PPT with methanol (MeOH) or acetonitrile (ACN), salting out LLE, subzero-temperature LLE, LLE with chloroform/MeOH mixture and SPE with HLB cartridge

Hence, different parameters influencing the extraction efficiency of the two analytes were studied hopefully to enhance the % recoveries. The type of the salt added for the salting out step was tested using 4.0 M NaCl and 2.0 M MgSO₄ solutions as well as NaCl solid form. The best % recoveries were obtained using NaCl solid form (Fig. 4.13 A). Therefore, the effect of the added amount of NaCl was studied from 0.05 to 0.25 g, and the highest % recoveries were obtained using 0.15 g of NaCl (Fig. 4.13 B).

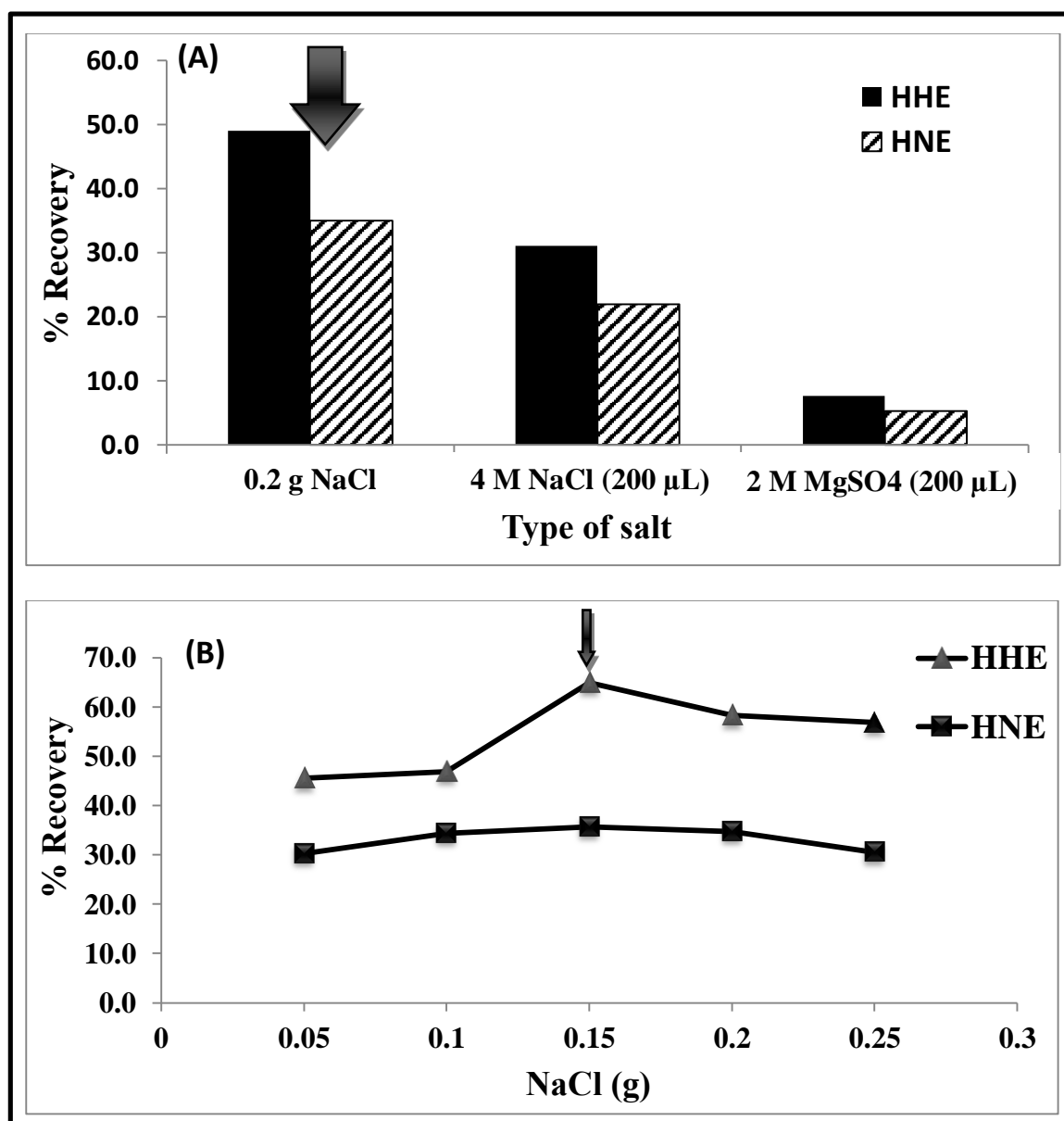


Fig. 4.13: Effects of (A) salt type and (B) salt amount used during salting out LLE on the % recoveries of the target analytes

In addition, different solvents were examined to select the most proper solvent for the LLE step. We first studied the derivatization reaction reactivity in different solvents and we found that the reaction of both HHE and HNE was completely hindered in acetone,

while tetrahydrofuran allowed the reaction of HHE but significantly inhibited HNE reaction. On the other hand, the reaction proceeded in the other studied solvents (acetonitrile, dioxane, *n*-propanol and isopropanol) with relative degrees of reactivities of 100, 55, 70, and 105%, respectively. Then, we tested these four solvents for salting out LLE procedure and acetonitrile and dioxane gave the highest % recoveries (Fig. 4.14). Since, the reaction proceeded with higher reactivity in acetonitrile than dioxane, thus acetonitrile was used as the solvent of choice.

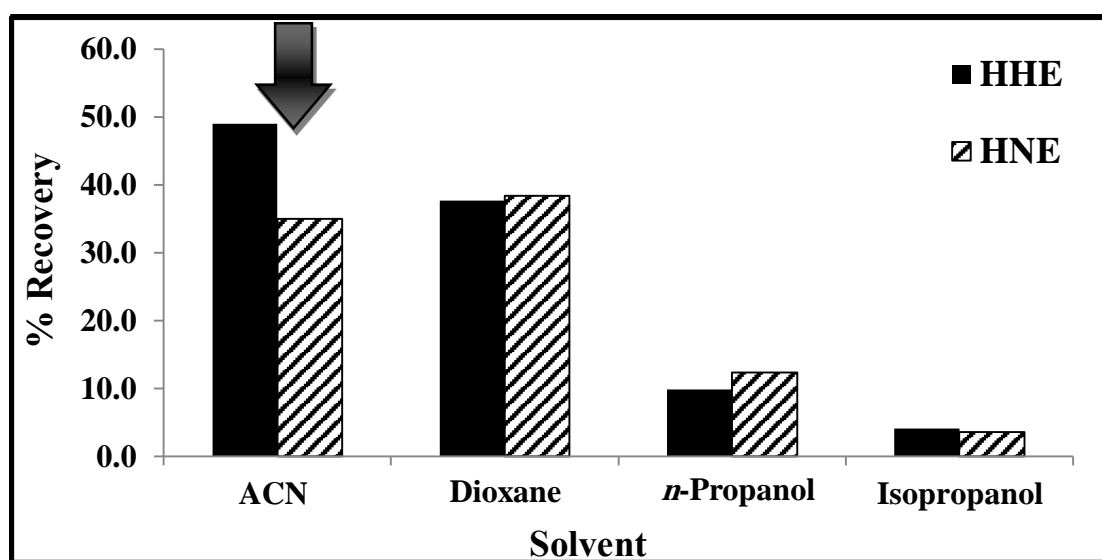
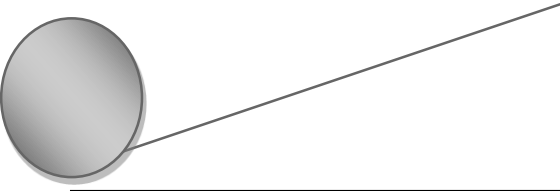


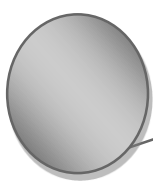
Fig. 4.14: Effect of the solvent used for salting out LLE on the % recoveries of target analytes

Yet, the values of the absolute % recoveries calculated by comparing the peak areas obtained from extraction of serum spiked with known amount of the studied aldehydes to the peak areas for standard aldehydes in the solvent (acetonitrile) were relatively low (40 and 62% for HHE and HNE, respectively). Keeping in mind the fact that the acetonitrile phase from salting out LLE usually contains 5-10% water¹²⁷, we conducted further experiments to investigate whether these low absolute % recovery values were due to a problem in the extraction efficiency or due to interference with the



derivatization reaction from either serum components or from the water content in the extracted acetonitrile phase. Thus, we compared the peak areas obtained from extraction of serum spiked with known amount of the studied aldehydes to those obtained for standard aldehydes extracted from water. Interestingly, the average relative % recoveries were found to be 92.0 and 99.0% for HHE and HNE, respectively. Such results mean that the low values of absolute % recoveries were attributed to inhibition of the derivatization reaction by the presence of water in acetonitrile not due to matrix effect from serum components.

To confirm our conclusion and to exclude any possibility that the low absolute % recovery is due to poor extraction efficiency, we performed two further experiments. First, we compared the peak areas obtained from extraction of serum spiked with known amount of the studied aldehydes to those obtained from standard aldehydes spiked to extracted acetonitrile phase from salting out LLE. Second, we compared the peak areas obtained from extraction of serum spiked with known amount of the studied aldehydes to those obtained from standard aldehydes in acetonitrile solution containing 5% water (to mimic the condition obtained after extraction of aldehydes solution in acetonitrile). In the first case, the average % recovery was found to be 98% for the two aldehydes, and in the second case they were 95 and 102.0 for HHE and HNE, respectively. These results confirmed our previous hypothesis that the low absolute % recovery (40-62%) is due to the presence of small amount of water in the extracted acetonitrile phase. Thus salting out LLE is suitable for the extraction of the target aldehydes, however, calibration should be carried out in matrix matched way. Thus the calibration was carried out in serum. For preparing the isotope labeled IS, the standard aldehydes were dissolved in water, then subjected to salting out LLE followed by heavy labelling with PQ/¹⁵N ammonium acetate.



4-3-7. Application of the proposed ICD LC/ESI-MS/MS method to determination of the target aldehydes in human serum

The high sensitivity, accuracy, rapidness and cost-effectiveness of the developed ICD LC/ESI-MS/MS make it a well suited choice for analysis of the two highly reactive 4-hydroxy-2-alkenals, HHE and HNE in human serum. The proposed method was applied for the determination of these two aldehydes in serum of 16 healthy subjects, as a control group, in addition to 5 diabetic, 8 rheumatic and 5 cardiac disorders patients. In all experiments, serum samples were extracted by salting out LLE followed by light labelling with PQ-¹⁴N ammonium acetate (solution A) and aldehydes standards in water were also extracted by salting out LLE followed by heavy labelling with PQ-¹⁵N ammonium acetate (solution B), then solutions A and B were mixed in 3:1 ratio then analyzed by LC/ESI-MS/MS. This ratio conveyed two extra-advantages to the developed method. First, maintaining a small dilution of the serum samples, thus, ensure the detection of the studied aldehydes at trace levels, and second, supporting the cost-effectiveness of the method by using small amount of ¹⁵N ammonium acetate. Typical chromatograms for aldehydes from healthy human subjects and diabetic, rheumatic and cardiac disorders patients are illustrated in Fig. 4.15. The levels of HNE and HHE in healthy and patients with different diseases are summarized in Table 4.4.

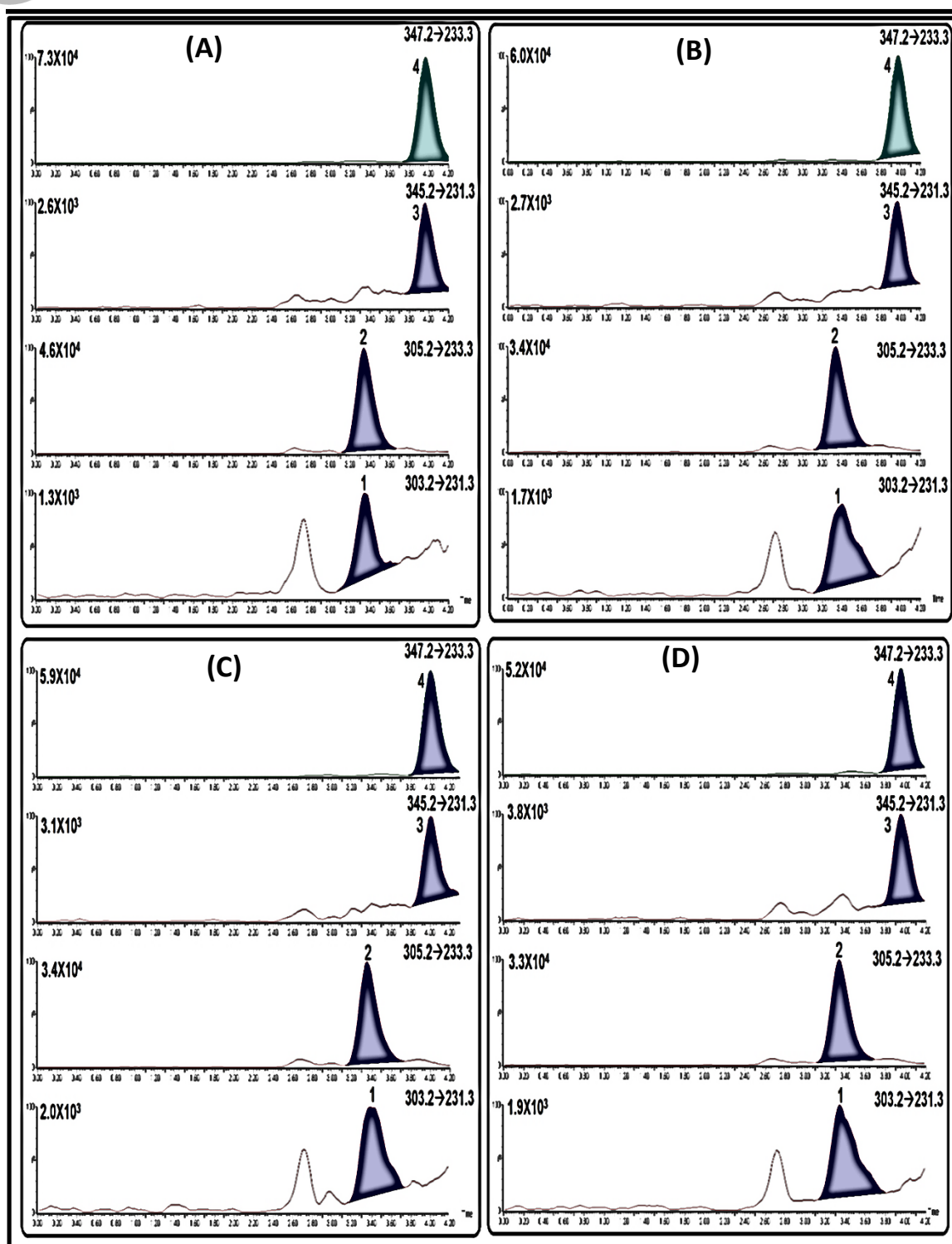


Fig. 4.15: Chromatograms of (A) healthy human serum, (B) diabetic patient serum, (C) rheumatoid arthritis patient serum, and (D) cardiac disorder patient serum; where peaks 1=HHE-PQ- ^{14}N , 2=HHE-PQ- ^{15}N , 3=HNE-PQ- ^{14}N , and 4=HNE-PQ- ^{15}N .

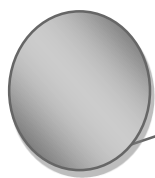


Table 4.4 Statistical analysis of the results for determination of the target aldehydes in healthy, diabetic, rheumatic, and cardiac disorders patients' sera.

Groups	Parameters	Reactive aldehydes data		
		HHE	HNE	
Control (C, n=16)	Range (nM)	30.5-65.3	7.6-19.2	
	Mean ± SE	41.8±2.5	15.1±0.8	
Diabetic patients (DM, n=5)	Range (nM)	50.7-123.7	22.8-29.3	
	Mean ± SE	87.2±15.1	26.6±1.3	
Rheumatic patients (RA, n=8)	Range (nM)	61.1-145.5	16.1-23.9	
	Mean ± SE	97.4±11.9	20.3±1.1	
Cardiac disorder patients (CD, n=5)	Range (nM)	109.5-156.1	27.8-39.7	
	Mean ± SE	132.5±7.5	35.6±2.1	
Statistical analysis	Bartlett	(p)	0.0008 ^a	0.7213 ^b
	Anova	(p)	-----	< 0.0001 ^{a,d}
	C vs DM	(p)	0.0365 ^{a,c}	< 0.0001 ^{a,d}
	C vs RA	(p)	0.0010 ^{a,c}	0.009 ^{a,d}
	C vs CD	(p)	0.0061 ^{a,c}	< 0.0001 ^{a,d}
	DM vs RA	(p)	0.8521 ^{b,c}	0.015 ^{a,d}
	DM vs CD	(p)	0.1567 ^{b,c}	0.001 ^{a,d}
	RA vs CD	(p)	0.3324 ^{b,c}	< 0.0001 ^{a,d}

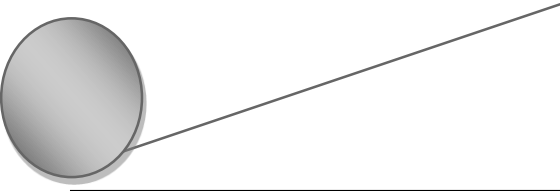
^a P < 0.05.

^b Non-significant.

^c Steel's Dwass test.

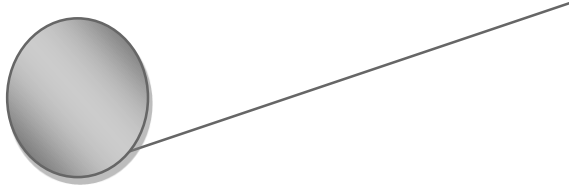
^d Tukey's multiple comparison test.

Comparing the levels of HNE and HHE in healthy and diseased conditions showed that their levels were significantly elevated in all of the studied diseases (Table 4.4) which agreed with the previous reports ^{21,27,28,61}. The levels of HNE and HHE are elevated in diabetic conditions due to the catalytic effect of free glucose and glycosylated collagen on lipid peroxidation ⁷⁵. Elevation of their levels in case of rheumatic arthritis is attributed to elevated level of ROS formed by activated polymorphonuclear cells and



injury resulting from ischemia and reperfusion in the inflamed joints ⁷⁷. Meanwhile, the increased levels of both aldehydes in cardiac disorders are probably due to increased oxidative stress as a result of the increase in ROS production due to catalysis of its formation by the oxidized LDL in cardiac disorder patients. Also, ROS are formed by injury resulting from ischemia and reperfusion of the heart tissues resulted from atherosclerosis, thrombosis or coronary artery spasm induced myocardial ischemia in cardiac disorder patients ¹²⁸.

In addition, we conducted comparisons between the levels of HHE and HNE in the investigated diseased conditions. The results are summarized in Table 4. We found that there is no significant difference in the level of HHE in diabetic conditions compared to rheumatic and cardiac disorders patients or rheumatic condition compared to cardiac disorders ones. In contrast, the level of HNE is significantly difference among the three diseased groups. HNE level was significantly higher in cardiac disorders patient higher than diabetic and rheumatic disorder patients. On the same time, HNE level in diabetic conditions was significantly higher than that in rheumatoid arthritis condition which is in contrast for the result obtained in chapter 2, thus we could attribute this increase to the status of disease progression not to the disease type. From these results we can conclude that the level of peroxidation of ω -6 PUFAs (source of HNE) is different among the three analyzed diseases and HNE level could be used to differentiate between diseases or their status of progression. On the other hand peroxidation of ω -3 PUFAs (source of HHE) is significantly increased in the three studied diseased conditions in the same manner without any significant difference between them. However, we recommend conducting further studies on a larger number of samples and linking the aldehydes levels with other diseases biomarkers to have a confirmed conclusion about this finding.

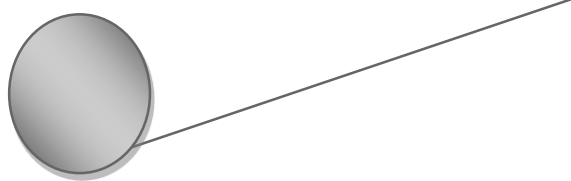


4-3-8. Comparison of the proposed and reported methods for simultaneous determination of HNE and HHE

Comparing the analytical performance of the developed ICD LC/ESI-MS/MS and that of the published methods for determination of HHE and HNE revealed advantages and superiority in many aspects. The developed method is the first one to determine these two aldehydes in serum of healthy and diseased humans, a fact which imparts a great importance and promising applications to it.

Table 4.5 illustrates a comparison of the proposed and reported methods for simultaneous determination of HHE and HNE. Most of the developed methods need long derivatization time^{64,96,102,122-124}, as well, the reported GC/MS method of van Kuijk et al.¹²¹ required time consuming preparation of deuterated IS (6d₃-HHE and 9d₃-HNE). In addition, the analytical methods which used hydrazine-based derivatizing reagents (DNPH and DNSH)^{64,96,123,124} for determination of HHE and HNE involved some disadvantages including poor selectivity, formation of two isomeric reaction products of each aldehyde as well as poor stability and safety of the reagent. Meanwhile, the two methods which used PFBHA derivatizing reagent entailed the formation of two reaction products for each aldehyde, *syn/anti* oxime derivatives, which is a source of analytical errors^{121,122}.

On the other hand, the developed method is rapid, requiring only 15 min for complete derivatization reaction; in addition, PQ is a very selective and highly stable derivatizing agent for aldehydes. The use of ¹⁴N/¹⁵N ammonium acetate as ICD derivatizing agent provided the merits of low cost, commercial availability and time



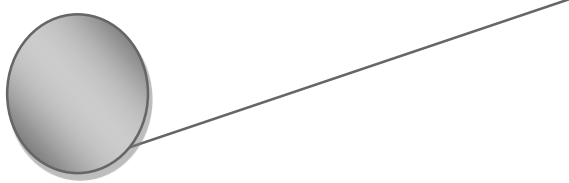
saving. The ICD technique is proved to be efficient in minimizing the matrix effects during LC/ESI-MS/MS analysis.

In addition, the proposed method exhibited ultra-sensitivity for both HNE and HHE which is much greater than all of the reported methods for their determination. The proposed method is about 20-32000 and 4-8700 times more sensitive than the published methods for HHE^{64,96,102,123,124} and HNE^{64,96,102,121,123,124}, respectively (Table 4.5). This great sensitivity makes the proposed method an excellent choice for the determination of these two aldehydes in biological fluids at trace and ultra-trace levels with high accuracy and precision.

Table 4.5 Comparison of the developed and reported methods for simultaneous determination of HHE and HNE

Method	Reagent	Condition (temp °C/ time)	LOD nM		matrix	Ref.
			HHE	HNE		
GC/MS	PFBHA	RT/10 min	N/A	(64)	Copper-oxidized human LDL	121
GC/MS	PFNHA	RT/2h	N/A	N/A	Mice liver	122
HPLC-UV	DNPH	RT/ overnight	(8764)	(6401)	vegetable oil	123
LC-MS/MS	DNPH	60/2h	1127	128	Linseed oil	124
LC-MS/MS	DNPH	RT/1h	0.3 (6)	0.6 (12)	Exhaled breath condensate	64
LC-MS/MS	CHD	60/1h	(351)	(128)	Oxidized plasma	102
LC-MS/MS	DNSH	RT/4h	0.2 (1.0)	0.2 (1.0)	Rat serum	96
LC-MS/MS	PQ/ ¹⁴ N- ¹⁵ N ammonium acetate	90/15 min	0.05(1.0)	0.01(0.2)	Human serum	Proposed method

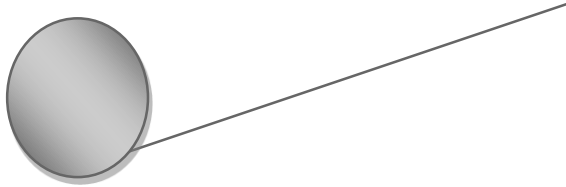
N/A: Data is not available.



4-3-9. Comparison of the proposed and previously reported ICD LC-MS/MS methods for aldehydes

Some ICD LC-MS/MS methods have been previously reported for the determination of some aldehydes in different matrices, *e.g.* aquatic products ¹⁰⁴, air ¹²⁹, exhaled breath condensate ¹³⁰ and pooled human liver microsomes ¹³¹. Yet, most of these methods depends on using of isotope coded analogues of DNPH including d_0/d_3 -DNPH ^{129,130} and $^{15}N_0/^{15}N_4$ -DNPH ¹³¹. Although DNPH is commercially available reagent but its isotope coded analogues are not, and their in-laboratory synthesis is expensive and sophisticated. The synthesis of d_0/d_3 -DNPH involved the use of d_0/d_5 -chlorobenzene as initial substrate ^{129,130}, while $^{15}N_0/^{15}N_4$ -DNPH is synthesized *via* 2 steps involving $^{15}N_0/^{15}N_1$ -nitric acid and $^{15}N_0/^{15}N_2$ -hydrazine as reactants ¹³¹. Additionally, a method depends on using d_0/d_3 -MPIA which is synthesized through a very time-consuming procedure and the introduction of isotope signature was accomplished using tri-deuterated iodomethane ¹⁰⁴. In all of these methods, the synthesis process represents a strong limitation of the methods applications due to very long time (reaching many days) required for synthesis, purification, drying and recrystallization steps of ICD reagents. Another disadvantage associated with ICD LC-MS/MS based on d_0/d_3 -reagents ^{104,129,130} is the chromatographic isotopic effect that emerges upon using d_0/d_3 -reagents. In contrast, $^{15}N/^{14}N$ ammonium acetate is commercially available and cheap reagent which made the proposed method very convenient, rapid and practical for wide spread use in analysis of aldehydes. In addition, the use of $^{15}N/^{14}N$ ammonium acetate completely overcome the chromatographic isotopic effect associated with the use of d_0/d_3 -reagents.

Only one of these methods determined HNE in a biological matrix, exhaled breath condensate ¹³⁰, however our method is about 10 times more sensitive than this method.



The excellent analytical performance and remarkable advantages of the developed ICD LC/ESI-MS/MS method suggests its significance for further applications to study the distribution of HNE and HHE in tissues and their contribution to tissue damage due to oxidative stress.

4-4. Conclusions

In this work we described an expedient, rapid and highly sensitive ICD technique based on using PQ and $^{14}\text{N}/^{15}\text{N}$ ammonium acetate as ICD reagent followed by LC/ESI-MS/MS for quantitative analysis of two highly reactive 4-hydroxy-2-alkenals, HHE and HNE, in human serum. The developed method was able to detect HHE and HNE with LOD down to 0.05 and 0.01nM, respectively. The developed method exhibited many advantages over published literatures for determination of these two aldehydes where it is time-saving, cost-effective, selective and it uses a safe and stable derivatizing agent (PQ), and a cheap and commercially available ICD reagent ($^{14}\text{N}/^{15}\text{N}$ ammonium acetate). Thus, we applied the developed method to determine the levels of these aldehydes in serum of diabetic, rheumatic and cardiac disorder patients, as well as a healthy control group. We found that the levels of HNE and HHE are significantly higher in all diseased conditions compared to the control group. In addition, no significant difference in the levels of HNE and HHE was observed in diabetic patients compared to rheumatic and cardiac disorder patients. On the other hand, the level of HNE was significantly higher in case of cardiac disorders relative to rheumatic arthritis condition, while, no significant difference was observed in the level of HHE in both diseases.

Chapter V

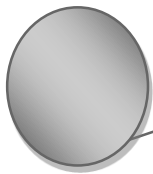
Determination of human serum semicarbazide-sensitive amine oxidase activity *via* flow injection analysis with fluorescence detection after online derivatization of the enzymatically produced benzaldehyde with 1,2-diaminoanthraquinone

Mahmoud H. El-Maghrabey, Naoya Kishikawa, Kaname

Ohyama, Takahiro Imazato, Yukitaka Ueki, Naotaka

Kuroda, *Analytica Chimica Acta* 881 (2015) 139–147.

DOI: 10.1016/j.aca.2015.04.006.

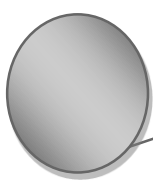


5-1. Introduction

Semicarbazide-sensitive amine oxidase (SSAO) is a family of heterogenous enzymes that can catalyze the deamination of various exogenous and endogenous monoamines. It is a copper-containing glycoprotein possessing topa-quinone as a cofactor. These enzymes are found in most of the mammals in two forms: tissue-bound and soluble isoforms (*i.e.* serum SSAO) ^{132,133}. The SSAO enzymes are different from the monoamine oxidases (MAO-A and MAO-B) in their inhibition pattern since they have tolerance to MAO inhibitors like clorgiline, pargyline and deprenyl, but sensitive to semicarbazide and other hydrazines ¹³⁴.

SSAO causes oxidative deamination to various amine compounds including dopamine, polyamines, tyramine, tryptamine, and benzylamine by converting them to the corresponding aldehydes with the generation of hydrogen peroxide and ammonia. Oxidation of methylamine, allylamine, and aminoacetone by SSAO gives rise to formaldehyde, ACR and methylglyoxal, respectively ¹³⁴. These products are all potentially cytotoxic, *e.g.*, formaldehyde is well known to be a major environmental risk factor, ACR and methylglyoxal may disrupt the functions of proteins, lipids, and enzymes, and hydrogen peroxide is a major generator of oxidative stress which is commonly associated with numerous diseases ¹³⁵.

The activity of serum SSAO has been reported to be increased in certain clinical conditions such as heart failure ¹³⁶ and diabetes mellitus ^{137,138}. Also, when the activity of SSAO is high, the increased enzymatic-mediated deamination is proposed to be involved in the pathogenesis of many vascular disorders ¹³⁹. Hence, the determination of SSAO might be a useful marker in the prognostic evaluation of diabetic angiopathy ¹⁴⁰.



Several methods have been described for the measurement of SSAO activity, mostly using benzylamine as the preferred substrate. By the action of SSAO, benzylamine is deaminated and oxidized to benzaldehyde with the generation of hydrogen peroxide, and ammonia. These methods include HPLC-FL after derivatization of benzaldehyde with dimedone¹⁴¹, HPLC-UV detection¹⁴² and light scattering measurement¹⁴³ after derivatization with DNPH, and radiometric method using [¹⁴C]-benzylamine as enzyme substrate¹⁴⁴. Other methods depended on direct measurement of the enzyme using LC-MS¹⁴⁵, reverse transcription polymerase chain reaction (RT-PCR)¹⁴⁶, and Western blot and immunoassays^{133,147}. Although some of these methods are sensitive enough to give valuable data about the SSAO activity, most of them suffer from various drawbacks such as time-consumption, tedious extraction procedures and poor recoveries of benzaldehyde from biological fluids^{142,143}, long derivatization reaction times^{141–143}, use of radioactive compounds¹⁴⁴, harsh condition (*e.g.*, 9 M sulfuric acid)¹⁴¹, and the use of sophisticated and expensive instruments^{133,145–147}. In addition, these methods that are based on the direct measurement of the SSAO enzyme^{133,145–147} do not reflect its activity inside the human body. In addition, the RT-PCR method¹⁴⁶ was not able to make a precise determination of the expression of SSAO neither *in vivo* nor *in vitro*. Also, the Western blot and immunoassays^{133,147} need expensive antibodies. So, these methods are not suitable for routine analysis of a large number of samples and there is a need to develop a sensitive, fast, simple, and convenient method for the determination of SSAO activity in serum.

In the present work, we aim at developing a rapid and highly sensitive flow injection analysis (FIA) method for the determination of SSAO activity in serum that allows the processing of a large number of samples within a short analysis time. The

method is based on incubation of serum with benzylamine, an exogenous SSAO substrate. Then the benzaldehyde generated by the SSAO activity is derivatized online with the novel aromatic aldehyde-specific reagent 1,2-diaminoanthraquinone (DAAQ) and the formed derivative will be determined by fluorescence detection (Fig. 5.1). The serum SSAO activity will be determined as benzaldehyde (nmol) formed per mL serum per hour.

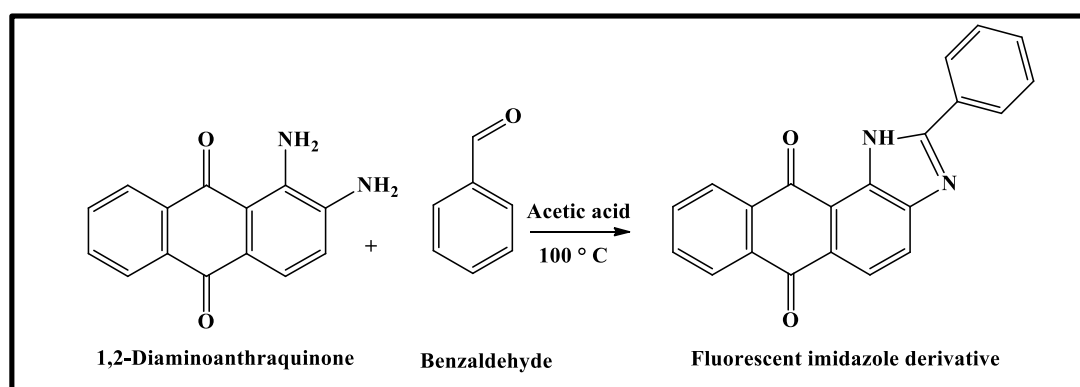


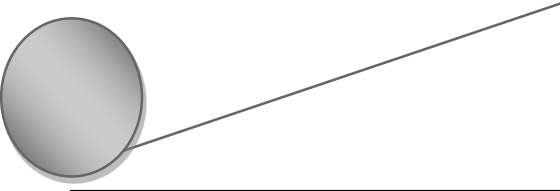
Fig. 5.1: Suggested mechanism for benzaldehyde reaction with DAAQ.

5-2. Experimental

5-2-1. Materials and reagents

Benzaldehyde, benzylamine, and glacial acetic acid were purchased from Wako Pure Chemical Industries. Sodium dihydrogenphosphate dihydrate ($\text{NaH}_2\text{PO}_4 \cdot 2\text{H}_2\text{O}$) and disodium hydrogen phosphate (Na_2HPO_4) were obtained from Nacalai Tesque. DAAQ and clorgiline were purchased from Sigma-Aldrich. Acetonitrile and methanol (HPLC grade) were obtained from Kanto Chemical Company. The water used was purified by a Simpli Lab UV (Millipore).

Phosphate buffer solution (0.1 M, pH 7.8) was prepared by dissolving 0.13 g of Na_2HPO_4 and 0.14 g of $\text{NaH}_2\text{PO}_4 \cdot 2\text{H}_2\text{O}$ in 100 mL distilled water and a Horiba F22 pH-



meter was used to check the pH of the buffer. Stock solution of benzaldehyde (10 mM) was prepared in acetonitrile and stock solutions of clorgiline (0.2 mM) and benzylamine (5.6 mM) were prepared in phosphate buffer solution. 8.0 mM and 0.8 mM solutions of DAAQ were prepared in glacial acetic acid. Because of the expected photo instability of DAAQ, its solution was kept in amber-colored glass bottles. It was found to be stable for at least 2 weeks when kept at 4 °C in the refrigerator.

5-2-2. Instrumentation and FIA conditions

A schematic diagram of the FIA system is shown in Fig. 5.2. The FIA system consisted of two Shimadzu LC-20AT pumps, a Rheodyne injector (Cotati, CA, USA) with a 20 μ L sample loop, a Shimadzu RF-20AXS fluorescence detector, and an EZ Chrom Elite chromatography data acquisition system (Scientific software, Pleasanton, CA, USA). Polytetrafluoroethylene (PTFE) tubing (10 m x 0.5 mm i.d., GL Sciences, Tokyo) was used as a reaction coil. Temperature of the reaction coil was kept at 100°C using a Shimadzu CTO-6A oven. Methanol and 0.8 mM DAAQ solution in glacial acetic acid were used as carrier and fluorogenic reagent streams, respectively. The flow rates of the carrier and fluorogenic reagent streams were set at 0.2 mL/min. Fluorescence detection was performed at 390 nm for excitation and 570 nm for emission.

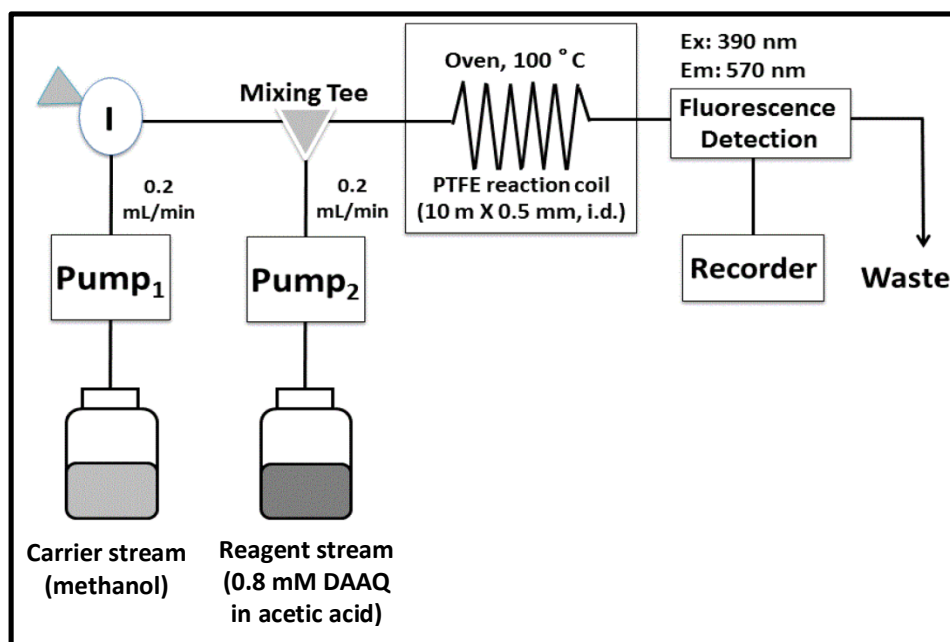


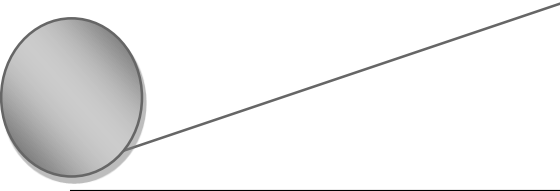
Fig. 5.2: Schematic diagram of the used FIA system.

5-2-3. Confirmation of the identity of benzaldehyde-DAAQ derivative

The method of Huang et al.¹⁴⁸ was followed for the synthesis of benzaldehyde-DAAQ derivative. The obtained yellowish-brown compound was subjected to electron impact-MS (EI-MS) to identify the molecular ion and ¹H NMR studies to prove the structure. The EI-MS spectra were recorded using JMS DX-303 mass spectrometer (Joel Ltd., Japan) and ¹H NMR spectra were recorded using Varian5-inova500 (500 Hz) spectrometer (Varian, CA, USA).

5-2-4. Fluorescence measurement of benzaldehyde after reaction with DAAQ

To a 100 μ L portion of methanolic solution of 0.2 mM benzaldehyde in a screw capped vial, 100 μ L of 8.0 mM DAAQ in acetic acid was added. After vortex mixing, the reaction mixture was heated at 100 °C for 30 min. The reaction mixture was diluted 10 times with methanol and the fluorescence spectra were recorded by a Shimadzu RF-1500



spectrofluorophotometer. A blank experiment was carried out simultaneously using 100 μL of methanol instead of benzaldehyde solution.

5-2-5. Clinical samples

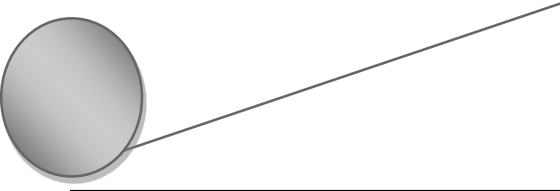
The present experiments were approved by the Ethics Committee of the School of Pharmaceutical Sciences, Nagasaki University, and performed in accordance with the established guidelines. Serum samples of 24 healthy human subjects (10 females, 14 males; mean age 49.2 ± 6.6) and 18 diabetic ones (10 females, 8 males; mean age 59.0 ± 12.0) were supplied by Sasebo Chuo Hospital and stored at $-80\text{ }^{\circ}\text{C}$ until analyzed.

5-2-6. Sample preparation procedure for SSAO enzyme activity

An aliquot of 50 μL human serum was pipetted into a 1.5 mL Eppendorf tube, to which 100 μL clorgiline (0.2 mM) was added to inhibit the MAO-A and B activities in serum. The tubes were vortexed for 1 min and incubated in a thermostatically controlled water bath at $37\text{ }^{\circ}\text{C}$ for 30 min. An aliquot of 250 μL of 5.6 mM benzylamine was added to each tube giving a final concentration of 3.5 mM, then vortexed for 1 min and incubated at $37\text{ }^{\circ}\text{C}$ for 1 h. An aliquot of 400 μL acetonitrile was immediately added to each tube, then was vortexed for 1 min and centrifuged at $1,200 \times g$ for 5 min. The mixture was then kept at $-30\text{ }^{\circ}\text{C}$ for 20 min to separate the acetonitrile phase from the aqueous phase. An aliquot of 20 μL of the acetonitrile phase was injected into the FIA system.

5-2-7. Method validation

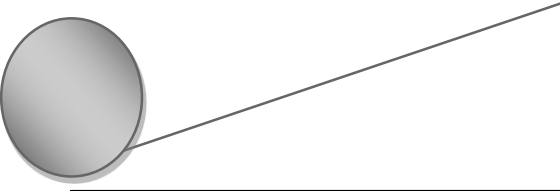
Method validation was performed in accordance with Guidance for Industry, Bioanalytical Method Validation (FDA)⁶⁶, where the fundamental parameters are calibration curve, selectivity, accuracy, precision, and recovery. The calibration curve was constructed by spiking seven samples covering the concentration range of 0.2-150.0



nmol/mL (including the LOQ) to the enzymatic reaction mixture (using 250 μ L of phosphate buffer solution instead of the SSAO's substrate, benzylamine). Each concentration was measured five times by applying the procedure described under section "5-2-6.". The LOQ was determined as the lowest concentration in the calibration curve where the analyte could be detected with acceptable accuracy (80-120%) and precision ($\% \text{RSD} \leq 20\%$). The LOQ was established using five independent serum samples spiked with standard benzaldehyde ⁶⁶. In addition, the LOD was determined as the concentration corresponding to the peak area of the blank plus three times of its standard deviation (blank+3SD).

Selectivity of the proposed method, defined as its ability to differentiate and quantify the analyte in the presence of other components in the serum, was evaluated by the analysis of blank serum samples obtained from six sources (six human volunteers).

Accuracy and precision of the proposed method were also evaluated by applying the procedure described under section "5-2-6." for replicate analyses of serum samples containing known amounts of the analyte. Benzaldehyde was spiked to enzymatic reaction mixture at three different concentration levels: low, medium, and high (0.2, 5.0, and 100.0 nmol/mL, respectively) using 250 μ L of phosphate buffer solution instead of the SSAO's substrate benzylamine. Each concentration was measured five times. The mean value was calculated and the deviation of the mean from the true value served as the measure of accuracy. Intra-day precision was investigated by calculating the $\% \text{RSD}$ for the peak areas for the five injections of benzaldehyde solution at these three concentrations in the same day; similarly, the inter-day precision (repeatability) was also investigated by calculating the $\% \text{RSD}$ for the peak areas of the three benzaldehyde concentrations on five successive days.



Recovery experiments were performed by comparing the analytical results for extracted enzymatic reaction mixtures (a) spiked at three concentrations of benzaldehyde (0.2, 5.0, and 100.0 nmol/mL) with un-extracted standards (b) that represent 100% recovery. % Recovery was calculated as follows: % Recovery = (a/b) x 100

5-2-8. Statistical analysis

In order to compare the levels of SSAO activity in the two studied groups (healthy and diabetic groups), variance ratio *F*-test was used to determine if there is a difference in their variances. Then, according to the result of the *F*-test we use either Student's *t*-test assuming equal variances or Student's *t*-test assuming unequal variances for comparing of the mean SSAO activity in each group¹⁴⁹. Tests were two-sided and the significance was established at $P < 0.01$.

5-3. Results and discussion

5-3-1. Fluorescence spectra and identification of benzaldehyde-DAAQ derivative

DAAQ is a non-cytotoxic and non-fluorescent probe that was used previously for nitric oxide sensing through the formation of a fluorescent triazole derivative which is detectable by means of fluorescence microscopy¹⁵⁰. The use of DAAQ as a derivatizing reagent for aldehydes has not been previously reported, which indicates the novelty of the proposed method.

The fluorescence spectra obtained from the reaction mixture of benzaldehyde with DAAQ in methanol are shown in Fig. 5.3. The formed imidazole derivative showed excitation and emission maxima of 390 and 545 nm, respectively. On the other hand, neither benzaldehyde nor DAAQ exhibited intrinsic fluorescence at the specified excitation and emission wavelengths. Since the reaction is a fluorogenic one, it can be

used for online derivatization in FIA determination of benzaldehyde formed by the action of serum SSAO.

In order to elucidate the structure of the fluorescent derivative, the yellowish-brown precipitate obtained from the reaction of benzaldehyde with DAAQ was analyzed by EI-MS and ^1H NMR. The most abundant ion peak was found at m/z 324 corresponding to the molecular formula of $\text{C}_{21}\text{H}_{12}\text{N}_2\text{O}_2$ and ^1H NMR (500 MHz, DMSO- d_6) δ (ppm): δ 7.56 (3H, d, $J = 8.5$ Hz), δ 7.87 (2H, t, $J = 7.0$ Hz), δ 8.04 (2H, d, $J = 7.0$ Hz), δ 8.16 (2H, m), δ 8.30 (2H, d, $J = 4.0$ Hz). These results conform to the those reported by Huang et al.¹⁴⁸ and the previous reports for the reaction of benzaldehyde with DAAQ or their analogues¹⁵¹. Thus, the derivatization reaction was suggested to proceed as shown in Fig. 5.1.

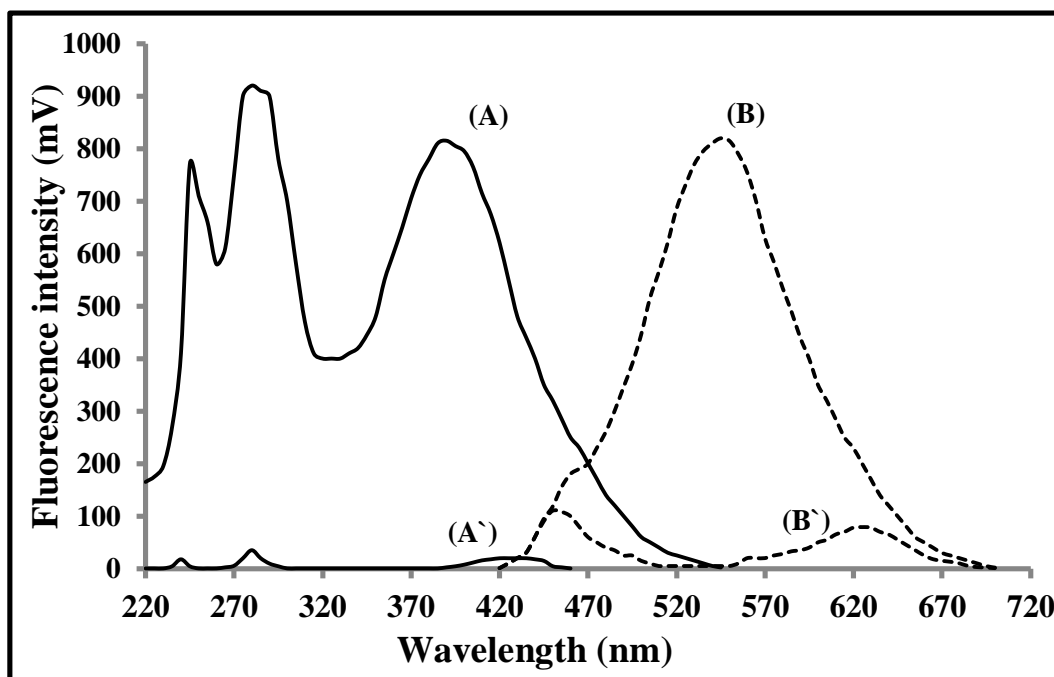


Fig. 5.3: Fluorescence spectra of benzaldehyde-DAAQ (10.0 μM benzaldehyde and 8.0 mM DAAQ) derivative and reagent blank (8 mM DAAQ alone). (A), (B): excitation and emission spectra of benzaldehyde-DAAQ derivative, respectively, (A'), (B'): excitation and emission spectra of reagent blank, respectively.

5-3-2. Optimization of derivatization conditions

In order to obtain the highest fluorescence intensity, we optimized the conditions for the fluorogenic derivatization reaction including DAAQ concentration, catalyst type and concentration and reaction temperature. The effect of DAAQ concentration on the fluorescence intensity was studied over the range of 0.1-1.0 mM. The fluorescence intensity increased with increasing the DAAQ concentration up to 0.4 mM then reached a plateau (Fig. 5.4). 0.8 mM of DAAQ was selected as the optimum reagent concentration to ensure method robustness.

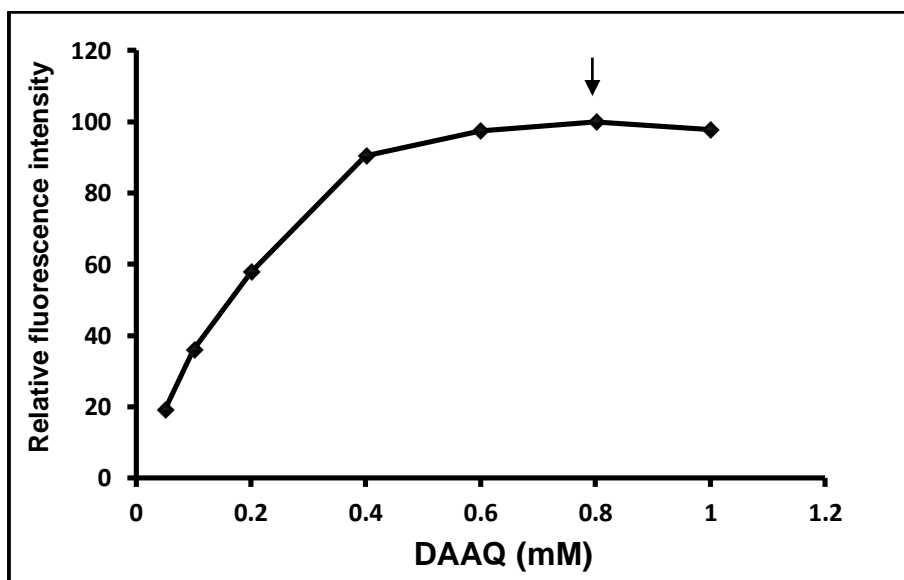


Fig. 5.4: Effect of DAAQ concentration on the fluorescence intensity of the reaction product with benzaldehyde (100 nmol/mL)

The influence of different catalysts on the fluorescence intensity was examined using acetic acid, acetic acid/sodium acetate, acetic acid/copper acetate, trifluoroacetic acid, sulfuric acid, acetic acid/Mn(III), and acetic acid/sodium metabisulfite as solvents for preparation of DAAQ. The study of these catalysts is based on previous reports for the synthesis of 2-arylbenzimidazoles from benzaldehyde and DAAQ or their

analogues¹⁵¹. Among these catalysts, the highest fluorescence intensity was obtained with acetic acid alone, so it was selected for subsequent experiments (Fig. 5.5 A). Subsequently, the effect of acetic acid concentration on the fluorescence intensity was studied over the concentration range of 10-100% using methanol as a diluent. The maximum fluorescence intensity was achieved using 100% acetic acid (Fig. 5.5 B); hence, it was used as a solvent for preparation of DAAQ.

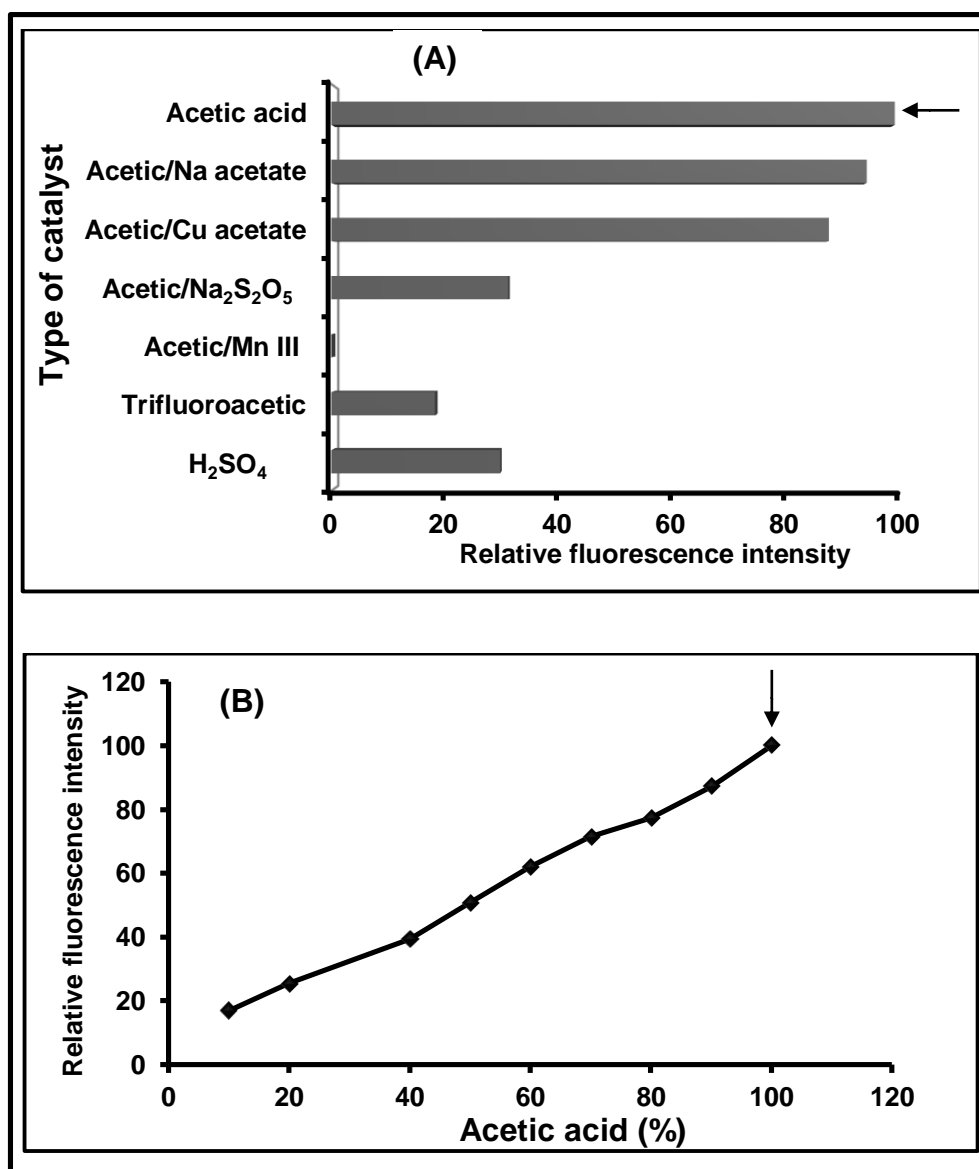


Fig. 5.5: Effect of (A) type of catalyst and (B) acetic acid concentration (%) on the fluorescence intensity of DAAQ-benzaldehyde derivative

The effect of the reaction temperature was examined (Fig. 5.6). The fluorescence intensity increased with increasing the temperature up to 100 °C. As a result, 100 °C was selected as the optimum reaction temperature.

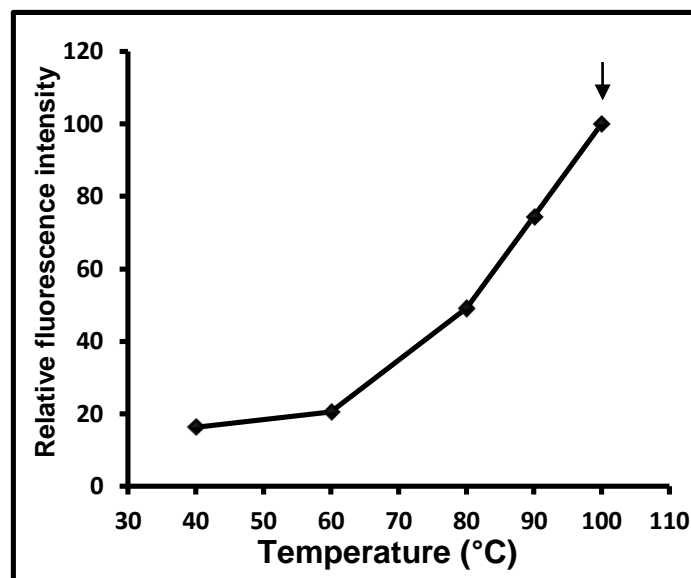


Fig. 5.6: Effect of the reaction temperature (°C) on the fluorescence intensity of DAAQ-benzaldehyde derivative

5-3-3. Optimization of FIA conditions

The FIA parameters such as the kind of carrier stream, flow rate of the carrier stream, flow rate of the fluorogenic reagent solution and reaction coil type and dimension were also optimized. Different solvents were tried as carrier streams including water, methanol, and acetonitrile. Methanol gave the highest fluorescence intensity, so it was chosen as the optimum carrier stream.

The effect of the flow rate of the two streams, the carrier and the fluorogenic reagent solutions, on the fluorescence signal and the residence time was investigated by changing their flow rate from 0.3 to 1.0 mL/min. A total flow rate of 0.4 mL/min was selected as a compromise between sensitivity and analytical throughput (Fig. 5.7) giving

a reasonable residence time of 5 min. Then, the flow rate ratio (carrier stream: fluorogenic reagent stream) was investigated maintaining a total flow rate of 0.4 mL/min. The highest fluorescence intensity was obtained at a flow rate of 0.2 mL/min for the two streams.

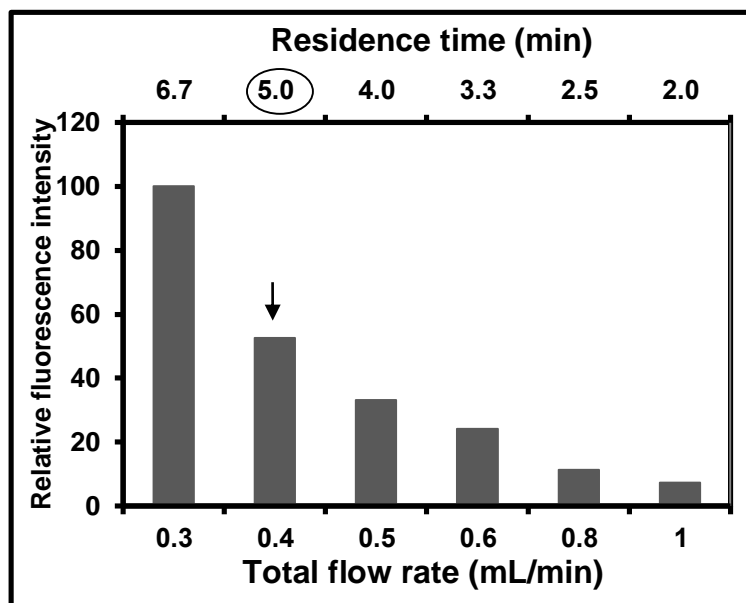


Fig. 5.7: Effect of total flow rate of the carrier and fluorogenic reagent streams on the fluorescence intensity of DAAQ-benzaldehyde derivative

Both PTFE and metal tubes were investigated as a reaction coil, and the PTFE one gave better fluorescence signal, so, it was selected as the optimum in subsequent experiments. The effect of the reaction coil dimension on the fluorescence intensity was investigated using different PTFE tubes while keeping a total residence time of 5 min by varying the flow rate. Three PTFE reaction coils were tested; the first one has dimensions of 10 m x 0.5 mm i.d. (coil volume of 2 mL) and the used flow rate was 0.4 mL/min, the second one was 15 m x 0.5 mm i.d. in dimensions (coil volume of 3 mL) and the used flow rate was 0.6 mL/min, and finally the third one was 10 m x 0.75 mm i.d. in dimensions (coil volume of 4.5 mL) and the used flow rate was 0.9 mL/min. The maximum fluorescence intensity was obtained using the first reaction coil (Fig. 5.8).

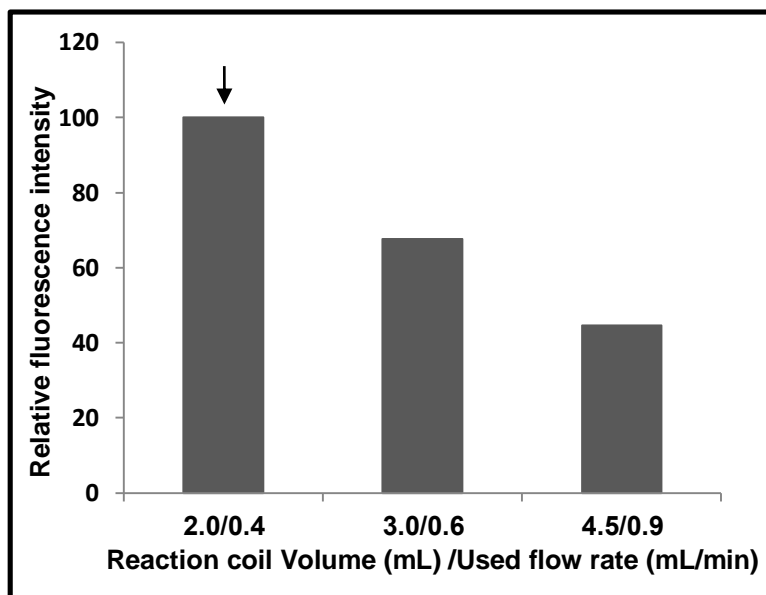


Fig. 5.8: Effect of reaction coil volume and flow rate on the fluorescence intensity of DAAQ-benzaldehyde derivative

In addition, an online study was conducted for selection of the optimum excitation and emission wavelengths of the reaction product. The highest fluorescence signal was obtained upon measuring the formed derivative at emission wavelength of 570 nm and excitation wavelength of 390 nm. A variation of the optimum emission wavelength of the product in the reaction medium from that in the online system was observed (545 and 570 nm, respectively), which is probably attributed to the difference in medium polarity. So, for achieving maximum sensitivity under the operating conditions, detection was done at 390/570 nm (excitation/emission).

Fig. 5.9 illustrates a representative detector response for benzaldehyde in enzymatic reaction mixture under the optimum FIA conditions.

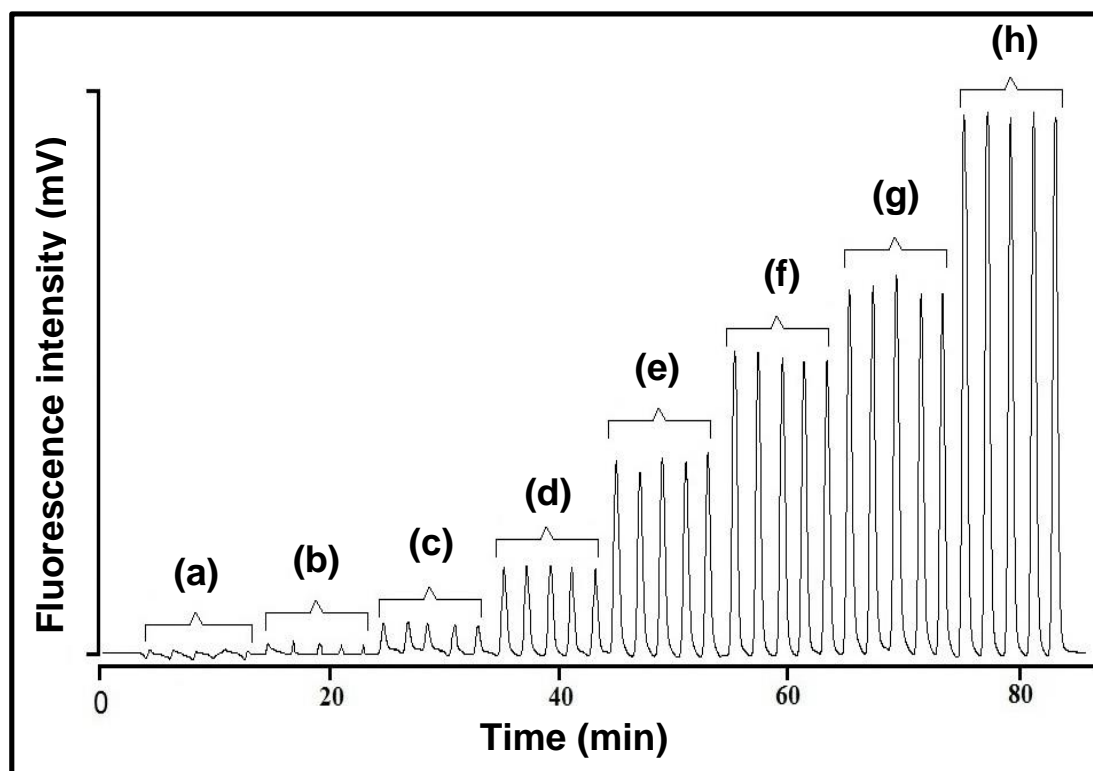


Fig. 5.9: FIA signals for the determination of benzaldehyde spiked to the enzymatic reaction mixture. Concentrations of benzaldehyde are: (a) 0 nmol/mL (blank), (b) 0.2 nmol/mL, (c) 5 nmol/mL, (d) 20 nmol/mL, (e) 50 nmol/mL, (f) 80 nmol/mL, (g) 100 nmol/mL and (h) 150 nmol/mL.

5-3-4. Pretreatment of serum samples for determination of SSAO activity and Michaelis-Menten constant (K_m)

To prevent the possible participation of plasma MAO in the conversion of benzylamine substrate to benzaldehyde, the reaction mixture was first incubated with 100 μ L clorgiline solution (0.2 mM) at 37 $^{\circ}$ C for 30 min. Under these conditions, clorgiline makes a complete and irreversible inhibition of both MAO-A and B ¹³⁴; meanwhile, SSAO is insensitive to clorgiline ¹⁴⁴. Clorgiline acts by binding the MAO enzyme active

sites stoichiometrically to form adduct with the flavine group in a 1:1 ratio ¹⁵². After incubation with clorgiline, the reaction was started by the addition of 250 μL of benzylamine. Different benzylamine concentrations were tried and the reaction rate was calculated each time as the amount formed of benzaldehyde in (nmol/mL/h). The apparent K_m (K') and V_{max} (V') of serum SSAO were estimated by the nonlinear curve fitting (Fig. 5.10) of Michaelis–Menten equation using GraphPad Prism trial version 6.05, (GraphPad Software, La Jolla, CA, USA):

$$V = (V_{max} \times [S]) / (K_m + [S])$$

Where V is the initial rate of reaction, V_{max} is the maximum reaction velocity, $[S]$ is the substrate concentration, and K_m is the Michaelis-Menten constant.

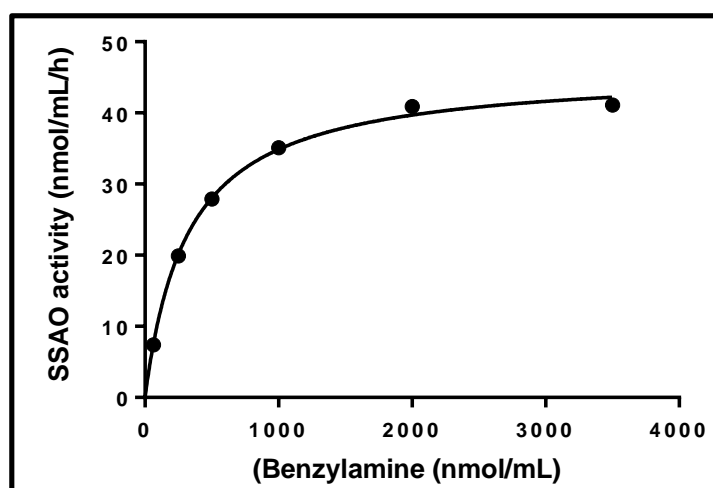
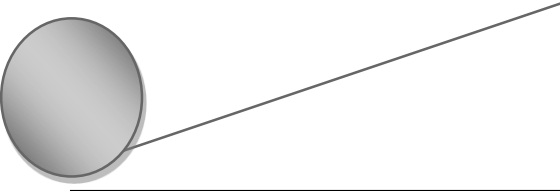


Fig. 5.10: Nonlinear fitting of Michaelis–Menten plot of SSAO activity *versus* benzylamine concentration in the enzymatic reaction mixture using GraphPad Prism trial version 6.05.



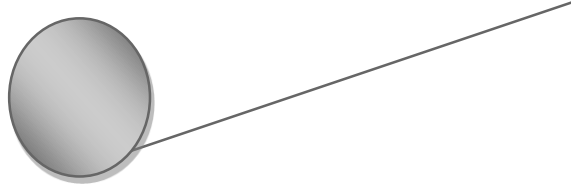
K' was found to be 322.2 ± 23.2 nmol/mL, where V' equals 46.1 ± 0.9 , which compares well with previously reported values ^{141,153}. Since it is usual to use a concentration of substrate about 10 folds higher than the K' value to determine the activity of an enzyme in a sample, a concentration of 3.5 $\mu\text{mol/mL}$ of benzylamine was used as the optimum substrate concentration in the incubation mixture.

For efficient extraction of benzaldehyde from human serum, we first attempted a simple PPT procedure with methanol or trichloroacetic acid for the pretreatment of serum samples. However, it was found that the presence of water in the reaction mixture interfered with the fluorogenic reaction. Therefore, in order to remove the water from the extracted solution, a subzero-temperature LLE based on the phenomenon that acetonitrile can be separated from the aqueous phase at a temperature below -20 °C ^{61,154}, was adopted. The application of this technique enabled water to be eliminated from the reaction mixture and the fluorogenic reaction then proceeded well. Moreover, the addition of acetonitrile terminated the action of SSAO on benzylamine *via* protein denaturation.

5-3-5. Validation study

To confirm the reliability of the proposed method, it was validated according to the Guidance for Industry on Bioanalytical Method Validation ⁶⁶.

The calibration curve prepared from the analysis of enzymatic reaction mixture spiked with standard benzaldehyde solution (seven-points curve) showed excellent linear relationship ($r = 0.9999$) between the concentrations and the average peak area over the concentration range of 0.2-150.0 nmol/mL according to the following regression equation:



$$Y = 0.388 \times 10^5 + 1.62 \times 10^5 X$$

Where: Y is the average peak area and X is benzaldehyde concentration, nmol/mL. The LOQ was found to be 0.2 nmol/mL with a % RSD of 9.4% and accuracy of -6.5%. The LOD (blank + 3 SD) was 0.06 nmol/mL.

To ensure selectivity of the proposed method and its ability to measure and differentiate benzaldehyde in the presence of components which may be expected to be present in the serum samples, serum samples from six healthy volunteers were analyzed and the response was compared to the signal of the analyte at the LOQ. Under these conditions, no interference from endogenous matrix components was observed indicating the selectivity of the proposed method for benzaldehyde. In addition an interference study has been carried out and will be discussed later in details.

The intra- and inter-day accuracy and precision of the proposed method were determined at 0.2, 5.0, and 100 nmol/mL. The results, expressed as the deviation of the mean value from the true one for accuracy and % RSD for precision, are shown in Table 5.1. The data showed good accuracy (intra-day -4.0 to -1.4 %; inter-day -6.5 to -0.6%) and adequate precision (intra-day % RSD of 2.9 to 6.7%; inter-day % RSD of 2.2 to 9.4%).

Recovery pertains to the extraction efficiency of the analytical method within the limits of variability. The % recoveries ranged from 94 to 98% with a standard deviation did not exceed 8.5% proving the high efficiency, precision, and reproducibility of the subzero-temperature LLE method. The results of recovery study are shown in Table 5.2.

The results of the validation procedure of the proposed FIA method agreed well with the requirements of the guidelines for Bioanalytical Method Validation⁶⁶.

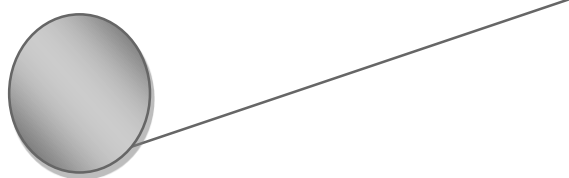
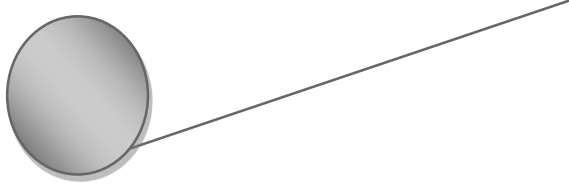


Table 5.1 Accuracy and precision of the proposed method for the determination of benzaldehyde in the spiked enzymatic reaction mixtures

Spiked concentration (nmol/ mL)	Found Conc. (nmol/mL)	Accuracy (%)	Precision (% RSD)
Intra-day (<i>n</i> = 5)			
0.2	0.192	-4.0	6.7
5.0	4.85	-3.0	3.4
100.0	98.6	-1.4	2.9
Inter-day (<i>n</i> = 5)			
0.2	0.187	-6.5	9.4
5.0	4.72	-5.6	4.5
100.0	99.4	-0.6	2.2

Table 5.2 Results of recovery study of benzaldehyde from spiked enzymatic reaction mixtures

Spiked level (nmol/mL)	% Recovery	SD
0.2	94	8.5
5.0	96	4.1
100.0	98	2.1

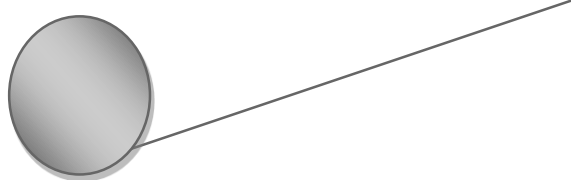


5-3-6. Interference investigation

In order to apply the proposed method to the determination of benzaldehyde formed by the action of serum SSAO, the influence of some aldehydes typically found in human serum was investigated. The aldehydes and their concentration ranges shown in Table 5.3 were selected for investigation of the interferences with the present method. Firstly, a mixed solution containing benzaldehyde (100 nmol/mL) and the aldehyde to be examined at constant concentration of 100 nmol/mL was injected into the carrier stream. The error due to the potentially interfering substances in the determination of benzaldehyde was determined by comparing the signal obtained for the mixed solution with that obtained for the 100 nmol/mL benzaldehyde solution without the interfering aldehyde.

Secondly, the same experiment was repeated in the enzymatic reaction mixture by spiking it with benzaldehyde (100 nmol/mL) and the aldehyde to be examined at constant concentration of 100 nmol/mL following the procedure mentioned in section "5-2-6." using 250 μ L of phosphate buffer solution instead of the SSAO's substrate benzylamine. Furthermore, both previous experiments were repeated using a mixture of all these possibly interfering aldehydes (100 nmol/ mL of each) and benzaldehyde (100 nmol/mL) and the error resulted from these aldehydes mixture was calculated.

The results of all experiments are illustrated in Table 5.3. It can be noted that the presence of GO, methylglyoxal, ACR, heptanal or MDA causes negligible small interferences in the direct determination of benzaldehyde, proving specificity of the reagent for aromatic aldehydes. In addition, the % error measured following the subzero-temperature LLE was obviously less than that measured upon direct injection of samples



into the FIA system. A % error of +1.1 was obtained upon analysis of serum sample spiked with benzaldehyde and mixed aldehydes following the subzero-temperature LLE *versus* +10.1% upon injection of the mixture directly into the carrier stream. These results evidenced the selectivity of the extraction procedure for benzaldehyde in presence of other aliphatic aldehydes.

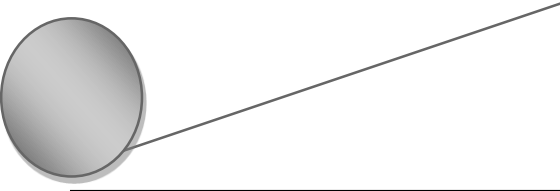
Table 5.3 Effects of some aldehydes normally exist in human serum on the determination of benzaldehyde (100 nmol/mL)

Aldehyde (100 nmol/mL)	Standard mixture	Enzymatic reaction mixture
	% Error ^{a,b}	% Error ^{a,c}
GO	+0.1	+0.2
Methyl glyoxal	+0.7	-0.5
ACR	+2.5	-1.1
Heptanal	+1.1	-0.3
MDA	+5.2	-1.2
Mixture of all previous aldehydes	+10.1	+1.1

^a Calculated as $(A_{B+I} - A_B)/A_B$. Where, A_{B+I} and A_B denote the peak area obtained for benzaldehyde solution containing the interfering aldehyde and that obtained for benzaldehyde without aldehyde, respectively.

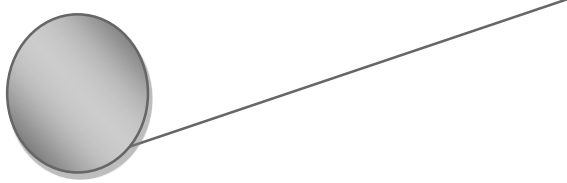
^b % Error calculated after direct injection of acetonitrile solutions containing benzaldehyde alone or with interfering aldehydes

^c % Error calculated after subzero-temperature LLE of serum samples spiked with benzaldehyde alone or with interfering aldehydes



Interference that may be encountered from benzylamine, the exogenous substrate of SSAO, with the derivatization reaction of benzaldehyde with DAAQ was also tested. A mixed solution containing benzaldehyde (100 nmol/mL) and benzylamine (3.5 mM) in acetonitrile was injected into the carrier stream. Comparing the signal obtained for this solution with that obtained for a standard benzaldehyde (100 nmol/mL), revealed a negative interference (-46.0%). The reason for this interference is probably due to condensation reaction of benzaldehyde with benzylamine forming a Schiff's base¹⁵⁵, such reaction abstracted benzaldehyde from the medium causing a negative interference with the assay.

Indeed, to mimic the actual assay conditions in serum, the same experiment was repeated in phosphate buffer (pH 7.8) (as a substitute for serum) then the solution was extracted by the subzero-temperature LLE procedure. 20 μ L of the acetonitrile phase was injected into the FIA system. Interestingly, a negligible positive deviation (+0.6%) from the actual value for benzaldehyde alone was observed. This indicates the high selectivity of the extraction procedure for benzaldehyde in the presence of benzylamine. This is because benzylamine has a distribution coefficient ($\log D$) = -0.56 at pH 7.4 (the physiological pH of blood serum), while that of benzaldehyde at the same pH is 1.61¹⁵⁶, which indicates very high polarity of benzylamine relative to benzaldehyde. From this, we can conclude that under the working condition (at pH 7.8); benzylamine is not extractable in acetonitrile phase while benzaldehyde is readily extracted in it, which offers high selectivity for the assay.



5-3-7. Application of the proposed method to determination of the SSAO activity in healthy and diabetic sera

The proposed FIA-FL method was applied to determine the human serum SSAO activity of 24 healthy human subjects and 18 patients with diabetes mellitus. Serum SSAO activity is defined as benzaldehyde (nmol) formed per mL serum per hour. The average SSAO activity in healthy human subjects (mean \pm SE) was found to be 58.9 ± 2.2 nmol/mL/h which agreed well with the previous results^{142,157,158}.

In the sera of diabetic patients, activity of SSAO was significantly higher compared to control healthy subjects at $P < 0.01$ (Table 5.4). This finding is in accordance with previous reports^{137,138,159-161}. Nunes et al. attributed the significant increase in SSAO activity in diabetic patients to the translocation of SSAO from the tissue-bound to plasma due to alterations in arterial permeability¹⁶². Thus, the measurement of serum SSAO activity is a valuable clinical biomarker for evaluation of the prognosis of diabetic complications¹⁴⁴.

Table 5.4 Statistical analysis of the results for determination of the SSAO activity in healthy and diabetics human subjects' sera

Parameter	Control healthy human subject	Diabetic patients
Number of samples (<i>n</i>)	24	18
SSAO activity range (nmol/mL/h)	29.7-79.3	59.9-84.4
SSAO activity mean \pm SE (nmol/mL/h)	58.9 ± 2.2	73.3 ± 1.8
Variance ratio <i>F</i> -test	$P = 0.09$ (NS) ^a	
Student's <i>t</i> -test	$P < 0.01$	

^a NS: no significant difference.

5-3-8. Comparison of the performance of the proposed method with that of reported literature for SSAO activity determination

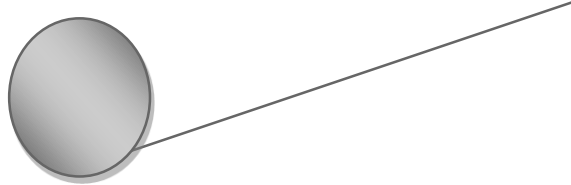
Table 5.5 illustrates a comparison of the performance of the proposed method with the reported literature for the determination of SSAO activity. The proposed method is 50 and 2 times more sensitive for benzaldehyde than the reported HPLC methods for determination of SSAO activity, respectively ^{141,142}. Even if the reported light scattering technique ¹⁴³ exhibited higher sensitivity than the proposed method, it suffers from some drawbacks such as tedious extraction procedure, long derivatization time, and poor recovery.

Table 5.5 Critical comparison of the performance of the proposed and reported methods for determination of SSAO activity

Method	Reagent	Reaction time (min)/ temperature (°C)	% Recovery	LOD (nmol/mL/h)	Remarks	Ref.
HPLC-FL	Dimedone	45/95	97	1.50	Derivatization required 9 M sulphuric acid	¹⁴¹
HPLC-UV	DNPH	30/37	64- 68	0.100	Unstable, flammable, and irritant reagent	¹⁴²
Light-Scattering	DNPH	30/40	68	0.002		¹⁴³
Radio-enzymatic assay	[¹⁴ C] Benzylamine	-----	N/A ^a	N/A ^a	Using radioactive compound	¹⁴⁴
FIA-FL	DAAQ	5/100	94-98	0.060	Automated online reaction	Present method

^a N/A: data is not available.

Although the time required for sample pretreatment and incubation period is a common feature of the proposed method and reported literature, the proposed FIA method



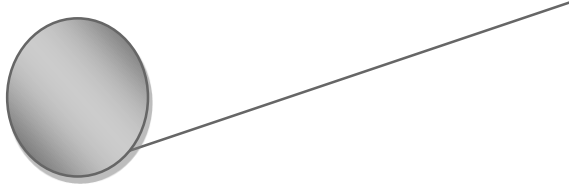
has the advantage of online derivatization reaction and short run time (5 min) which offers high sample throughput (27 sample/h). In addition, the proposed method uses small serum volume (50 μ L), these attributes, together with the excellent recovery and selectivity obtained adopting the subzero-temperature LLE procedure, make the proposed method very suitable for the routine measurement and comparison of serum SSAO activity in healthy and diabetic subjects.

The results of the proposed FIA method were statistically compared with those obtained using the reported HPLC-UV detection method ¹⁴² by applying both methods for the analysis of serum samples from ten healthy volunteers (4 females, 6 males; mean age 51.2 ± 5.6) for determination of SSAO activity. Statistical comparison of the results of the proposed and reported methods by two-sided paired Student *t*-test and variance ratio *F*-test revealed no significant difference between the performances of the two methods with regard to accuracy and precision ¹⁴⁹. Results of the comparison study are illustrated in Table 5.6.

Table 5.6 Statistical comparison of the proposed FIA method and a reference method for the determination of SSAO activity in human sera

Parameter	Proposed FIA method	Comparison HPLC-UV method ¹⁴²
Number of samples (n)		10
SSAO activity range (nmol/mL/h)	35.7-63.1	33.9-63.6
SSAO activity mean \pm SE (nmol/mL/h)	48.9 ± 3.4	47.6 ± 3.3
Variance ratio <i>F</i> -test		$P = 0.44$ (NS) ^a
Paired student's <i>t</i> -test		$P = 0.19$ (NS) ^a

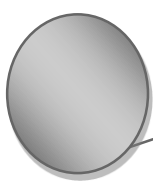
^aNS: no significant difference.



5-4. Conclusions

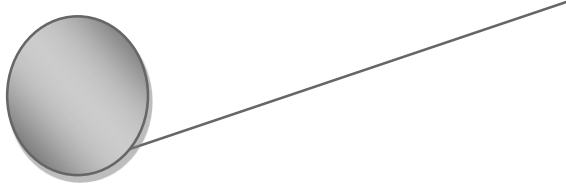
Herein, a novel fluorogenic derivatizing agent (DAAQ) was used to convert benzaldehyde, generated by the action of SSAO on benzylamine, into a fluorescent imidazole derivative. DAAQ showed high selectivity for benzaldehyde and there was no significant interference from aliphatic endogenous biological aldehydes. Based on this finding, a well optimized and validated FIA-FL method was developed for the assay of human serum SSAO activity employing a highly selective subzero-temperature LLE procedure. Serum SSAO activity was expressed as benzaldehyde (nmol) formed per mL serum per hour. The excellent validation results together with the high sensitivity and high sample throughput (27 samples/h) make the proposed method an excellent choice for determination of serum SSAO activity. The proposed method was applied to monitor the difference in SSAO activities in the sera of healthy and diabetic human subjects. A significant increase in serum SSAO activity was detected in case of diabetic patients relative to healthy human subjects.

General conclusions



Reactive aldehydes are produced due to oxidative stress in many diseased conditions and they are involved in the complications and progression of many diseases such as diabetes mellitus, rheumatoid arthritis and cardiac disorders. Hence, some aldehydes have been used as biomarkers of oxidative stress and diseases progression. Therefore, the development of highly sensitive, selective and simple analytical methods for aldehydes quantification in human samples is very important. Determination of aldehydes in biological fluids is considered very challenging due to their high polarity, lack of chromophores, poor chromatographic behavior, as well as difficulty of their extraction from biological matrices. In our laboratory, we started to develop new analytical methods for determination of different aldehydes in biological fluids ^{54,55,61,65}. In this thesis, we went on with this aim to develop novel, highly sensitive, simple and selective analytical methods for determination of aldehydes in serum of healthy and diseased human subjects hopefully to detect the differences in their levels in different diseases and to predict their pattern in correlation with diseased conditions.

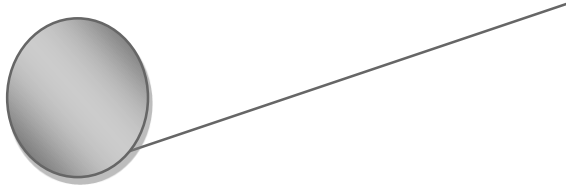
Firstly, we used 2,2'-fural as a selective and sensitive fluorogenic derivatizing agent for the determination of four LPRRAs (GO, ACR, MDA and HNE) in human serum by HPLC-FL method. Selection of these target analytes is based on their high reactivity and ability to initiate endogenous damages and harmful effects. The developed method enabled selective quantification of the levels of the four LPRRAs in serum of healthy subjects, diabetic and rheumatic patients. We conducted a comparison study of the levels of the four aldehydes in healthy and diseased human subjects, and we found that the levels of the four LPRRAs are elevated in diabetic and rheumatic arthritis patients compared to healthy control group. Additionally, we found that the levels of GO and ACR in diabetic



patients are higher than their levels in rheumatic ones, while the levels of MDA and HNE are higher in rheumatic patients than in diabetic ones.

In the second stage of this research, we developed an ultra-sensitive LC/ESI-MS/MS method for screening and quantification of a series of *n*-alkanals (C₃-C₁₀) in human serum. The method is based on the reaction of the α,β -diketo reagent PQ with the target aldehydes in the presence of ammonium acetate forming imidazole derivatives. The PQ-aldehydes derivatives were detected by ESI⁺-MS/MS using the transition m/z [M+H]⁺ \rightarrow m/z 231.9. The developed method was applied for the quantification of the analytes (C₃-C₁₀) in human serum using a simple salting out LLE method. The prominent ultra-sensitivity and simplicity of the developed method made it superior to the reported methods for these aldehydes.

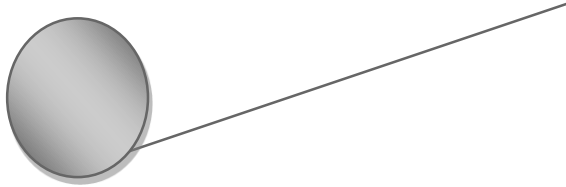
The interesting characteristics of PQ-aldehydes derivatives at MS/MS detector (including high sensitivity, simple and clear product ion spectra) as well as the simplicity of the reaction motivated us to initiate the next step of this study. In this part, we developed the first ICD LC/ESI-MS/MS for the simultaneous determination of two highly reactive 4-hydroxy-2-alkenals, HNE and HHE, in human serum. The method is based on the reaction of PQ with HNE and HHE in the presence of ¹⁴N/¹⁵N ammonium acetate as ICD reagent followed by LC/ESI⁺-MS/MS with detection at the transitions m/z [M+H]⁺ \rightarrow m/z 231.3 and m/z [M+2+H]⁺ \rightarrow m/z 233.3 for ¹⁴N and ¹⁵N-labeled analytes, respectively. The use of ¹⁴N/¹⁵N ammonium acetate as ICD reagent is very beneficial since it is cheap and commercially available. The high sensitivity and selectivity of the developed method enabled its application for the determination of HHE and HNE in human serum employing an expedient salting out LLE method. We applied the developed method to compare the levels of HHE and HNE in serum of healthy



subjects, diabetic, rheumatic and cardiac disorders patients. We found that the levels of the two aldehydes are significantly higher in all diseased conditions relative to healthy control. While, no significant difference exists between the levels of both aldehydes in diabetic compared to rheumatic and cardiac disorders patients. On the other hand, the level of HNE in cardiac disorders patients was significantly higher than its level in rheumatic arthritis patients, and there was no significant difference in level of HHE in both types of patients. The developed method is the first method to simultaneously determine HHE and HNE in human serum, so we believe that it will be very helpful for researchers to investigate their concomitant roles in the onset and progression of different diseases.

Finally, in the last step of this research we developed a highly simple, rapid and sensitive FIA method for the determination of serum SSAO activity. The method is based on incubation of serum with benzylamine as an exogenous SSAO substrate. The produced benzaldehyde was extracted by subzero-temperature LLE. Then, the benzaldehyde produced by the SSAO activity is online derivatized with the novel aromatic aldehyde-specific reagent DAAQ followed by FL detection. The developed method is very rapid allowing the processing of 27 samples per h. The method was applied to compare the activity of serum SSAO in healthy and diabetic human subjects and we found that the serum SSAO activity was significantly higher in the diabetic patients than in the healthy group. The developed FIA method is superior to the published methods in terms of sensitivity, accuracy and rapidness.

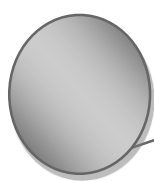
The four developed analytical methods were based on condensation reaction of aldehydes with either α,β -diketo compound in the presence of ammonium acetate or α,β -



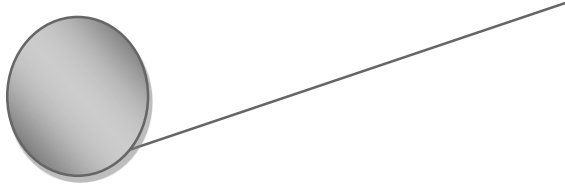
diamino compound forming imidazole derivatives with interesting fluorescence and/or ionization properties.

The developed analytical methods offered a promising approach for analysis of clinically significant aldehydes at trace and ultra-trace levels in healthy and diseased conditions (diabetic, rheumatic and cardiac disorders patients). They enabled detection of alteration in the levels of target analytes at these different clinical conditions. The developed methods would be useful for elucidation of the patterns of aldehydes levels and the patterns of activity of the aldehyde-producing enzyme, SSAO, at different clinical conditions. If these methods are applied to a great number of biofluids, they would help in the discovery of new diseases' biomarkers and more understanding of diseases development, individual biochemical response to the diseases, and mechanistic relationship of aldehydes and diseases progression.

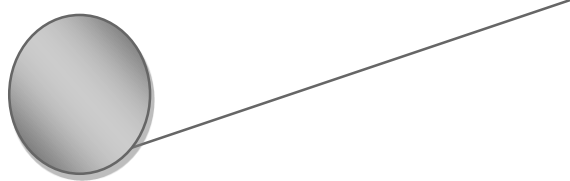
References



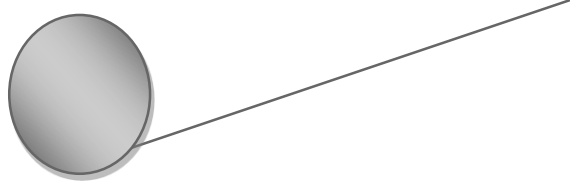
-
- (1) O'Brien, P. J.; Siraki, A. G.; Shangari, N. *Crit. Rev. Toxicol.* **2005**, *35* (7), 609–662.
 - (2) Feron, V. J.; Til, H. P.; de Vrijer, F.; Woutersen, R. A.; Cassee, F. R.; van Bladeren, P. J. *Mutat. Res. Toxicol.* **1991**, *259* (3-4), 363–385.
 - (3) Sood, C.; O'Brien, P. J. *Br. J. Cancer. Suppl.* **1996**, *27*, S287–S293.
 - (4) Kapetanovic, I. M.; Torchin, C. D.; Strong, J. M.; Yonekawa, W. D.; Lu, C.; Li, A. P.; Dieckhaus, C. M.; Santos, W. L.; Macdonald, T. L.; Sofia, R. D.; Kupferberg, H. J. *Chem. Biol. Interact.* **2002**, *142* (1-2), 119–134.
 - (5) Heimbrook, D. C.; Sartorelli, A. C. *Mol. Pharmacol.* **1986**, *29* (2), 168–172.
 - (6) Walsh, J. S.; Reese, M. J.; Thurmond, L. M. *Chem. Biol. Interact.* **2002**, *142* (1-2), 135–154.
 - (7) McMurry, J. *Organic Chemistry*; Brooks/Cole: Monterey, CA, 1984.
 - (8) Ellis, E. M. *Pharmacol. Ther.* **2007**, *115* (1), 13–24.
 - (9) Esterbauer, H.; Cheeseman, K. H.; Dianzani, M. U.; Poli, G.; Slater, T. F. *Biochem. J.* **1982**, *208* (1), 129–140.
 - (10) Esterbauer, H.; Schaur, R. J.; Zollner, H. *Free Radic. Biol. Med.* **1991**, *11* (1), 81–128.
 - (11) Shibamoto, T. *J. Pharm. Biomed. Anal.* **2006**, *41* (1), 12–25.
 - (12) Rindgen, D.; Nakajima, M.; Wehrli, S.; Xu, K.; Blair, I. A. *Chem. Res. Toxicol.* **1999**, *12* (12), 1195–1204.
 - (13) Uchida, K.; Kanematsu, M.; Morimitsu, Y.; Osawa, T.; Noguchi, N.; Niki, E. *J. Biol. Chem.* **1998**, *273* (26), 16058–16066.
 - (14) Benedetti, A.; Comporti, M.; Esterbauer, H. *Biochim. Biophys. Acta* **1980**, *620* (2), 281–296.
-



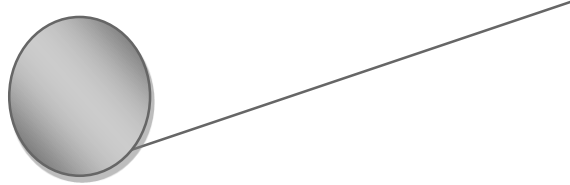
-
- (15) Lovell, M. A.; Xie, C.; Markesbery, W. R. *Neurobiol. Aging* **2001**, *22* (2), 187–194.
- (16) Calingasan, N. Y.; Uchida, K.; Gibson, G. E. *J. Neurochem.* **1999**, *72* (2), 751–756.
- (17) Williams, T. I.; Lynn, B. C.; Markesbery, W. R.; Lovell, M. A. *Neurobiol. Aging* **2006**, *27* (8), 1094–1099.
- (18) Kawaguchi-Niida, M.; Shibata, N.; Morikawa, S.; Uchida, K.; Yamamoto, T.; Sawada, T.; Kobayashi, M. *Acta Neuropathol.* **2006**, *111* (5), 422–429.
- (19) Asselin, C.; Bouchard, B.; Tardif, J.-C.; Des Rosiers, C. *Free Radic. Biol. Med.* **2006**, *41* (1), 97–105.
- (20) Leonarduzzi, G.; Chiarpotto, E.; Biasi, F.; Poli, G. *Mol. Nutr. Food Res.* **2005**, *49* (11), 1044–1049.
- (21) Toyokuni, S.; Yamada, S.; Kashima, M.; Ihara, Y.; Yamada, Y.; Tanaka, T.; Hiai, H.; Seino, Y.; Uchida, K. *Antioxid. Redox Signal.* **2000**, *2* (4), 681–685.
- (22) Niedowicz, D. M.; Daleke, D. L. *Cell Biochem. Biophys.* **2005**, *43* (2), 289–330.
- (23) Romero, M. J.; Bosch-Morell, F.; Romero, B.; Rodrigo, J. M.; Serra, M. A.; Romero, F. J. *Free Radic. Biol. Med.* **1998**, *25* (9), 993–997.
- (24) Marnett, L. J. *Toxicology* **2002**, *181-182*, 219–222.
- (25) Dib, M.; Garrel, C.; Favier, A.; Robin, V.; Desnuelle, C. *J. Neurol.* **2002**, *249* (4), 367–374.
- (26) Slatter, D. A.; Bolton, C. H.; Bailey, A. J. *Diabetologia* **2000**, *43* (5), 550–557.
- (27) Luczaj, W.; Gindzienska-Sieskiewicz, E.; Jarocka-Karpowicz, I.; Andrisic, L.; Sierakowski, S.; Zarkovic, N.; Waeg, G.; Skrzydlewska, E. *Free Radic. Res.* **2016**, *50* (3), 304–313.
-



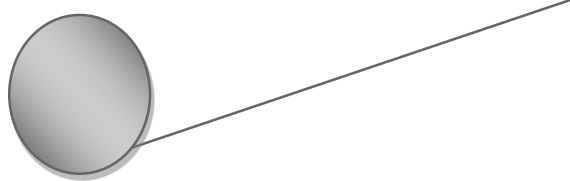
- (28) Uchida, K. *Free Radic. Biol. Med.* **2000**, 28 (12), 1685–1696.
 - (29) Odani, H.; Shinzato, T.; Usami, J.; Matsumoto, Y.; Brinkmann Frye, E.; Baynes, J. W.; Maeda, K. *FEBS Lett.* **1998**, 427 (3), 381–385.
 - (30) Thornalley, P. J.; Langborg, A.; Minhas, H. S. *Biochem. J.* **1999**, 344 Pt 1, 109–116.
 - (31) Simpson, G. L.; Ortwerth, B. J. *Biochim. Biophys. Acta* **2000**, 1501 (1), 12–24.
 - (32) Benov, L.; Fridovich, I. *J. Biol. Chem.* **1998**, 273 (40), 25741–25744.
 - (33) Thornalley, P. J.; Stern, A. *Biochim. Biophys. Acta* **1984**, 804 (3), 308–323.
 - (34) Ukeda, H.; Hasegawa, Y.; Ishi, T.; Sawamura, M. *Biosci. Biotechnol. Biochem.* **1997**, 61 (12), 2039–2042.
 - (35) Thornalley, P. J. *Gen. Pharmacol.* **1996**, 27 (4), 565–573.
 - (36) Li, W.; Yuan, X.-M.; Ivanova, S.; Tracey, K. J.; Eaton, J. W.; Brunk, U. T. *Biochem. J.* **2003**, 371 (Pt 2), 429–436.
 - (37) Seiler, N. *Neurochem. Res.* **2000**, 25 (4), 471–490.
 - (38) Conklin, D. J.; Boyce, C. L.; Trent, M. B.; Boor, P. J. *Toxicol. Appl. Pharmacol.* **2001**, 175 (2), 149–159.
 - (39) Yu, P. H.; Zuo, D. M. *Diabetologia* **1997**, 40 (11), 1243–1250.
 - (40) Clejan, L. A.; Cederbaum, A. I. *FASEB J. Off. Publ. Fed. Am. Soc. Exp. Biol.* **1992**, 6 (2), 765–770.
 - (41) Kukielka, E.; Cederbaum, A. I. *Toxicol. Lett.* **1995**, 78 (1), 9–15.
 - (42) Bondoc, F. Y.; Bao, Z.; Hu, W. Y.; Gonzalez, F. J.; Wang, Y.; Yang, C. S.; Hong, J. Y. *Biochem. Pharmacol.* **1999**, 58 (3), 461–463.
 - (43) Headlam, H. A.; Davies, M. J. *Free Radic. Biol. Med.* **2002**, 32 (11), 1171–1184.
 - (44) Anderson, M. M.; Hazen, S. L.; Hsu, F. F.; Heinecke, J. W. *J. Clin. Invest.* **1997**,
-



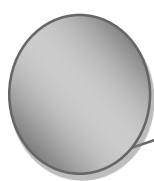
- 99 (3), 424–432.
- (45) Adam, W.; Kurz, A.; Saha-Moller, C. R. *Free Radic. Biol. Med.* **1999**, *26* (5-6), 566–579.
- (46) Long, E. K.; Picklo, M. J. S. *Free Radic. Biol. Med.* **2010**, *49* (1), 1–8.
- (47) Eggink, M.; Wijtmans, M.; Kretschmer, A.; Kool, J.; Lingeman, H.; De Esch, I. J. P.; Niessen, W. M. A.; Irth, H. *Anal. Bioanal. Chem.* **2010**, *397* (2), 665–675.
- (48) Wu, M.-Y.; Chen, B.-G.; Chang, C. D.; Huang, M.-H.; Wu, T.-G.; Chang, D.-M.; Lee, Y.-J.; Wang, H. C.; Lee, C.-I.; Chern, C.-L.; Liu, R. H. *J. Chromatogr. A* **2008**, *1204* (1), 81–86.
- (49) Zardari, L. A.; Khuhawar, M. Y.; Laghari, A. J. *Chromatographia* **2009**, *70* (5-6), 891–897.
- (50) Espinosa-Mansilla, A.; Duran-Meras, I.; Canada, F. C.; Marquez, M. P. *Anal. Biochem.* **2007**, *371* (1), 82–91.
- (51) Ojeda, A. G.; Wrobel, K.; Escobosa, A. R. C.; Garay-Sevilla, M. E.; Wrobel, K. *Anal. Biochem.* **2014**, *449*, 52–58.
- (52) Paci, A.; Rieutord, A.; Guillaume, D.; Traore, F.; Ropenga, J.; Husson, H. P.; Brion, F. *J. Chromatogr. B. Biomed. Sci. Appl.* **2000**, *739* (2), 239–246.
- (53) Bohnenstengel, F.; Eichelbaum, M.; Golbs, E.; Kroemer, H. K. *J. Chromatogr. B. Biomed. Sci. Appl.* **1997**, *692* (1), 163–168.
- (54) Imazato, T.; Kanematsu, M.; Kishikawa, N.; Ohyama, K.; Hino, T.; Ueki, Y.; Maehata, E.; Kuroda, N. *Biomed. Chromatogr.* **2015**, *29* (9), 1304–1308.
- (55) Ali, M. F. B.; Kishikawa, N.; Ohyama, K.; Mohamed, H. A.-M.; Abdel-Wadood, H. M.; Mahmoud, A. M.; Imazato, T.; Ueki, Y.; Wada, M.; Kuroda, N. *J. Chromatogr. B, Anal. Technol. Biomed. life Sci.* **2014**, *953-954*, 147–152.
-



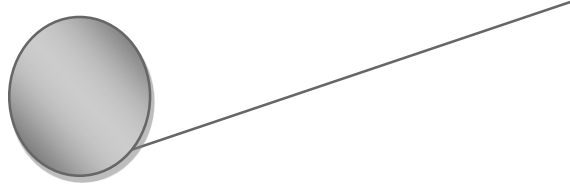
-
- (56) Giera, M.; Lingeman, H.; Niessen, W. M. A. *Chromatographia* **2012**, *75* (9-10), 433–440.
- (57) Zhang, G.; Tang, Y.; Shi, X.; Gao, R.; Sun, Y.; Du, W.; Fu, Q. *Anal. Biochem.* **2013**, *443* (1), 16–21.
- (58) Cooley, J. C.; Lunte, C. E. *Electrophoresis* **2011**, *32* (21), 2994–2999.
- (59) Zhang, D.; Haputhanthri, R.; Ansar, S. M.; Vangala, K.; De Silva, H. I.; Sygula, A.; Saebo, S.; Pittman, C. U. J. *Anal. Bioanal. Chem.* **2010**, *398* (7-8), 3193–3201.
- (60) Strohmaier, H.; Hinghofer-Szalkay, H.; Schaur, R. J. *J. Lipid Mediat. Cell Signal.* **1995**, *11* (1), 51–61.
- (61) Imazato, T.; Shiokawa, A.; Kurose, Y.; Katou, Y.; Kishikawa, N.; Ohyama, K.; Ali, M. F. B.; Ueki, Y.; Maehata, E.; Kuroda, N. *Biomed. Chromatogr.* **2014**, *28* (6), 891–894.
- (62) Santaniello, E.; Repetto, A.; Chiesa, L. M.; Biondi, P. A. *Redox Rep.* **2007**, *12* (1), 55–58.
- (63) Miyake, T.; Shibamoto, T. *Food Chem. Toxicol.* **1996**, *34* (10), 1009–1011.
- (64) Andreoli, R.; Manini, P.; Corradi, M.; Mutti, A.; Niessen, W. M. A. *Rapid Commun. Mass Spectrom.* **2003**, *17* (7), 637–645.
- (65) Fathy Bakr Ali, M.; Kishikawa, N.; Ohyama, K.; Abdel-Mageed Mohamed, H.; Mohamed Abdel-Wadood, H.; Mohamed Mohamed, A.; Kuroda, N. *J. Chromatogr. A* **2013**, *1300*, 199–203.
- (66) Food and Drug Administration. Guidance for Industry, Bioanalytical Method Validation, **2001** (accessed 18 Jan 2014)
<http://www.fda.gov/downloads/Drugs/Guidances/ucm070107.pdf>
- (67) Kobayashi, K.; Pillai, K. S.; Sakuratani, Y.; Abe, T.; Kamata, E.; Hayashi, M. *J.*
-



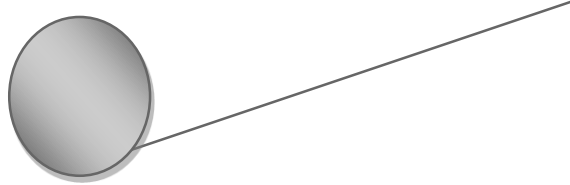
-
- Toxicol. Sci.* **2008**, 33 (1), 97–104.
- (68) Eggink, M.; Wijtmans, M.; Ekkebus, R.; Lingeman, H.; De Esch, I. J. P.; Kool, J.; Niessen, W. M. A.; Irth, H. *Anal. Chem.* **2008**, 80 (23), 9042–9051.
- (69) Wang, S.; Gu, Q.; Chen, X.; Zhao, T.; Zhang, Y. *Eur. J. Chem.* **2011**, 2 (2), 173–177.
- (70) Delgado, M.; Desroches, M.; Ganachaud, F. *RSC Adv.* **2013**, 3 (45), 23057.
- (71) Sakata, K.; Kashiwagi, K.; Sharmin, S.; Ueda, S.; Irie, Y.; Murotani, N.; Igarashi, K. *Biochem. Biophys. Res. Commun.* **2003**, 305 (1), 143–149.
- (72) Sim, A. S.; Salonikas, C.; Naidoo, D.; Wilcken, D. E. L. *J. Chromatogr. B, Anal. Technol. Biomed. Life Sci.* **2003**, 785 (2), 337–344.
- (73) Del Rio, D.; Stewart, A. J.; Pellegrini, N. *Nutr. Metab. Cardiovasc. Dis.* **2005**, 15 (4), 316–328.
- (74) Dalle-Donne, I.; Rossi, R.; Colombo, R.; Giustarini, D.; Milzani, A. *Clin. Chem.* **2006**, 52 (4), 601–623.
- (75) Hicks, M.; Delbridge, L.; Yue, D. K.; Reeve, T. S. *Biochem. Biophys. Res. Commun.* **1988**, 151 (2), 649–655.
- (76) Han, Y.; Randell, E.; Vasdev, S.; Gill, V.; Gadag, V.; Newhook, L. A.; Grant, M.; Hagerty, D. *Mol. Cell. Biochem.* **2007**, 305 (1-2), 123–131.
- (77) Gambhir, J. K.; Lali, P.; Jain, A. K. *Clin. Biochem.* **1997**, 30 (4), 351–355.
- (78) Stevens, J. F.; Maier, C. S. *Mol. Nutr. Food Res.* **2008**, 52 (1), 7–25.
- (79) Furumitsu, Y.; Yukioka, K.; Kojima, A.; Yukioka, M.; Shichikawa, K.; Ochi, T.; Matsui-Yuasa, I.; Otani, S.; Nishizawa, Y.; Morii, H. *J. Rheumatol.* **1993**, 20 (10), 1661–1665.
- (80) Bhor, V. .; Raghuram, N.; Sivakami, S. *Int. J. Biochem. Cell Biol.* **2004**, 36 (1),
-



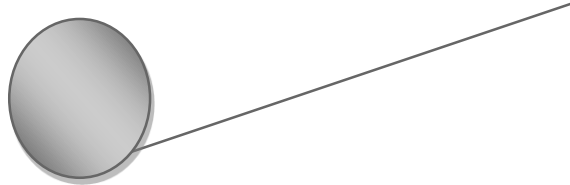
- 89–97.
- (81) Shacter, E. *Drug Metab. Rev.* **2000**, 32 (3-4), 307–326.
- (82) Alhamdani, M.-S. S.; Al-Kassir, A.-H. A. M.; Jaleel, N. A.; Hmood, A. M.; Ali, H. M. *Am. J. Nephrol.* **2006**, 26 (3), 299–303.
- (83) Martelli, A.; Canonero, R.; Cavanna, M.; Ceradelli, M.; Marinari, U. M. *Mutat. Res.* **1994**, 323 (3), 121–126.
- (84) Fiamegos, Y. C.; Stalikas, C. D. *Anal. Chim. Acta* **2008**, 609 (2), 175–183.
- (85) Büldt, A.; Karst, U. *Anal. Chem.* **1999**, 71 (9), 1893–1898.
- (86) Prieto-Blanco, M. C.; Iglesias, M. P.; López-Mahía, P.; Lorenzo, S. M.; Rodríguez, D. P. *Talanta* **2010**, 80 (5), 2083–2092.
- (87) Lin, Y. L.; Wang, P. Y.; Hsieh, L. L.; Ku, K. H.; Yeh, Y. T.; Wu, C. H. *J. Chromatogr. A* **2009**, 1216 (36), 6377–6381.
- (88) Baños, C. E.; Silva, M. *Talanta* **2009**, 77 (5), 1597–1602.
- (89) Xu, H.; Lv, L.; Hu, S.; Song, D. *J. Chromatogr. A* **2010**, 1217 (16), 2371–2375.
- (90) Lili, L.; Xu, H.; Song, D.; Cui, Y.; Hu, S.; Zhang, G. *J. Chromatogr. A* **2010**, 1217 (16), 2365–2370.
- (91) Zhang, H. J.; Huang, J. F.; Lin, B.; Feng, Y. Q. *J. Chromatogr. A* **2007**, 1160 (1-2), 114–119.
- (92) Mainka, A.; Bächmann, K. *J. Chromatogr. A* **1997**, 767 (1-2), 241–247.
- (93) Nakashima, K.; Hidaka, Y.; Yoshida, T.; Kuroda, N.; Akiyama, S. *J. Chromatogr. B. Biomed. Appl.* **1994**, 661 (2), 205–210.
- (94) Xiong, X.-J.; Wang, H.; Rao, W.-B.; Guo, X.-F.; Zhang, H.-S. *J. Chromatogr. A* **2010**, 1217 (1), 49–56.
- (95) Xu, H.; Song, D.; Cui, Y.; Hu, S.; Yu, Q.-W.; Feng, Y.-Q. *Chromatographia*
-



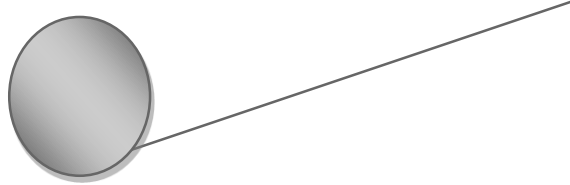
-
- 2009**, 70 (5-6), 775–781.
- (96) Tomono, S.; Miyoshi, N.; Ohshima, H. *J. Chromatogr. B Anal. Technol. Biomed. Life Sci.* **2015**, 988, 149–156.
- (97) Vogel, M.; Büldt, a; Karst, U. *Fresenius. J. Anal. Chem.* **2000**, 366 (8), 781–791.
- (98) Tsai, S. W.; Chang, C. M. *J. Chromatogr. A* **2003**, 1015 (1-2), 143–150.
- (99) Li, N.; Deng, C.; Yao, N.; Shen, X.; Zhang, X. *Anal. Chim. Acta* **2005**, 540 (2), 317–323.
- (100) Holley, A. E.; Walker, M. K.; Cheeseman, K. H.; Slater, T. F. *Free Radic. Biol. Med.* **1993**, 15 (3), 281–289.
- (101) Matsuoka, M.; Imado, N.; Maki, T.; Banno, K.; Sato, T. *Chromatographia* **1996**, 43 (9), 501–506.
- (102) O’Brien-Coker, I. C.; Perkins, G.; Mallet, A. I. *Rapid Commun. Mass Spectrom.* **2001**, 15 (12), 920–928.
- (103) Williams, T. I.; Lovell, M. A.; Lynn, B. C. **2004**, 339 (10), 1–2.
- (104) Sun, Z.; Wang, X.; Cai, Y.; Fu, J.; You, J. *Talanta* **2014**, 120, 84–93.
- (105) Higashi, T.; Ogawa, S. *J. Pharm. Biomed. Anal.* **2016**.
- (106) Levi, E. M.; Hauser, C. R. *J. Org. Chem.* **1969**, 34 (8), 2482–2484.
- (107) Buck, J. S.; Jenkins, S. S. *J. Am. Chem. Soc.* **1929**, 51 (7), 2163–2167.
- (108) KOBAYASHI, Y.; KUBO, H.; KINOSHITA, T. *Anal. Sci.* **1987**, 3 (4), 363–367.
- (109) Wasey, A.; Bansal, R. K.; Satake, M.; Puri, B. K. *Bull. Chem. Soc. Jpn.* **1983**, 56 (12), 3603–3607.
- (110) Wasey, A.; Puri, B. K.; Katyal, M.; Satake, M. *Int. J. Environ. Anal. Chem.* **1986**, 24 (3), 169–182.
- (111) Wasey, A.; Bansal, R. K.; Puri, B. K.; Katyal, M. *Bull. Environ. Contam.*
-



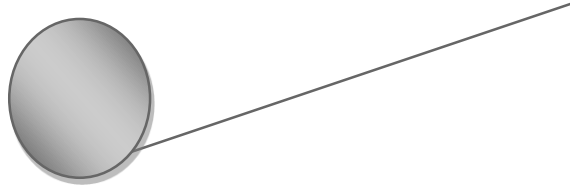
-
- Toxicol.* **1984**, 32 (3), 324–332.
- (112) Schaur, R. J. *Mol. Aspects Med.* **2003**, 24 (4-5), 149–159.
- (113) Grasse, L. D.; Lame, M. W.; Segall, H. J. *Toxicol. Lett.* **1985**, 29 (1), 43–49.
- (114) Brambilla, G.; Sciaba, L.; Faggin, P.; Maura, A.; Marinari, U. M.; Ferro, M.; Esterbauer, H. *Mutat. Res.* **1986**, 171 (2-3), 169–176.
- (115) Eckl, P. M.; Ortner, A.; Esterbauer, H. *Mutat. Res.* **1993**, 290 (2), 183–192.
- (116) Bacot, S.; Bernoud-Hubac, N.; Chantegrel, B.; Deshayes, C.; Doutheau, A.; Ponsin, G.; Lagarde, M.; Guichardant, M. *J. Lipid Res.* **2007**, 48 (4), 816–825.
- (117) Long, E. K.; Murphy, T. C.; Leiphon, L. J.; Watt, J.; Morrow, J. D.; Milne, G. L.; Howard, J. R. H.; Picklo, M. J. S. *J. Neurochem.* **2008**, 105 (3), 714–724.
- (118) Berhane, K.; Widersten, M.; Engstrom, A.; Kozarich, J. W.; Mannervik, B. *Proc. Natl. Acad. Sci. U. S. A.* **1994**, 91 (4), 1480–1484.
- (119) Hubatsch, I.; Ridderstrom, M.; Mannervik, B. *Biochem. J.* **1998**, 330 (Pt 1), 175–179.
- (120) Brichac, J.; Ho, K. K.; Honzatko, A.; Wang, R.; Lu, X.; Weiner, H.; Picklo, M. J. *S. Chem. Res. Toxicol.* **2007**, 20 (6), 887–895.
- (121) van Kuijk, F. J.; Siakotos, A. N.; Fong, L. G.; Stephens, R. J.; Thomas, D. W. *Anal. Biochem.* **1995**, 224 (1), 420–424.
- (122) Kawai, Y.; Takeda, S.; Terao, J. *Chem. Res. Toxicol.* **2007**, 20 (1), 99–107.
- (123) Seppanen, C. M.; Csallany, A. S. *J. Am. Oil Chem. Soc.* **2001**, 78 (12), 1253–1260.
- (124) Douny, C.; Tihon, A.; Bayonnet, P.; Brose, F.; Degand, G.; Rozet, E.; Milet, J.; Ribonnet, L.; Lambin, L.; Larondelle, Y.; Scippo, M.-L. *Food Anal. Methods* **2015**, 8 (6), 1425–1435.
-



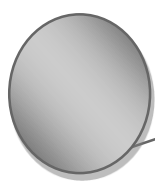
-
- (125) Bruheim, P.; Kvitvang, H. F. N.; Villas-Boas, S. G. *J. Chromatogr. A* **2013**, *1296*, 196–203.
- (126) Dai, W.; Huang, Q.; Yin, P.; Li, J.; Zhou, J.; Kong, H.; Zhao, C.; Lu, X.; Xu, G. *Anal. Chem.* **2012**, *84* (23), 10245–10251.
- (127) TABATA, M.; KUMAMOTO, M.; NISHIMOTO, J. *Anal. Sci.* **1994**, *10* (3), 383–388.
- (128) Dhalla, N. S.; Temsah, R. M.; Netticadan, T. *J. Hypertens.* **2000**, *18* (6), 655–673.
- (129) Zurek, G.; Karst, U. *J. Chromatogr. A* **2000**, *869* (1-2), 251–259.
- (130) Manini, P.; Andreoli, R.; Sforza, S.; Dall'Asta, C.; Galaverna, G.; Mutti, A.; Niessen, W. M. A. *J. Chromatogr. B, Anal. Technol. Biomed. life Sci.* **2010**, *878* (27), 2616–2622.
- (131) Prokai, L.; Szarka, S.; Wang, X.; Prokai-Tatrai, K. *J. Chromatogr. A* **2012**, *1232*, 281–287.
- (132) Abella, A.; Marti, L.; Camps, M.; Claret, M.; Fernandez-Alvarez, J.; Gomis, R.; Guma, A.; Viguerie, N.; Carpena, C.; Palacin, M.; Testar, X.; Zorzano, A. *Diabetes* **2003**, *52* (4), 1004–1013.
- (133) Abella, A.; Garcia-Vicente, S.; Viguerie, N.; Ros-Baro, A.; Camps, M.; Palacin, M.; Zorzano, A.; Marti, L. *Diabetologia* **2004**, *47* (3), 429–438.
- (134) Lyles, G. A. *Int. J. Biochem. Cell Biol.* **1996**, *28* (3), 259–274.
- (135) Hernandez, M.; Sole, M.; Boada, M.; Unzeta, M. *Biochim. Biophys. Acta* **2006**, *1763* (2), 164–173.
- (136) Boomsma, F.; de Kam, P. J.; Tjeerdsma, G.; van den Meiracker, A. H.; van Veldhuisen, D. J. *Eur. Heart J.* **2000**, *21* (22), 1859–1863.
-



- (137) Boomsma, F.; Derkx, F. H.; van den Meiracker, A. H.; Man in 't Veld, A. J.; Schalekamp, M. A. *Clin. Sci. (Lond)*. **1995**, *88* (6), 675–679.
- (138) Garpenstrand, H.; Ekblom, J.; Backlund, L. B.; Orelund, L.; Rosenqvist, U. *Diabet. Med.* **1999**, *16* (6), 514–521.
- (139) Yu, P. H.; Zuo, D. M. *Diabetes* **1993**, *42* (4), 594–603.
- (140) Matyus, P.; Dajka-Halasz, B.; Foldi, A.; Haider, N.; Barlocco, D.; Magyar, K. *Curr. Med. Chem.* **2004**, *11* (10), 1285–1298.
- (141) van Dijk, J.; Boomsma, F.; Alberts, G.; Man in 't Veld, A. J.; Schalekamp, M. A. *J. Chromatogr. B. Biomed. Appl.* **1995**, *663* (1), 43–50.
- (142) Li, H.; Luo, W.; Lin, J.; Lin, Z.; Zhang, Y. *J. Chromatogr. B, Anal. Technol. Biomed. life Sci.* **2004**, *810* (2), 277–282.
- (143) Tan, X.; Rang, W.-Q.; Wang, Y.-S.; Yang, H.-X.; Xue, J.-H.; Shi, L.-F.; Yang, H.-M.; Liu, L.; Zhou, B. *Anal. Lett.* **2012**, *45* (18), 2774–2784.
- (144) Meszaros, Z.; Karadi, I.; Csanyi, A.; Szombathy, T.; Romics, L.; Magyar, K. *Eur. J. Drug Metab. Pharmacokinet.* **1999**, *24* (4), 299–302.
- (145) Zhang, Y.; Xiao, S.; Wang, L.; Wang, H.; Zhu, Y.; Li, Y.; Deng, Y. *Anal. Bioanal. Chem.* **2010**, *397* (2), 709–715.
- (146) Gokturk, C.; Nordquist, J.; Sugimoto, H.; Forsberg-Nilsson, K.; Nilsson, J.; Orelund, L. *Biochem. Biophys. Res. Commun.* **2004**, *325* (3), 1013–1020.
- (147) Garcia-Vicente, S.; Abella, A.; Viguerie, N.; Ros-Baro, A.; Camps, M.; Testar, X.; Palacin, M.; Zorzano, A.; Marti, L. *J. Physiol. Biochem.* **2005**, *61* (2), 395–401.
- (148) Huang, H.-S.; Chen, T.-C.; Chen, R.-H.; Huang, K.-F.; Huang, F.-C.; Jhan, J.-R.; Chen, C.-L.; Lee, C.-C.; Lo, Y.; Lin, J.-J. *Bioorg. Med. Chem.* **2009**, *17* (21),



- 7418–7428.
- (149) Miller, J. N.; Miller, J. C. *Statistics and chemometrics for analytical chemistry*, Fifth Ed.; Prentice Hall: England, 2005.
- (150) Heiduschka, P.; Thanos, S. *Neuroreport* **1998**, *9* (18), 4051–4057.
- (151) Panda, S.; Malik, R.; C. Jain, S. *Curr. Org. Chem.* **2012**, *16* (16), 1905–1919.
- (152) Fowler, C. J.; Orelan, L.; Callingham, B. A. *J. Pharm. Pharmacol.* **1981**, *33* (6), 341–347.
- (153) Lyles, G. A.; Holt, A.; Marshall, C. M. *J. Pharm. Pharmacol.* **1990**, *42* (5), 332–338.
- (154) Yoshida, M.; Akane, A. *Anal. Chem.* **1999**, *71* (9), 1918–1921.
- (155) Rodríguez-Lugo, R. E.; Trincado, M.; Grützmacher, H. *ChemCatChem* **2013**, *5* (5), 1079–1083.
- (156) Advanced Chemistry Development, Inc.,: Toronto, On, Canada 2012.
- (157) Januszewski, A. S.; Mason, N.; Karschimkus, C. S.; Rowley, K. G.; Best, J. D.; O’Neal, D. N.; Jenkins, A. J. *Diabetes Vasc. Dis. Res.* **2014**, *11* (4), 262–269.
- (158) Roessner, V.; Uebel, H.; Becker, A.; Beck, G.; Bleich, S.; Rothenberger, A. *Behav. Brain Funct.* **2006**, *2*, 5.
- (159) Gokturk, C.; Garpenstrand, H.; Nilsson, J.; Nordquist, J.; Orelan, L.; Forsberg- Nilsson, K. *Biochim. Biophys. Acta* **2003**, *1647* (1-2), 88–91.
- (160) Obata, T. *Life Sci.* **2006**, *79* (5), 417–422.
- (161) Nunes, S. F.; Figueiredo, I. V.; Pereira, J. S.; Soares, P. J.; Caramona, M. M.; Callingham, B. *Acta Diabetol.* **2010**, *47* (2), 179–182.
- (162) Nunes, S. F.; Figueiredo, I. V.; Pereira, J. S.; de Lemos, E. T.; Reis, F.; Teixeira, F.; Caramona, M. M. *Physiol. Res.* **2011**, *60* (2), 309–315.
-



Acknowledgement

First, all my praise, gratitude and thanks to ALLAH, the most kind and merciful, who enabled me to complete this work.

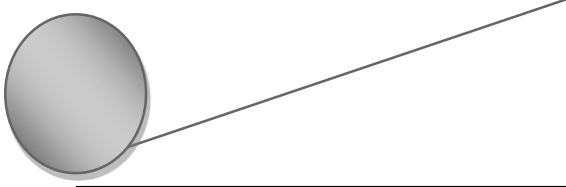
I would like to express my sincere gratitude and appreciation to my supervisor, *Professor Naotaka Kuroda* for his continuous support to my PhD study, for his patience, inspiration and enormous knowledge. His guidance, discussions and valuable suggestions helped me a lot in all times of my research. It was a great opportunity to conduct my PhD study in his laboratory and being one of his students.

I honestly thank my thesis committee: *Professor Morio Nakayama* and *Professor Koyo Nishida* for their insightful comments, constructive and detailed discussions that contributed to this thesis.

My sincere thanks go also to *Associate professor Naoya Kishikawa* for his stimulating discussions, beneficial help and the superb support he offered to me throughout my researches. Also, I would like to thank *Associate professor Kaname Ohyama* for his help, suggestions and fruitful comments.

I am also very thankful to my colleagues in the Graduate School of Biomedical Sciences, Nagasaki University, for providing a great work environment and beneficial discussions.

I would like to express my deepest appreciation and gratitude to all my professors in the Department of Pharmaceutical Analytical Chemistry, Faculty of Pharmacy, Mansoura University, for their unlimited support and continuous encouragement.



Acknowledgement

I'm also very grateful to the Japanese Ministry of Education, Culture, Sports, Sciences and Technology (MEXT) for the scholarship to conduct my PhD in Japan and to the Cultural, Educational and Science Bureau in the Embassy of the Arab Republic of Egypt in Japan for encouragement, help, and support.

My deepest thanks to my mother for loving, encouraging and supporting me spiritually throughout this thesis and throughout my whole life. Also, I would like to thank my brothers for their support and help. My special thanks and appreciation is extended to my beloved wife Rania Nabih for her love, understanding, continuous support and cordial assistance to me while performing this work.

Mahmoud Hamed ElMaghrabey